

THE LIGHT FIELD IN PRACTICE

A study into the lower order properties of the light field and their influence on visual comfort in daylight office spaces



 **TU Delft**

Master thesis

N.A. Debets

THE LIGHT FIELD IN PRACTICE

A study into the lower order properties of the light field
and their influence on visual comfort in daylit office spaces

in partial fulfilment of the requirements for the degree of

Master of Science
in Civil Engineering
at the Delft University of Technology,
to be defended publicly on Thursday March 1, 2018 at 16:00h

by

Noor Debets



Thesis committee, from the Delft University of Technology:

Prof. dr. Ir. R. Nijssen
dr.ir. H.R. Schipper
dr. G.J. Hordijk,
Prof. dr. S.C. Pont

faculty of Civil Engineering
faculty of Civil Engineering
faculty of Architecture and the Built Environment
faculty of Industrial Design Engineering

to my tutors, family and friends

ABSTRACT

In the development of the lighting practice, progress has been made to eliminate bad lighting and to contribute to a visual comfortable scene. Metrics, and subsequent recommendations, have been established to provide uniform horizontal illuminance. In addition, performance-based metrics are developed. For example, various lighting levels for different tasks. However, the conventional metrics and current lighting standards fail to describe the spatial quality of light that provides a human observer with information about its surroundings contributing to one's well-being. And so, increased emphasis is on three-dimensional light distribution in a space creating good lighting. Currently, renewed attention goes to the application of a theory to examine the visual appearance of light in a space: the light field. The light field can be subdivided in the light intensity, the light direction and diffuseness simultaneously. Hence, it is wondered to what extent the analysis of the light field is an effective alternative to predict visual comfort in a daylight office meeting space?

The research answers this main question in three parts, using literature review, in-field measurements and simulated data. The first part of the research concentrates on literature about the conventional visual comfort metrics (luminance Contrast Ratio and Daylight Glare Property), and the (mathematical) description of the light field. The second part of research deals solely with the light field. It examines how its properties can be measured and visualised, in researching the application of tool use. In part three knowledge about the conventional performance-based measuring techniques and the analysis of the properties of the light field (light intensity, light direction and diffuseness) are brought together and compared in a case study of a visual uncomfortable experienced office space.

Based upon the results obtained during the research, it is proven that the analysis of the light field is a promising candidate describing an uncomfortable setting in terms of light direction and diffuseness rather than luminance and illuminance. It is a view independent metric that can predict visual uncomfortable situations generated by a strong directional lighting combined with a low diffuseness, resulting in disturbing shades. Simultaneously, it is found that the current metrics for luminance Contrast Ratio and the simplified Daylight Glare probability, that try to predict the likelihood of visual comfort, lack a full description of the perceived level of visual comfort. Finally, the level of visual comfort for the human observer in the office space of the case study has been improved.

Keywords: *daylight, light metrics, visual comfort, luminance contrast ratio, daylight glare probability, light field, light direction, light intensity, diffuseness, light field,*

PREFACE

“The unconscious tactile ingredient in vision is particularly important and strongly present in historical architecture, but badly neglected in the architecture of our time”

(Pallasmaa J. , 2012, p.29).

Supported by this quote I realised that the sensitivity I had for good and/or bad lighting was not misguiding at all. And so, I wondered why this topic that seemed so natural and obvious to me was still very unknown. Longing for a more sensible and social side of the built environment during my bachelors civil engineering, I finally attempted to understand the *tactile ingredient* of light in a space during my master thesis. During almost a year I worked fascinated and inspired on gaining knowledge about the quality of light in a space that definitely changed the way I see light.

This master thesis is the outcome of research into a new field of study for me: the light field. Extensive investigation allowed me to answer the main research question and opened up a new world to me.

I would like to thank my thesis committee Roel Schipper, Rob Nijssse and Sylvia Pont for their guidance and support during the process. A special thanks for committee member Truus de Bruin Hordijk for the trust you gave me going my own way, and the helpful discussions during our meetings, answering the many questions I had. I would also like to thank Raquel Viula for her assistance with the luminance camera and Tatiana Kartashova for the possibility of using her web application.

Furthermore, I would like to thank my friends for keeping me motivated and inspiring me to get as much out of this project as possible. Mimmo, thank you for your support in finding the mathematician in me, and listening to me for all those hours *searching for the light to find*. Jan, Mom, Dad, thank you for being, as always, inspirational to me and willing to give me advice any time any place. Thank you so much.

Noor Debets,
Rotterdam, February 19, 2018

TABLE OF CONTENT

The pdf version of this thesis is different from the print version. Page numbers in the table of content do not match the page numbers of the print file.

ABSTRACT	5
PREFACE	6
1. Introduction	10
1.1 Background	10
1.2 The problem definition	12
1.3 Limitations	13
1.4 Methodology & outline	14
PART I - LITERATURE REVIEW	
2. Quality of Daylight and Visual Comfort	17
2.1 A definition of daylighting	17
2.2 Third stage of daylighting design	18
2.2 Visual comfort metrics	19
3. An introduction to the Light Field	22
3.1 Physics of the light field	22
3.1.1 Introduction to the light field: Light density and light vector	22
3.1.2 Introduction to the light field: Diffuseness	26
3.1.3 Tools to measure the light field	27
3.2 How to make the light field visible	29
3.2.1 The visual characteristics of diffuseness- a history	29
3.2.2 The visual light field – its concept and analysis	30
3.3 The light field - its application	33
4. Conclusion Part I	35
PART II - RESEARCHING APPLICATION OF TOOL USE	
5. Measurement method	39
5.1 A spatial description of room BK01.West.050	39
5.2 Cubic illuminance meter and light field visualization: over time	40
5.2.1 The cubic illuminance meter	40
5.2.2 Visualization: Light field depicted by objects	42
5.2.3 Visualization: A web application	43
5.3 Cubic illuminance meter and light field visualization: different positions	43
5.3.1 The cubic illuminance meter	44
5.3.2 Visualization: Light field depicted by objects	44
5.3.3 Visualization: A web application	44
6. Measurement results	45
6.1 Cubic illuminance meter and light field visualization: over time	45
6.1.1 The cubic illuminance meter	45
6.1.2 Visualization: Light field depicted by objects	46
6.1.3 Visualization: A web application	49
6.2 Cubic illuminance meter and light field visualization: different positions	49
6.2.1 The cubic illuminance meter	49

6.2.2 Visualization: Light field depicted by objects	50
6.2.3 Visualization: A web application	52
7. Discussion Part II	53
7.1 Cubic illuminance meter	53
7.2 Light field visualization	55
8. Conclusion part II	58
PART III - RESEARCHING THE LIGHT FIELD THROUGH A CASE STUDY	
9. Case Study Method	61
9.1 Problem Description Case Study	61
9.2 Measurement	62
9.2.1 Spatial design Ct2.72	62
9.2.2 Visual comfort metrics: LCR and DGP	62
9.2.3 Cubic illuminance meter	63
9.2.4 Light Field visualization	63
9.3 Computer-generated measurements	64
9.3.1 Set-up Rhino model- Validation	64
9.3.2 Simulation	65
10. Case Study Results	67
10.1 Measurement	67
10.1.1 Spatial design Ct2.72: Room surface reflectance	68
10.1.2 Visual comfort metrics: LCR and DGP	68
10.1.3 Cubic illuminance meter	69
10.1.4 Light Field visualization	71
10.2 Computer-generated results	72
10.2.1 Validation	72
10.2.2 Simulation	74
11. Discussion Part III	80
11.1 Measurement	80
11.2 Computer-generated results	82
11.2.1 Validation	82
11.2.2 Simulation	83
12. Conclusion Part III	86
13. Final conclusion & recommendation	88
REFERENCES	90
APPENDICES	
A. The description of light & photometric quantities	93
B. The light field as a spherical harmonics representation	94
C. The cubic illuminance meter	95
D. Light Visualization by Kartashova	97
E. Measurement protocol	98
E1. Cubic illuminance meter	98
E2. Object visualization with luminance camera	98

F. Measurement results	101
F1. September 15	101
F2. October 26	103
F3. October 21	105
G. Fish-Eye lens	107
H. Room surface reflectance	108
I. Result Case-Study: November 21	109
J. Result Case-Study: December 1- 10:15h & 11:30h	111
K. Radiance	112
K1. simulation protocol	112
K2. advanced parameters	112
L. Validation	113
M. Simulation:	115
M1. November 3, 11:00h, Clouded Sky	115
M2. November 3, 11:00h, Clear Sky	118
N. Additional visualization	122

1

INTRODUCTION

In order to research the three-dimensional characteristics of lighting and construct new design guidelines for this topic, an understanding is required about existing lighting design guidelines. This chapter will therefore elaborate on the history of the lighting profession and the origin of according legislation formed - and used up to this date.

Paragraph 1. introduces terminology in a literature review about the current state of the lighting design practice. This results in a problem definition in paragraph 1.2 in which the main research question and the sub questions are presented. The limitations are examined in paragraph 1.3. Paragraph 1.4 presents the method of research and the overall outline of the thesis.

1.1 BACKGROUND

Practice and theory can be considered as parallel lines which once in a while intersect and influence each other. This thesis aims to make practice and theory intersect (Cuttle 2008). This aim stems from several assumptions that are extracted from a critical review of the literature and the state of lighting design in practice.

The development of the lighting profession legislation

For much of the last century, lighting design was conditioned by the invention of the fluorescent lamp in the late 1930s. Pursuing *uniform* horizontal illuminance levels, lighting engineers started to develop photometric data¹, with illuminance as a measure of intensity (appendix A). Hence, the role of lighting recommendations increased to eliminate 'bad lighting', which is defined as light that make us able to see without being visual uncomfortable (Boyce, 2013). The first established recommended lighting levels dates from 1936. Over time, illuminance levels became more strictly defined. For example, in 1994, lighting became more performance based, when *CIBSE Guide for Interior Lighting* included lists of tasks and applications to be illuminated properly (Mills & Borg, 1999). Today, illuminance uniformity is still included in the European standards for indoor lighting (EN12464-1:2011), outlined by the average two-dimensional illuminance on a

¹ Other than *radiometry*, that describes the whole range of the electromagnetic spectrum, *photometry* considers light in the visible spectrum, in relation to the human visual response. For example, a photometric equivalent of Radiance is Illuminance, measured in Lux.

horizontal plane set to maintain a certain level of comfort.

The way we looked at artificial lighting, influenced the daylighting approach as well. Artificial lighting allowed us to work 24/7, significantly impacting the design of buildings considering daylight. For example, a decrease in the window-wall ratio and an increase in floor depth (Banham, 1984). Likewise, photometric daylight data applied to Building Codes like NEN12464-1, set minimal requirements for a.o. the static *Daylight Factor* and minimum daylight surfaces in the facade of 2,5 - 10% of the floorplan of a room. Also visual comfort gained increased attention, controlled by glare-related contrast ratio (cd/m²) between the lowest and the mean illuminance in an area (Bouwbesluit, 2017). However, these luminance-based metrics are still up to the designer to decide how to deal with it, based on a few generic descriptions of tasks (Mills & Borg, 1999).

Since it emerged in 1900, the development of the lighting practice, and the discussion surrounding light has seen great development. Last decade, literature review shows many theories about lighting being more than a mean that allows us to see: it has to influence our mood as well (Cuttle, 2008). In this line of thought, Boyce defined 'good lighting' as light that "allows you to see what you need to see quickly and easily and does not cause visual discomfort, but does raise the human spirit." (Boyce, 2013, p2)

The desire of 'good lighting' is mainly advocated by Cuttle, who stated that we are "firmly stuck" in the concept of work plane illuminance which "dominates not only our standards, but more damagingly, our thinking" (Cuttle, 2010, p.82). Cuttle criticizes the lighting standards because they claim to be performance based, while Cuttle says that they "cannot be justified on the basis of visual performance" (Cuttle, 2010, p.76). Hence, he overlooked the development of the lighting profession to analyse the themes that determined the objectives of the lighting practice. This resulted in the notation of three stages within the development of the lighting practice: a (1) first stage that illuminates work planes uniformly, (2) a stage of lighting adapted to human needs and tasks based on visual performance and, (3) a stage of more perception based lighting. Today, we should swiftly move towards this third stage focussing on lighting a space (Cuttle, 2010).

Cuttle is not alone in his statement about the search for an improved description of qualitative lighting design. It is true that Richard Kelly already reflected on the quality of light in the early 1950s, which relates to the third stage of Cuttle. Kelly was one of the first to describe lighting in terms of quality, differentiating three basic functions of light, namely 'focal glow', 'ambient luminescence' and 'play of brilliance', to: "(1) make it easier to see (2) make surroundings safe and reassuring and (3) stimulate the spirit" (Kelly, 1952, p.26). In his description, Kelly refers to the use of visual perception to collect most of our knowledge about our surroundings. He already suggested what Ganslandt&Hofmann (1992, p.77) mentioned regarding the three-dimensional quality of space, that "the shaping of our environment through light and shade is of prime importance for our perception of spatial forms and surface structures." Because, "if this information is missing [...] we feel the environment to be unnatural and even threatening". (Ganslandt & Hofmann, 1992, p.117). This suggests a new opportunity of research, one to explore light as at three-dimensional concept. Because "the conventional light measuring techniques fail to describe the quality of illumination in its form-revealing sense" (Mury, 2009, p.4). Therefore, a better understanding of the light field in a three-dimensional space seems to be required.

It is only in 2015 that theoretical developments could not be denied by those who put theory into practice. One of such improvements is the WELL Building Standard that aims for human health and wellness. The standard includes performance metrics among which they intent to promote the quality of (day)light (WELL, 2016). It's an early example of light being more than just horizontal lux (Boyce, 2013). As Mardaljevic stated: "If the standards are proving to be insufficient to ensure good daylighting design, then we should look to improving them rather than ignoring or ditching them altogether." (Cuttle & Mardaljevic, 2012, p.16).

Given this situation, a tension appears between the growing awareness of 'good lighting' in combination with the little attention in practice regarding photometric data. As Cuttle mentions, the third proposed stage of good lighting requires knowledge about our surroundings. A visual comfortable apperance of a scene is possible, and largely influenced, by light. Increasingly, the emphasis is on the light distribution in a space. This research investigates to what extent the three-dimensional light distribution can be used to collect knowledge creating 'good lighting'.

1.2 THE PROBLEM DEFINITION

Regarding the development in the lighting profession, the first stage comprises uniform illuminance on a horizontal plane, the objective of the second stage is based on visual performances preventing visual discomfort, and the objective of the third stage is to reveal the potential of the three-dimensional light distribution (Cuttle, 2010). It is suggested that the second stage has fall short with regard to visual comfort, so that the lighting standards are not performance-based at all. The notion that light is more than illuminance in the horizontal plane increases. Gradually, research lay emphasis on the three-dimensional light distribution in a space. This is in line with the proposed move to a third stage in the lighting profession that includes 'good lighting' (Boyce, 2013)(Cuttle, 2010).

Against this background, the central question that motivates this research is:

To what extent is the analysis of the light field an effective alternative to predict visual comfort in a daylit office meeting space?

The aim of the research is twofold: (i) to apply the analysis techniques regarding three-dimensional light distribution (i.e., light field) for daylight analysis in offices rooms, and (ii) to predict visual discomfort by analysing (changes in) the light field. The findings are meant to provide parameters for the design of comfortable (office) spaces and to make designers aware that light is more than lux in the horizontal plane.

To answer the posed research question, 5 subquestions were derived:

1: *How is visual comfort currently determined?*

The first sub-question forms a base for this research, analyzing the current performance-based metrics that determine the visual uncomfortable aspects of daylight, and the increasing demand for better metrics. The theoretical findings enable us to give a comprehensive answer to the the question how visual comfort is determined.

2: *How can the analysis of the light field contribute to improved light qualities?*

The second sub-question analyses the literature available regarding the light field and how the analysis of the light field does add to the existing daylighting metrics. This research primarily focusses on the 'visible' properties of the light field (i.e. the lower order properties): the light intensity, the light direction and the light diffuseness. A better

understanding of these terms from a physical and visual perspective facilitates the measurements and simulation afterwards.

3: *How can (variations in) the light field in a daylit scene be measured with a cubic illuminance meter?*

The third sub-question examines the use of a self-built cubic illuminance meter as an instrument to measure the light field. A MDF-cube with 6 KONICA MINOLTA luminance meters attached, functions as a base for the cubic illuminance meter. Results will be processed by using the KONICA MINOLTA Excel Add-in.

4: *How can the light field be visualized?*

The fourth sub-question aims for researching the tools to use for visualizing the light field. This is two-fold: First, this research seeks for a relation between the measured light field and object's appearances. In a measurement, the interaction of the light field with the white matt objects is captured with a luminance camera with a normal lens. LMK LABSOFT software processes these images into false colour luminance images. Second, the light field is visualized by using a web application of Kartashova.

5: *What is the difference between the analysis of the light field and the analysis of the Luminance Contrast Ratio on the measured level of visual comfort?*

The fifth sub-question analyses the effect of variations in the light field on visual discomfort in terms of glare in a case study. The aim is to examine the differences between the light field analysis and often used visual comfort metric; the luminance Contrast Ratio.

For the case study, an office meeting room at the faculty of Civil Engineering is selected as a reference model. The room is known as visual uncomfortable when an observers faces the window. Variations in the light field are obtained in a simulation model in twofold: by (i) including the dynamic aspects of daylight regarding the different sky types during study, and (ii) by alternating the materials' (i.e. reflectivity) appearances.

An in-field measurement functions as a base model for further simulations of which adjusted models are analysed. This is aligned with the following sub-question.

6: *How can scene adjustments influence the level of comfort in a room?*

The sixth sub-question analyses the effect of adjustments in the reference room, as part of the case study. This question aims for a practical application regarding the light field to improve the visual comfort level in office meeting space Ct2.72.

1.3 LIMITATIONS

This research is part of the master program Building Engineering, at the faculty of Civil Engineering of Delft University of Technology. The case study measurements took place at this faculty. The research has to deal with limited rooms and measurement tools have been accessible. Since the master thesis has a delimited time span, limited time is available.

The measurements were conducted in Delft, The Netherlands. Not only the environmental conditions of the time and place effect the results, the layout and the material reflectivity of the scene have influence too: the window-glass, the interior surfaces and objects and surrounding buildings that influence the incident daylight.

Concentrating on the objects only, the appearance of the shapes, perceived by humans, is influenced by the geometry of the shape, the roughness and colour of the material. This research solely focusses on their shape as a parameter, using white objects only. To decrease the effect of surface reflectance, the objects are positioned on black absorbing paper.

1.4 METHODOLOGY & OUTLINE

The structure of this thesis comprises three parts: A literature review (part I), and two empirical parts (part II, part III)(figure 1.1).

Part I introduces the field of topic in a literature review.

Chapter 2 explores the current daylighting practice, that results in a need to explore light in a three-dimensional way. This is linked to the third stage proposed by Cuttle (2008). Furthermore, the performance-based visual comfort metrics is examined, related to the second stage of the lighting profession (Cuttle, 2008). The knowledge of this chapter leads to a literature review about the light field.

Chapter 3 explores light as a three-dimensional entity, known by the 'light field'. A theoretical framework explores the various studies and concepts that have been proposed. The physical aspect and the visual concepts are both elaborated on.

The conclusion in *chapter 4* concludes on the literature findings and formulate various learning points that are used in subsequent research (Part II).

Part II comprises an empirical part.

Chapter 5 and 6 research the use of the tools to measure the light field. And so, the use of the cubic illuminance meter is introduced. Its application is proven in previous research (chapter 3). In this part the self-built cubic illuminance meter was tested in a verification trial. The appearances of several objects that interact with the light field are used as a verification tool.

In *chapter 7 and 8* we discuss the results and conclude on how to measure the light field and how the light field can be visualized.

Part III presents an empirical analysis through a case study.

Chapter 9 and 10 combines research of the light field with metrics for the level of visual comfort. An in-field measurement is conducted in a visual uncomfortable experienced office room at the faculty of Civil Engineering. A digital model of the room is set-up to function as a measurement tool for further simulations. The effect of variations in the light field on visual comfort is analysed, and to what extent scene adjustments influence the level of visual comfort.

Chapter 11 and 12 discuss and conclude on the results of Part III.

Lastly, the main research questions, that covers the entire research, will be answered in *chapter 13*. The recommendations advice on developments that are needed.

METHODOLOGY AND OUTLINE

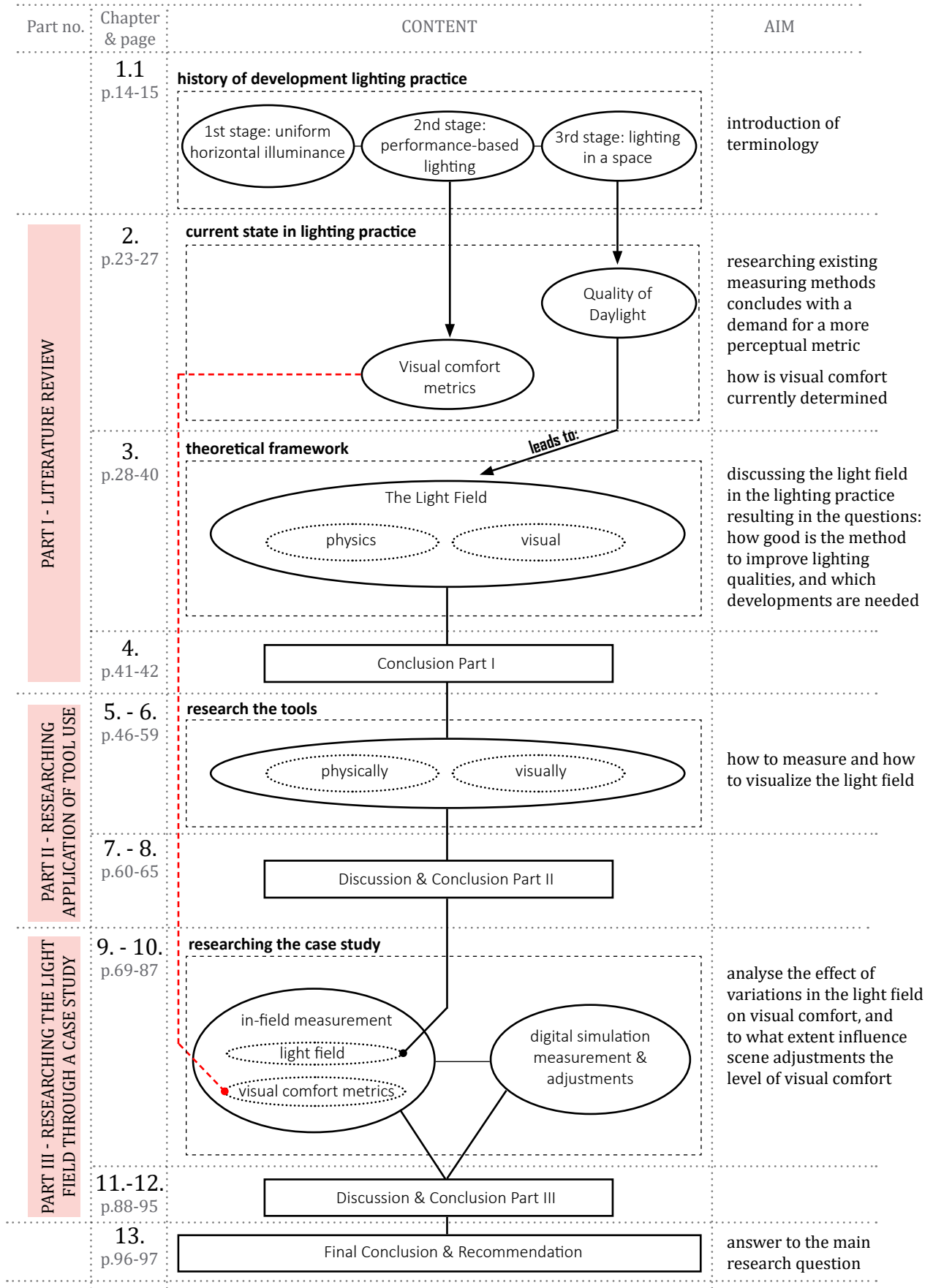


Figure 1.1 A schematic overview of the research outline.

PART I
LITERATURE REVIEW

2

VISUAL COMFORT AND QUALITY OF DAYLIGHT

This chapter examines the demand for qualitative daylighting, and introduces the existing metrics related to visual comfort. But first, in paragraph 2.1 the definition of daylight and daylighting is given. Paragraph 2.2 introduces the desire to elaborate on a better use of daylight for the architectural practice, specifically regarding the 'third stage of lighting' (Cuttle, 2008). Paragraph 2.3 describes how visual comfort is defined today.

2.1 A DEFINITION OF DAYLIGHTING

This paragraph defines the term daylight, and subsequently its derived term daylighting.

As the psalm (113.3) tells us: *from the rising of the sun, to its setting*, natural light surrounds us. Daylight is defined by a combination of both direct and indirect sunlight during the day. The intensity and the quality of daylight depend on the extent to which sunlight is diffuse or direct.

The derived architectural and technical term, daylighting, can be interpreted as “the controlled use of natural light in and around buildings” (Reinhart, 2014, p.9). Natural light is assessed differently, from the perspective of visual comfort, energy and/or its availability. In this research we evaluate visual comfort. Because visual comfort improves the spatial quality and 'raises the human spirit' (Boyce, 2013).

A desired lighting effect is created by reflection, scattering and/or blocking of the daylight. Such lighting effects are applied for centuries, with the Pantheon (AD128) in Rome as an early example.

That daylighting is as old as architecture itself, does not imply that it is an easy light source to work with. Natural light is hard to forecast due to its dynamic character, resulting in design difficulties. If these challenges are not dealt with in a good way, the presence of daylight could lead to visual uncomfortable situations like high brightness i.e. glare, and high contrasts by disturbing shadow patterns. If the design makes use of these dynamics, a comfortable building will be the result.

The tradition of lighting is based on engineering. This is reflected in the existing lighting standards which mostly require quantitative measures of two-dimensional work plane

illumination. This is a technical perspective that ignores the perception of the user. This is in contrast with the 'humane' approach of the visual effects in architecture, like enhancing well-being (Skarlatou, 2010)(Boyce, 2013). For example, architect Pallasmaa states that "the unconscious tactile ingredient in vision is particularly important and strongly present in historical architecture, but badly neglected in the architecture of our time", (Pallasmaa J., 2012, p.29).

Although light is important to the experience of architecture, most architects do not extent their findings more than just the presence or absence of daylight (Fontenelle, 2008). The reason for this could be the broad and vague phenomenon of light effects: The technical description misses out on information, and does not give enough data to provide a complete image of an architectural scene. "While we know that perceptual impacts of daylight such as contrast and temporal variability are important factors, we are left with an imbalanced set of performance indicators" (Rockcastle and Andersen, 2014). It underlines the need to explore the perceptual aspects of space and form-giving characteristics of daylight even more (Chamilothori, Wienold en Andersen, 2016) (Rockcastle and Andersen, 2013).

2.2 THE THIRD STAGE OF DAYLIGHTING

Recently, theoretical developments seem to proof the increasing accordance on the desire to elaborate on daylighting for the architectural practice (Skarlatou, 2010) (Madsen, 2010). Especially in regard of making a step towards the third stage of the lighting profession, (Cuttle, 2010), daylighting could contribute to a visual pleasant environment (Boyce, 2013)(Steane and Steemers, 2004).

Some studies focus on a completely new approach for the assessment of daylight (Madsen, 2010), others (Galasiu and Veitch, 2006) aim for an expansion of the range of luminous conditions beyond the simple horizontal illuminance. "According to human perception researchers, the lighting of vertical surfaces is more important than the lighting of the work plane, especially in working spaces" (Galatioto and Beccali, 2016, p.853).

In an attempt to assess daylight in architecture differently, Madsen (2010) considered daylight in space as a combination of Light Zones. Therefore she developed a graphical concept and tool in architecture to examine the form-giving and spatial characteristics of daylight (figure 2.2). However, the variables important to the space and form-giving characteristics: intensity, direction, distribution and colour of daylight, did not give any insight in lighting quality as such (Madsen, 2010). Furthermore, Chamilothori tried to join the architectural notion of light with a practice-driven level. She made a request for "traditionally non-quantifiable aspects of daylight in space, such as its ambience, with quantifiable metrics". (Chamilothori, Wienold and Andersen, 2016, p.5). They conducted an experimental study, in which 30 subjects used VR glasses. Results showed a preference for irregularity in façade and daylight features with the exception of daylight dynamics (see figure 2.1). In addition, research of Rockcastle *et al.* (2014, 2015) compared existing visual comfort metrics with perceptual qualities, i.e., contrast and temporal variation, which they derived from ten case studies with varies daylight compositions. The conducted simulations presented the ability to assess dynamic contrast-based effects, next to the existing glare-based discomfort.

It is clear that the focus of research lay on how to define vidual comfort differently. However, visual comfort has no distinct definition. In fact, there may be ambiguity about the interpretation of visual discomfort. This is partly ascribed to the lack of agreement about the difference between comfort and visual comfort (Jakubiec, 2014). For example, a fairly

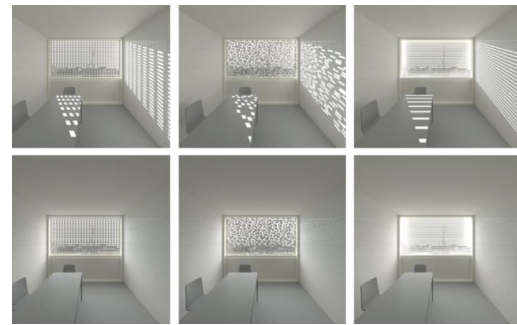
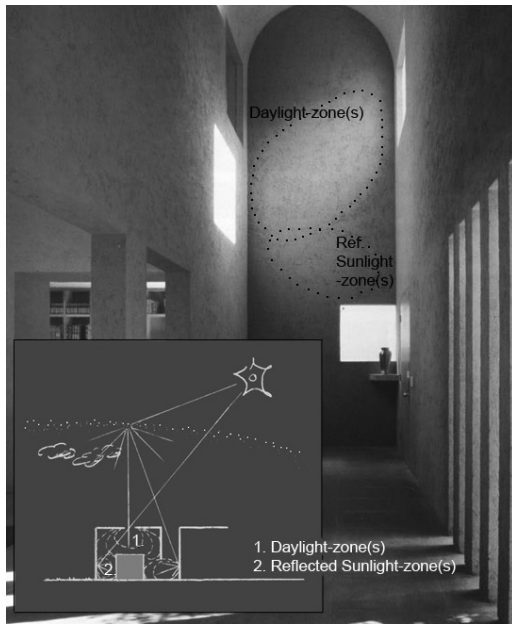


Figure 2.1 (top) Rendered images for an experimental study with VR headset regarding the perceptual impression of a space. On the vertical axis the sky type, and on the horizontal axis the facade variations (Chamilothori, *et al.*, 2016)

Figure 2.2 (left) The Legorreta Arquitectos (Mexico), in which Madsen considers a space's daylight as bubbles of light that meet the space itself. In this way daylight is considered as a composition of light zones (Madsen, 2010).

stable concept like atmosphere or liveliness can be linked to more than (day)lighting alone (Vogels, 2008). A widely used perspective is that "comfort is not discomfort" (Iacomussi *et al.*, 2015, p.729). In the next paragraph we introduce two existing metrics regarding visual comfort.

2.3 VISUAL COMFORT METRIC

Many metrics try to predict the likelihood of experiencing comfortable visual daylit scenes. Discomfort due to daylight has many parameters, like direct sunlight, monitor contrast or discomfort glare. It is usually not distinct which method to use, other than "keep direct sunlight away from vertical task planes" (Jakubiec 2014, p.41).

Most metrics that analyse visual comfort performances, evaluate discomfort glare (Carlucci, 2015). Discomfort glare can be described by the condition that causes visual discomfort due to unacceptable luminance distribution or by high contrasts in the visual field, higher than to the adaption level of the eyes (Bellia, *et al.* 2008). The phenomenon is difficult to quantify. Despite the known disadvantages related to glare there is no standard set in the NEN 12464-1 for daylight, except for guidance like matt wallcovering and light ceilings.

Most metrics are defined in terms of illuminance. Illuminance is defined as the total amount of luminous flux incident on a surface quantified in Lux and solely relates to the aspect of light (appendix A) (Reinhart, 2014). And so, illuminance-based metrics ignores the link between light and the objects being lighted in a space. Conversely, luminance, which describes the amount of light reflected or emitted from a surface, concerns light and the object. Hence, luminance-based analysis forms the base of the image we perceive. However, it misses out on information about the environment (Jakubiec, 2014). Specifically, as Ganslandt and Hofman (1992) state "luminance and luminance distribution do not provide an adequate basis for the planning of visual impressions" (p.76).

In many studies for visual discomfort (Bellia, 2008) (Jakubiec, 2014) (Yacine, *et al.* 2017), multiple metrics are compared with each other, of which most of them focus on vertical

illuminance, while being view dependent. However, as Jakubiec (2014) found in a survey study, visual discomfort is often caused by various sources independently. So, to predict visual discomfort, all the different effects must be avoided. Hence, a successful metric differs in every situation.

An often-used luminance-based approach, to plan a comfortable visual scene, is to avoid high luminance ratios in the field of view. High brightness is perceived when high luminance ratios are measured, resulting in visual discomfort. The field of view of an observer can be subdivided into a central zone, i.e. the ergorama (30°), and an adjacent zone, i.e. the panorama (60°) (figure 2.3). According to law of Dutch working conditions (Arboret) a ratio in the ergorama of 1:10 is acceptable, and 1:3 fairly good. They recommend that a ratio in the panorama should not exceed 1:30.

To measure luminance ratios, the following procedure can be executed: A luminance camera equipped with a fish eye lens photographs a series of under-, normal, and overexposed images. Then, these images are combined in a High Dynamic Range (HDR) image that can be processed into a false-color luminance map (in cd/m²)(figure 2.4). From these false-color images, the luminance ratio in the ergorama and the panorama are calculated as follows:

$$\text{Luminance Contrast Ratio Ergorama} = \frac{\text{average luminance (cd/m}^2\text{)}}{\text{maximum luminance (cd/m}^2\text{)}} \quad (1)$$

$$\text{Luminance Contrast Ratio Panorama} = \frac{\text{average luminance (cd/m}^2\text{)}}{\text{maximum luminance (cd/m}^2\text{)}} \quad (2)$$

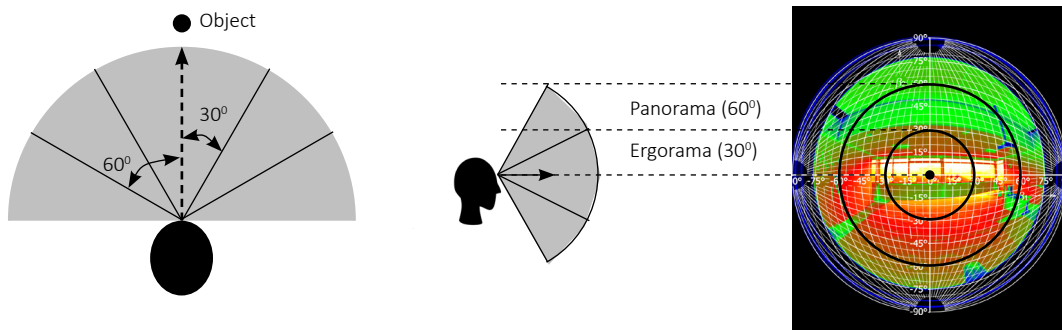


Figure 2.3 The field of view consisting of the ergorama (30°) and the panorama (60°) that is captured within a fisheye image.



Figure 2.4 An under-, normal- and overexposed fish eye image, resulting in a luminance false-color map.

Although the Luminance Contrast Ratio (LCR) is commonly used in daylight analysis, it is discussed that this metric lacks a perception-based approach and that further research is required to improve the ratios (Jakubiec, 2014). This could be ascribed to the definition, which is just one of many.

Lately, renewed interest in visual comfort resulted in the Daylight Glare Probability (DGP) (Wienold, 2009). An often used simplified version of the metric ($DGPs|_{Wienold}$) reduces computation time and just relates the vertical illuminance (E_v) at eye's level to the chance of glare. $DGPs|_{Wienold}$ considers high brightness and contrasts and ranges from 0-1, presenting multiple comfort levels (table 2.1). For example, a $DGPs|_{Wienold}$ of 0,35 estimates that 35% of occupants would experience visual discomfort in such situation. The formula is indicated with:

$$DGPs|_{Wienold} = 6,22 \cdot 10^{-5} \cdot E_v + 0,184 \quad (3)$$

Table 2.1 The relation between the level of DGP and subjective glare ratings.

	imperceptible	perceptible	disturbing	intolerable
DGP	< 0,35	0,35- 0,40	0,40- 0,45	> 0,45

However, despite the fact that the simplified DGP is very similar to the actual DGP, it is suggested that it "cannot be used for absolute glare factor conditions that include a direct view of glare sources in the field of view of the observer" (Carlucci, 2015, p.25).

Still, the metric forms a base for further research. For example, Torres and Lo Verso (2015) examined the relation between DGP and cylindrical illuminances, the latter determined as "the average of all vertical illuminances in all directions around the considered point" (p.700). In a simulation study with Radiance, they proposed a new metric based upon the cylindrical illuminance, resulting in a view independent metric. With "the advantage of retaining the vertical component of illuminance, while being view independent" (p.700), it shows the interest to examine visual comfort regarding, light, the object and how it is perceived.

3

THE LIGHT FIELD

Before doing practical research, we first need to understand the meaning of the term Light Field. Therefore, this chapter gives a theoretical background from two perspectives: (i) the physical light field, and (ii) the visual light field. First, paragraph 3.1, introduces the light field physically. It comprises a detailed description about the basic properties of the light field and how we can measure these. Secondly, paragraph 3.2, describes the light field as a visual entity, reviewing the attempts made to formulate a quantitative description of it.

3.1 PHYSICS OF THE LIGHT FIELD

Within some lighting studies, one tries to get grip on the technical measures that define the spatial characteristics in a room (Gershun, 1939) (Mury, 2009)(Cuttle, 2008). For this purpose we'll make use of their concept: the light field. First, paragraph 3.1.1 contains an introduction to the light density and light vector. Then, paragraph 3.1.2 elaborates on a third property of the light field: the light diffuseness. Then, a description is given of how these properties of the light field can be measured.

3.1.1 INTRODUCTION TO THE LIGHT FIELD: LIGHT DENSITY AND LIGHT VECTOR

In an attempt to make illuminating engineers aware of new methods of photometric and radiometric calculations, Gershun (1939) was one of the scientists who considered light as a field, "much like the magnetic field" (Mury, 2009, p.3) He stated that the traditional photometry was a case of "arrested development" and proposed a systematic physical theory regarding the visual appearance of a space: *the light field*. Several studies (Mury, 2009)(Adelson and Bergen, 1991) (Kartashova, *et al.* 2016) (Xia, *et al.*, 2014; 2016; 2017) have looked at this topic. This paragraph examines the mathematical description of it.

The principle of the light field is introduced by Gershun, who was one of the first to define a 'Light Vector' and a quantity named the 'Space Illumination'. In a mathematical approach Gershun described the radiance as a function of location and direction. He expressed it in a 5-dimensional numerical function to term the light, the radiance, traveling in every direction (polar angle θ , and azimuth angle φ) through any point in space (x,y,z). (Gershun, 1939).

In addition, Mury (2009) took the work of Gershun that had “not been extended essentially since”. (p.2). Mury conducted research into the global structure of the light field beyond Gershun’s three-dimensional description. Instead, he suggested the Fourier description as convenient, and clarified the complex light field in terms of spherical harmonics. So, “when the spherical harmonics decomposition is applied, the radiance distribution function at a point can be represented as a sum of its frequency components” (Mury, 2009, p12). Clearly, the light field is complex, but it can be approximated with a few terms only.

In a physical context, the spherical harmonic development is expressed in a ‘multipole’ expansion, which is a mathematical series that describe a function that depends on the two the angles of a sphere. Figure 3.1 presents two of its terms: the 0th order (its initial term), and the 1st order. The zeroth order (monopole), is a scalar and describes the average radiance from all directions, independent of angle, i.e. ambient light, or light density. The first order (dipole) represents the positive and negative mode around a sphere, and transforms as a light vector (not equal to light rays). For example, the dipole contribution is high in a situation with an overcast sky, and when the monopole dominates the overcast sky adds on a snow cover. (Mury, 2009) It should be noted that the multipole expansion consists of a 2nd and higher orders too. Muryy et al. indicated the strong relation between the lower order components, including the 2nd order, and the geometrical layouts. The lower order properties seemed quite constant over a scene, whereas high order components appeared not to (Mury, Pont en Koenderink, 2007).

However, research of Xia *et al.* suggested only the 0th and 1st order as the lower order properties, namely the light density and the light direction. In turn she added ‘light diffuseness’ as a basic property of the light field (Xia, *et al.* 2016-II). In paragraph 3.2 the light diffuseness will be elaborated on.

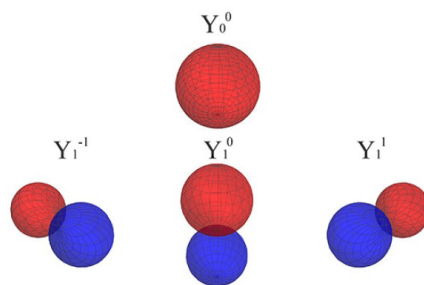


Figure 3.1 A plot of spherical harmonic basic functions. Y_0^0 represents the 0th order (monopole) that describes the average radiance from all directions. The second row, containing Y_1^{-1}, Y_1^0, Y_1^1 shows the 1th order (dipole) that represents the light vector (Xia, 2016).

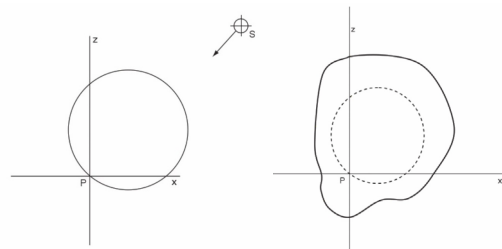


Figure 3.2 (left) The ideal spatial illumination defined by a cosinus distribution due to the light source S, and (right) the illumination solid in a real space (Cuttle, 2008).

Besides the expanded mathematical analysis of the light field (Gershun, 1939) (Mury, 2009), Cuttle (1971, 2008) examined the three-dimensional illuminance distribution by using a more practical, visual-based method (Simons and Bean, 2001). He defined Gershun's *Light Vector* as the *Illumination vector* and the *Space Illumination* as *Scalar illuminance*, in which the latter describes the average illuminance in a point, or over a surface of a sphere.

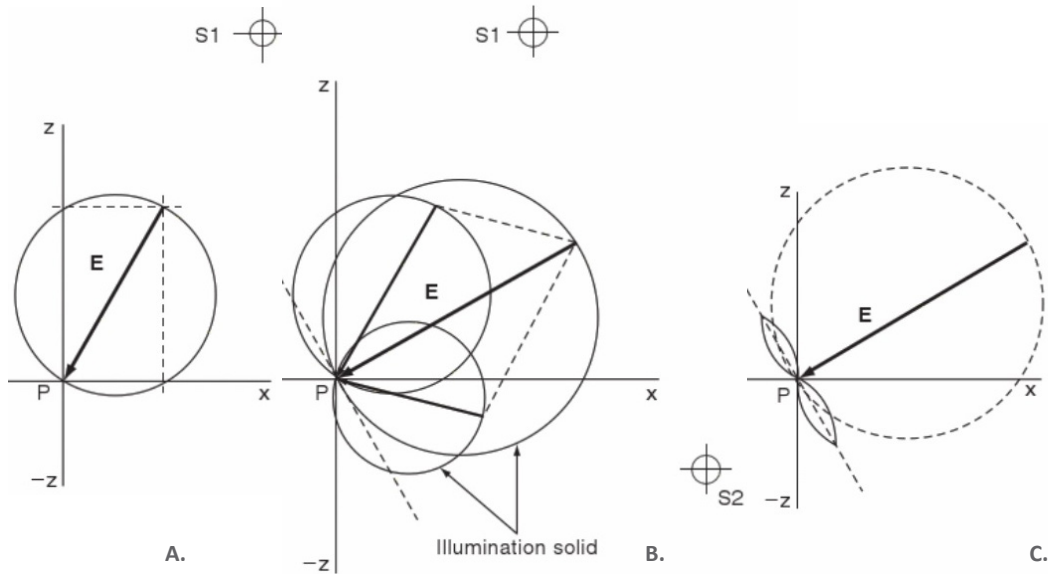


Figure 3.3 (a) The vector distribution caused by light source S1 defines the illumination solid. (b) When a second light source (S2) is added, the two source vector distributions define the illumination solid. (c) The illumination solid includes two components: (i) A asymmetric vector component (dashed) that is subtracted from the illumination solid resulting in (ii) a remaining symmetric solid (Cuttle, 2008).

Cuttle characterized the three-dimensional illuminance distribution by vector-algebra, based upon an imaginary 'illumination solid' that represents "how the illumination at that point varies according to the direction of the measuring surface" (figure 3.2)(Cuttle, 1971, p.173). This illumination solid in a space forms a base for the average illuminance in a point and comprises two components: a *vector component* and a *symmetric component*. An illumination solid is defined by the vector distribution of a single source S1 (figure 3.3). When a second source S2 is added, this results in an illumination solid defined by the summation of two source vector distributions in which **E** becomes the resultant vector. Then, the (dashed) vector component is subtracted from the illumination solid and the (solid) symmetric component remains.

The vector components is described as follows,

$$\mathbf{E}_u = (E_{(+u)} - E_{(-u)}); \quad (4)$$

$$\mathbf{E}_v = (E_{(+v)} - E_{(-v)}); \quad (5)$$

$$\mathbf{E}_w = (E_{(+w)} - E_{(-w)}); \quad (6)$$

Resulting in the magnitude of the illumination vector:

$$|\mathbf{E}| = \sqrt{(\mathbf{E}_u^2 + \mathbf{E}_v^2 + \mathbf{E}_w^2)} \quad (7)$$

The *vector component* is a scalar, thus independent of the axes.

The *symmetric component* has a magnitude which is in any direction equal to the magnitude in the opposite direction.

$$\sim E_u = ((E_{(+u)} + E_{(-u)}) - |E_u|) / 2 \quad (8)$$

$$\sim E_v = ((E_{(+v)} + E_{(-v)}) - |E_v|) / 2 \quad (9)$$

$$\sim E_w = ((E_{(+w)} + E_{(-w)}) - |E_w|) / 2 \quad (10)$$

The total *symmetric illuminance* can be written as,

$$\sim E = (\sim E_u + \sim E_v + \sim E_w) / 3 \quad (11)$$

The *vector component* and the *symmetric component* form a base to calculate the average value of the illumination solid, i.e. the *Scalar Illuminance*:

$$E_{sr} = 0,25 * |E| + \sim E \quad (12)$$

In addition, the *vector components* form a base to calculate the average *light direction*, in terms of the altitude (angle α) and the azimuth (angle φ)(figure 3.4):

$$\alpha = \arctan[E_z / (E_x^2 + E_y^2)^{0,5}] \quad (13)$$

$$\varphi = 180 - \arctan(E_x / E_y) \quad (14)$$

The presented altitude and azimuth are obtained by measurements in the familiar (x, y, z)-plane. When the axes of the cube are indicated in a different (u,v,w)-plane a transformation is needed. Cuttle used the following formula to compute the vector direction in $e_{(x,y,z)}$;

$$e_{(x)} = 0,707e_{(v)} - 0,707e_{(w)} \quad (15)$$

$$e_{(y)} = 0,816e_{(u)} - 0,408e_{(v)} - 0,408e_{(w)} \quad (16)$$

$$e_{(z)} = 0,577e_{(u)} + 0,577e_{(v)} + 0,577e_{(w)} \quad (17)$$

With:

$$e_{(u)} = E_{(u)} / |E| \quad (18)$$

$$e_{(v)} = E_{(v)} / |E| \quad (19)$$

$$e_{(w)} = E_{(w)} / |E| \quad (20)$$

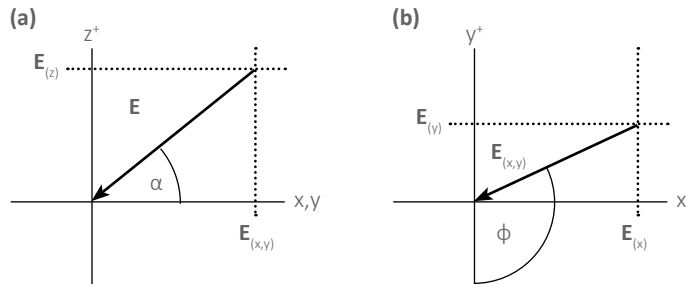


Figure 3.4 (a): Vertical section of the altitude angle (α) of the illumination vector, and (b): Horizontal section of the azimuth angle (ϕ). (Cuttle, 2008)

The transformation in formula 11-13 can be attained when the (x, y, z)-axis are rotated by an angle of 35° by “which the u, v, and w axes are tilted relative to the horizontal plane, [...] the axis is assumed to lie in the same vertical plane as the y axis” (Cuttle, 2008, p.33).

Following this procedure², the u-, v-, w- unit vectors depend on the x-, y-, z- unit vectors in the following matter,

$$\begin{pmatrix} e_{(u)} \\ e_{(v)} \\ e_{(w)} \end{pmatrix} = \begin{pmatrix} 0 & \cos(35,3^\circ) & \sin(35,3^\circ) \\ \cos(35,3^\circ)\sin(120^\circ) & \cos(35,3^\circ)\cos(120^\circ) & \sin(35,3^\circ) \\ \cos(35,3^\circ)\sin(240^\circ) & \cos(35,3^\circ)\cos(120^\circ) & \sin(35,3^\circ) \end{pmatrix} \begin{pmatrix} e_{(x)} \\ e_{(y)} \\ e_{(z)} \end{pmatrix} = \quad (21)$$

$$\begin{pmatrix} 0 & 0,816 & 0,577 \\ 0,707 & -0,408 & 0,577 \\ 0,707 & -0,408 & 0,577 \end{pmatrix} \begin{pmatrix} e_{(u)} \\ e_{(v)} \\ e_{(w)} \end{pmatrix}$$

With this description of the scalar illuminance as the average illumination in a point, and the light vector in terms of altitude and azimuth, Cuttle provided a clear tool for the three-dimensional analysis of light.

3.1.2 INTRODUCTION TO THE LIGHT FIELD: DIFFUSENESS

After a description of the average *light intensity* and the *light vector* in a point, this subparagraph introduces the mathematical concept of *light diffuseness*.

Several studies (Kelly, 1952) (Cuttle, 2008) (Xia, *et al.*, 2016-II) have looked at light diffuseness even though they did not have any consensus about a proper definition. Some related it to “an open white sandy beach on an overall cloudy day” (Kelly, 1952, p.29), others termed it as the ‘flow of light’(explained in paragraph 3.2)(Cuttle, 2008). Xia defined diffuseness as:

“... the isotropy of a light distribution around a point in a space. It ranges from fully collimated light via hemispherical diffuseness to completely diffuse light. Fully collimated light comes from a single direction; in contrast, completely diffuse light comes from a sphere of directions. Light diffuseness can highly influence the appearance of scenes and objects in it” (Xia, 2016, p.100).

It was Xia *et al.* who noted that both Gershun and Mury lacked a description of diffuseness as a basic property of the light field. While beyond the light density and the light direction, the light diffuseness appears to have large influence on the characteristics of a space too (Koenderink, *et al.* 2007). Thus, Xia reviewed four previous described 'modelling indices' which were strongly related with the light diffuseness and thus considered the same (Xia, *et al.*, 2016-II). In addition, she introduced a new metric, D_{xi} , which was ‘conceptually equivalent’ to the reviewed diffuseness metric of Cuttle (D_{cuttle}). Inspired by the work of Mury, Xia considered the ratio of D_{cuttle} “similar to the ratio between the strength of

² “to set up the tripod with the y axis (‘eye’ axis) aligned with the long axis of the space so that when the photocell is facing in the y+ direction the horizontal scale reads 00, and then ‘x is a-cross’ with x+ to the right. [...] The measurement procedure is then straightforward. Set the photocell tilt to +350 [...], and read E(u+) at 00, E(v+) at 1200, and E(w+) at 2400. Reset the photocell tilt to -350, and read E(u-) at 1800, E(v-) at 300, and E(w-) at 600.” (Cuttle, 2014, p.33) It should be noted that in the actual procedure Cuttle uses a rotation of 35,30 , since the faces of the tilted cube should all have the same distance to the z-axis.

the first order (i.e., the light vector) and the zeroth order (i.e., the light density) of the SH representation of the light field”, in which “the diffuseness metric DX_i is entirely based on a mathematical description of the physical light distribution” (Xia, *et al.*, 2016-II, p.101). Cuttle calculated ‘his’ diffuseness metric as follows:

$$\text{vector scalar ratio} = |E| / E_{sr} \quad (22)$$

The normalised term of diffuseness as:

$$(D_{\text{cuttle}})_{\text{normalized}} = 1 - (|E_{\text{vector}}| / E_{\text{scalar}}) / 4 \quad (23)$$

“with ‘0’ corresponding to fully collimated light and ‘1’ corresponding to fully diffuse light” (Xia, *et al.*, 2016-II, p.108).

With the light intensity, the light direction and the light diffuseness described as the basic properties of the light field, the next paragraph elaborates on how to measure these.

3.1.2 TOOLS TO MEASURE THE LIGHT FIELD

The lower order properties of the light field (light intensity, light direction, diffuseness) are numerically defined to be measured in a real scene. Regarding the development of a tool to measure the light field, a number of instruments are considered. All developed instruments are based on the use of photodiodes, measuring lux. However, their size and amount of faces differ.

As one of the first, Mury developed a plenopter to measure up to the 2nd order of the spherical harmonical representation (figure 3.5)(appendix B). Spherical harmonics of the 2nd order contain nine free parameters (appendix B). To measure this, a dodecahedron-shaped device was used, containing 12 photodiodes. This “Plenopter” (plenus, complete, and optic), presented the simplest regular polyhedron with >9 faces. By using the plenopter at random points in a daylight scene, the light field could sufficiently be restored (Mury, 2009).

However, the influence on the spatial characteristics of a scene, of the 2nd order of the spherical harmonics representaion, seemed low. Therefore, Xia (2016) introduced a cubic device having 6 faces instead of 12 (figure 3.5). The instrument related to a the cubic tool of Cuttle which he used for his vector-algebra method (Xia, *et al.*, 2016-III).

As explained with formula 21, Cuttle rotated his cube +-45 degrees and +-35 degrees around the x- and y-axis. Xia *et al.* (2016-II) found that the diffuseness metric proposed by Cuttle (formula 22, 23) was affected by the orientation of the cube. Therefore, she analysed the effect of various orientations of the cubic illuminance meter relative to the light source (figure 3.6). After research she stated that for positioning the cube it should be prevented to orient the cube parallel to the light source (attitude 1,2), or to have faces similiry lighted (attitude 4).

Furthermore, Xia (2016) proved that the orientation negatively influences the scalar illuminance, resulting in a less accurate value. “One difficulty with cubic illumination meters is that they are sensitive to orientation in the presence of strongly directional lighting, with a maximum possible variance of 33 percent for the scalar illuminance.” (Xia, 2016, p.146). The magnitude and direction of illumination vector are well-measured.



Figure 3.5 Tools to measure the light field: (left) The custom-made plenopter of Mury with 12 photodiodes (Mury, 2009) (middle) A Cubic Illuminance meter using a single Lux Meter (Cuttle, 2009). (right) The cubic illuminance meter of Xia *et al.* (2016-III) with six photodiodes (right).

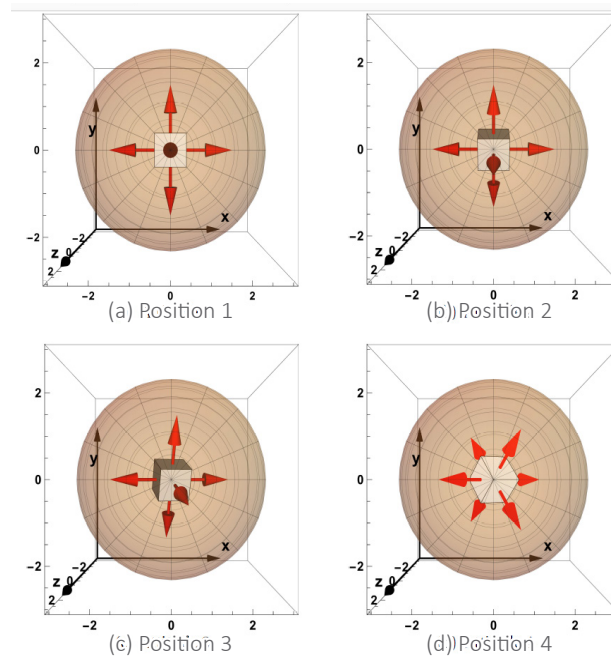


Figure 3.6 In research of Xia the effect of the orientation relative to the light source was investigated. Four attitudes were simulated with the light vector aligned with the z-axis: (a) Position 1: The cubic illuminance meter was positioned with four faces parallel to the z-axis, resulting in a symmetric orientation, (b) Position 2: the cubic illuminance meter was rotated for 20 degrees around the x-axis with some of the faces parallel to the light source, (c) Position 3: an additional 15 degrees rotation around the y-axis, and (d) Position 4: rotated 45 degrees around the x-axis and 35 degrees around the y-axis, resulting in similarly lightened faces (Xia, *et al.*, 2016-III).

3.2 MAKE THE LIGHT FIELD VISUAL

The previous paragraph elaborated on the light field from the physical perspective. However, it takes observation to understand (the variations) in illuminance distribution. In practice, painters (Gurney, 2010), designers and architects (Ganslandt and Hofmann, 1992) (Pallasmaa, 2012) use their artistic intuition to visualize the interaction of the light field with their surroundings. A space or an object in a scene is affected by the distribution of light. Unless there's an object that manifests the light field's appearance, human observers can't see a light field in itself. However, a scientific descriptions and similar visualization of a three-dimensional light field is rather needed, to make a useful tool for engineers, architects and designers.

This paragraph elaborates on the light field from visual perspective. First, we elaborate on the work of Frandsen and Cuttle who both were at the start of how lighting affects objects appearances. Secondly, building on the idea that probes can visualize the light field, applications and further research is reviewed.

3.2.1 THE VISUAL CHARACTERISTICS OF DIFFUSENESS - HISTORY

The spatial distribution of light and how it influences the appearance of objects has been repeatedly subject of practical studies (Frandsen, 1989) (Cuttle, 2008). Were the mathematical approach started to define the *light vector* and the *average (scalar) illuminance* in a point, studies into the visual appearances of the light field considered the relation between the two: namely the light diffuseness.

As one of the first, research carried out by Frandsen (1987, 1989) showed how the characteristics of light diffuseness can be described in a conceptual framework. Frandsen tried to frame the various types of shadows a person can determine by using a sphere under an increasing solid angle of light (0° to 180°)(figure 3.7). He considered not only the strict difference between soft and sharp shades, using a white probe in a dark space (no reflection), but inserted a ten-steps Scale of Light including 11 types of shadow.

In line with research of Frandsen, Cuttle (2008) worked with the shadow pattern on 3D spheres in a space as well. Although he didn't mention any of Frandsen's Scale of Light in his studies, Cuttle seemed to confirm the potential of a matt white sphere to reveal a shadow pattern. Therefore, he situated three objects in a room, each interacting differently with the light field (figure 3.8). The glossy black sphere displays a highlight pattern, the peg on a disc defines a sharp shadow and the white matt sphere reveals a shading pattern. However, the aspects of lighting that reveal the highlight and shadow patterns are different from those generating the shading patterns*. Cuttle (2008) defined these two aspects as (i) the *sharpness* of lighting, generating shadow and highlight patterns, and (ii) the *flow of light* causing of shading patterns.

Both studies form a base for further research. For example, Xia used work of Frandsen in her study to compare it to other diffuseness metrics. And so, she extended the scale towards a full range in computer renderings (Xia, *et al.*, 2016-II; 2016-III). Besides, Pont verified Cuttle's intuitive method showing that the appearances of objects are indeed affected by their shape, material properties and by the light field. Similarly, the appearance of each of the objects give cues about shape, material property and the light field too (Pont, *et al.* 2009)

³ "The terms shadow pattern and shading pattern tend to be confused, but their appearances are distinct, as are the means by which they are formed. The shadow pattern requires a shadow caster and a receiving surface, whereas the shading pattern is formed by the changing orientation of a convex three-dimensional surface" (Cuttle, 2008, p.81).

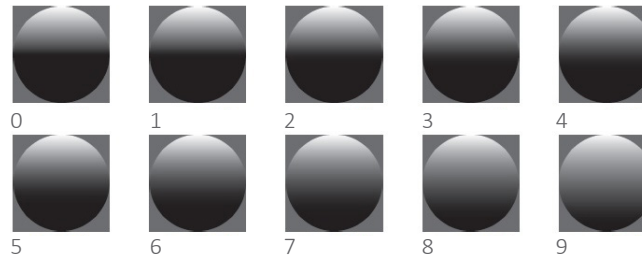


Figure 3.7A The Scale of Light (0-9) defined by Fandsen (1989) rendered by Xia *et al.* (2016-II)

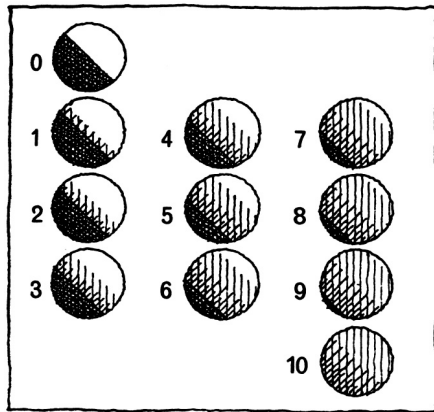


Figure 3.7B The Scale of Light defined by Fandsen (1989)

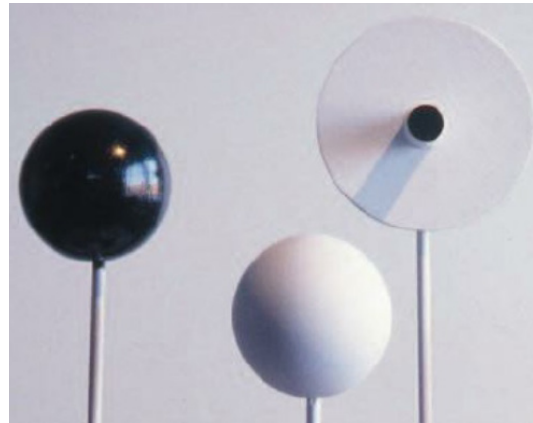


Figure 3.8 Three objects each interacting differently with the light field (Cuttle, 2008).

3.2.2 THE VISUAL LIGHT FIELD – ITS CONCEPT AND ANALYSIS

Beyond the research into the interaction of the light field with objects, Koenderink *et al.* (2007) was the first to speak about the ‘visual light field’ that doesn’t just comply to objects, so as well described as ‘visual space’. His study was able to demonstrate that human observers have expectations of how an object can look like. By using a ‘visual fit’, participants were able to match the appearance of a given surface to a stereoscopic scene by adjusting the (1) light intensity of the scene, (2) the direction of the light, and (3) the light diffuseness (Koenderink, *et al.* 2007). Subsequently, Schirillo confirmed in a review analysis that human observers can indeed infer⁴ the light field (Schirillo, 2013). This positive result about the reliability of the probe’s appearances interacting with the light field, is further developed. In this paragraph recent research on the topic will be examined.

In her PhD-thesis Xia (2016) proved that individuals are able to both separate and simultaneously adjust lighting qualities (direction, intensity and diffuseness). This added to the finding that individuals can distinguish the three basic properties of the light field. In contrast to the work of Koenderink *et al.* (2007), Xia worked with observers looking to a real scene, i.e. a disk in a viewing box (figure 3.9) in which the light on both the scene and the disk could be manipulated. Besides her finding about the possibility of observers to simultaneously adjust lighting qualities, she also found image ambiguities between intensity-diffuseness, intensity-direction and diffuseness-direction. Nevertheless they concluded that the three lower order light field properties have “distinguishable effects on the appearances of the objects” (Xia, 2014, p.21).

In the same line of thought, Madsen and Donn (2006) questioned themselves the same ambiguity in a case study they conducted with their students. In a virtual experiment using Radiance, named the light-flow meter [Cuttle] she examined renderings

of matte white spheres, see figure 3.10. In this visual evaluation of form-giving and spatial characteristics of the light scene she proved the tool to be successful in locating the area where daylight from different directions ‘meet’. However, diffuseness and direction variations appeared confounded and different view directions influenced the shading patterns (Madsen and Donn, 2006).

A considerable amount of studies has been published on the visual light field using a white matt probe as a gauge object. In the experiment of Xia *et al.* (2016-II; 2016-III) a rough sphere was added, resulting in the finding that observers are sensitive for texture or roughness on a sphere. This was constituted from an improved readability for the light direction and diffuseness. However, it didn’t improve the readability of the intensity changes (Xia, *et al.*, 2016-II). They also found similar results in a real setting in which the dodecahedron was suggested as best compared to shapes derived from a pentagon body. A study of De Bruin-Hordijk *et al.* (2008) reported this as well, noticing an improved readability of fine distinctions in lighting quality using a dodecahedron instead of a sphere. De Bruin – Hordijk *et al.* is also one of the few conducting research on the interaction of the light field in a practical daylight interior setting. She reported too that the number of visible faces of an object makes the accuracy of the light direction better. In line with Frandsen, they developed a false-colour scale (Scale of Shadow), set up in a laboratory setting (figure 3.11). Objects were photographed with a luminance camera in a real office room, and related to the images of the Scale of Shadow. Although the false-colour images improved the quantitative readability of the objects, as did Madsen and Donn (2006), they reported that “deeper in the room the differences with the steps of the shadow scale are more pronounced”, which can be a problem during other research (De Bruin-Hordijk, Hellinga and Pont 2008).

With respect to the previous studies, Kartashova *et al.* (2016) noticed that a gap appeared between the measures and comparisons of the structure of the physical and corresponding visual light fields. She wanted to confirm the conclusion of Mury *et al.* (2009) who reported that only a few points could sufficiently reconstruct the global structure of the physical light field. Therefore, Kartashova *et al.* (2016) conducted an experiment consisting of a visual measurement in which a furnished living room was photographed under three artificial-light conditions. Probes were positioned on a 36-positions- grid in a computer-generated render, see figure 3.12. Participants were expected to adjust the probe’s lighting (direction, intensity of directed and ambient light) to make it fit in the scene. They compared these results with measurements with the Cubic Illuminance meter [design by Xia *et al.* 2016]. It appeared that human observers’ have, partly due to due to subtle (inter)reflections “a robust impression of the light field that is simplified with respect to the physical light field” (Kartashova, *et al.* 2016). However, when humans are present in a space, their perception could be bypassed (Xia, *et al.*, 2016-III).

Images of a scene are 2D, a space lay-out is three-dimensional and the light field can be described as a five-dimensional function. Information is lost when 5 dimensions are projected on a 2D image (Pont, *et al.* 2009). The orders of a HDR image (over, normal and under exposed) are minimal in comparison with the real world containing about ten orders (Xia, 2016. p.67). Unlike previous studies focussing on visualizing the light field in an image, Kartashova presented three-dimensional projections to prevent information loss while reconstructing the visual light field.

⁴ Schirillo (2013): “The term *infer* is used, after Helmholtz (1866/1962), rather than *perceive*, because it clarifies that one is aware of both surfaces and the light in front of them, without the additional specific qualities of transparency.”

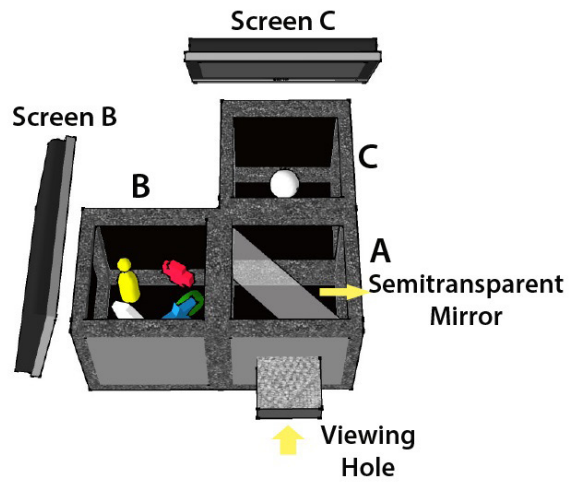


Figure 3.9 Illustration of the set-up of the viewing box Xia *et al.* (2014) used in a research in which observers had to match the light properties of a disk to a real background scene.

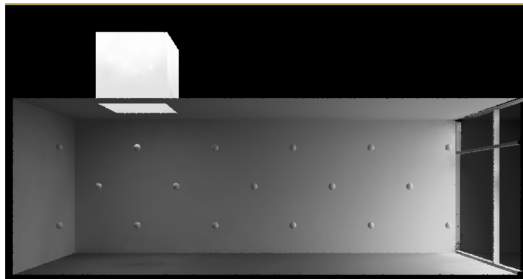


Figure 3.10 A rendering of the 'light-flow-meter' in a space with two daylight openings, that clearly defines the light direction (Madsen and Donn, 2006)

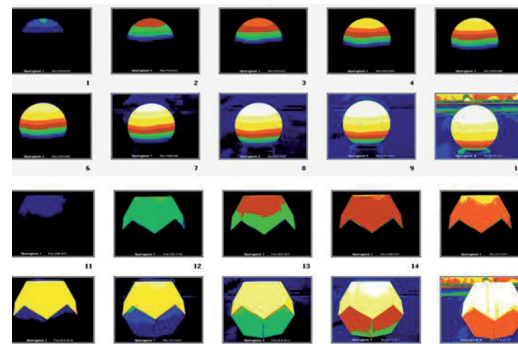


Figure 3.11 (Top) A false colour Scale of Shadow defined in a laboratory setting, and (below) the set-up of a real space measurement (De Bruin-Hordijk, 2008).



Figure 3.12 Measurement set-up of a real room with rendered white probes (Kartashova, 2016).

3.3 THE LIGHT FIELD - ITS APPLICATION

The light field has a mathematical character (Gershun, 1939)(Mury, 2009)(Xia, 2016) and a visual aspect (Frandsen, 1989)(Koenderink, et al. 2008)(Pont, 2009) (Cuttle, 2008). Up until now, research includes research into how to calculate and visually reconstruct the light field. Yet, practice-based architectural applications are minimal.

Regarding diffuseness, Cuttle (2008) examined in an interview series that people's preferences for the vector/scalar ratio lay between 1,2-1,8, corresponding to the normalized diffuseness between 0,55 and 0,7, see table 3.1. (Xia, *et al.*, 2016-II;III) (Cuttle, 2008). Frandsen (in Xia, *et al.*, 2016-II;) found that the range of diffuseness mostly lay between 0,21-0,30, when parallel light dominates. This is probably in line with findings of Cuttle (2010) that estimated observers' preferences for the vector altitude to be in a range of 15° and 45° degrees. Furthermore, it appeared that observers often estimate higher diffuseness levels than actual measured (Xia, *et al.*, 2016-II;III). This knowledge could provide additional information about the charactersitiss in the room, as Ganslandt and Hofman (1992) stated that "Lighting that consists of both diffuse and directed lighting produces soft shadows. Forms and surface structures can be recognised clearly. There are no disturbing shadows." (p.77)(figure 3.13).

An other frequently named aspect of the light field that is matched with a certain level of comfort is the ratio between the directionality of light and the diffuseness (figure 3.14), or as Inanici (2007) named it "The directionality of light is defined as the balance between the diffuse and directional components of light within an environment." (p.1182). A distinct ratio is, as far as the author knows, not yet defined. However, that the ratio has an effect on the visual comfort seems apparent, see figure 3.12 and 3.13 in which the visual appearance of the ratio is presented (Xia, 2016) (Ganslandt and Hofman, 1992)

As far as known, one of the only examples related to architectural applications is the research of Duff (2013) who did an attempt to use the formulas 4-20 to compare in-field measurements in artificial lighted Radiance simulations, analysing the effect of variations in reflection. The results support the idea that Radiance is an accurate modelling software. However, he only focused on the cylindrical illuminance, a single metric derived from the give formula set.

Table 3.1 Assessment of appearance of the Vector/Scalar ratio according to research of Cuttle

Vector/scalar ratio	Assessment of apperance	Application
4.0 (max)		
3.5	Dramatic	
3.0	Very strong	Strong contrasts, detail in shadows not discernible
2.5	strong	Suitable for display; too harsh for human features
2.0	Moderately strong	Pleasant apperance for distant faces (normal)
1.5	Moderately weak	Pleasant apperance for near faces (informal)
1.0	Weak	Soft lighting for subdued effects
0.5	Very weak	Flat shadow-free lighting
0 (min)		



Figure 3.13 An illuminated plastered face with diffuseness levels from low (left) to high (right) (Xia, 2016).

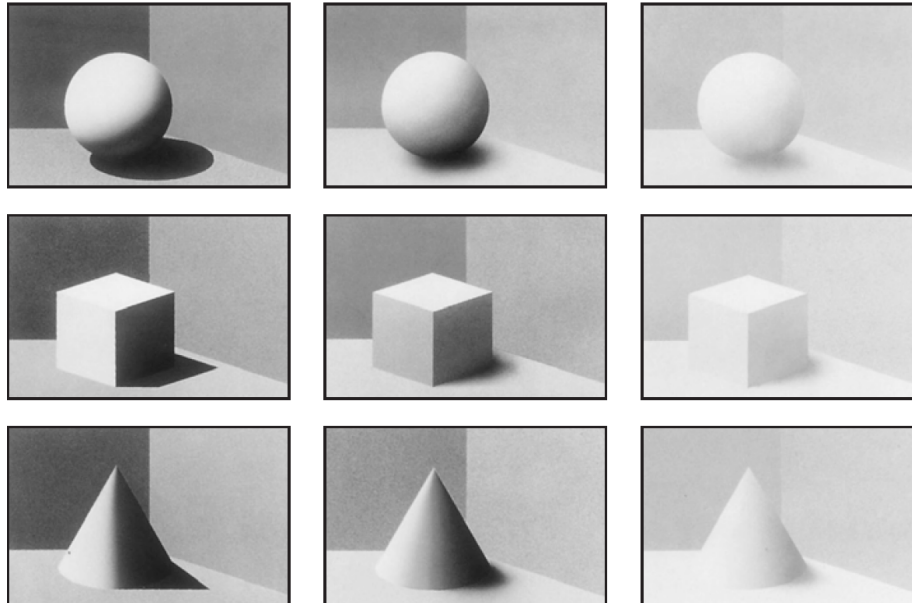


Figure 3.14 The perception of several forms under various lighting conditions. The left row present directed light causing strong shadows and shaping effects. The middle row shows a lighting setting in which light is both diffuse and directional resulting in soft, no disturbing, shadows. The right row shows diffuse light in which shapes are poorly recognizable (Ganslandt & Hofman, 1992).

4

CONCLUSION PART I

Part I elaborated on literature subdivided over two chapters: Chapter 2 examined the research about the existing and new measuring methods for daylight in a space, and described the current visual comfort metrics. Chapter 3 presented a theoretical framework describing the light field in a physical and visual manner.

This chapter will conclude answering two sub-questions. Furthermore, a number of learning points is given that enables the use of the light field in practice.

In chapter 2 we looked for an answer to the question:

How is visual comfort currently determined?

A literature review has been carried out analyzing the often used performance-based metrics that determine the visual uncomfortable aspects of daylight in a space. The research reveals the limitation surrounding the current daylighting practice, and shows that visual comfort has no distinct definition yet. Current metrics do not perform sufficient. It is argued that luminance-based metrics are too much focused on the aspect of light only, and that illuminance metrics take objects in account but miss out on information about the environment. Still, often used examples are the simplified luminance based Daylight Glare Probability (DGP) and the luminance Contrast Ratios (CR).

Recent research in daylight attempts to link visual comfort metrics to new perceptual qualities derived from user experiences or architectural case studies. This should result in a link between an architectural notion of light and a practice-based approach. This research makes an attempt to do so.

Chapter 3 seeks for an answer on the question:

How can the analysis of the light field contribute to improved light qualities?

A theoretical framework was set up to examine how other studies have defined the concept of the light field. The literature analysis showed that the light field is often examined in properties that human observers are able to perceive. These properties are defined by a variety of terms, summarized in table 4.1. For the unity of this research we will speak of the (i) the light intensity, (ii) the light direction and the (iii) light diffuseness only.

The analysis of the lower order properties of the light field fits within the need for a more

Table 4.1 An overview of equivalent terms for three properties of the light field: the Light Intensity, Light Vector and Diffuseness.

Equivalent	Meaning
Light Intensity	
0th order component of the SH representation	
Light density	Constant illumination from all directions
Ambient light	Constant illumination from all directions – used in computer graphics
Scalar illumination	The mean spherical illuminance without direction – the average value of the illumination solid – a measure of the ambient light level at a point
Light Vector	
1st order component	
Illumination vector	the average illumination direction and strength
Primary illumination direction	the average illumination direction and strength
Light direction	the average illumination direction and strength
Diffuseness	
Vector/scalar ratio	A diffuseness metric
Flow of light	The potential of lighting to describe distinct shading patterns
Illumination flow	Lighting diffuseness and directions

perception-based lighting profession. Other than luminance and illuminance distribution, perception-based lighting design seeks for information about the environment in which light, object (material and shape), and space perception interact with each other. The light field meets this qualitative demand, describing not only the illuminance distribution but the direction and the diffuseness of light. This suggests that the light field can contribute to an improved analysis of lighting qualities.

Studies have reported about the behaviour of the light field, in a range of settings. As far as the author knows, most of them are conducted in a laboratory setting or related to artificial light. Despite fundamental research about the mathematical description and visual appearance of the light field, architectural application related to daylighting is yet little.

Both aspects stem in questions about how good the light field analysis works and which developments are needed. This research will find an answer to these questions in the following parts to, subsequently, answer the main research question.

LEARNING POINTS

Besides the clarification on the posed sub-questions, a number of learning points are formulated that relate to the application of the light field. These points form a base for the in-field measurements in part II of this research.

- The light intensity, light direction (in terms of altitude and azimuth) and diffuseness aspects of the light field can be measured using the vector-based formulas (formula 4-23).
- The measurements of these three properties of the light field can be measured by using a cubic illuminance meter.
- To visualize the light field immediately, objects could function as a gauge object.

- A more subjective analysis of the visual light field can be performed by using a luminance camera.
- However, within the transition of a 3D object to a 2D image, direction-diffuseness and intensity-diffuseness ambiguity appears.
- A visualization of the measured light field can be given with the visualization application by Kartashova based upon cubic illuminance measurements. This results in a visual impression of the light field in multiple points in a scene.

PART II
RESEARCHING
APPLICATION OF TOOL USE

5

MEASUREMENT METHOD

This chapter explores how (variations in) the light field can be measured and visualized for understanding the light field by empirical observation. To obtain these variations, we conducted two types of measurements analyzing the light field in an office meeting space: (i) a measurement over time and (ii) a measurement with a variation of position.

Paragraph 5.1 gives a spatial description of the measured office space, room BK01.West.50. Paragraph 5.2 elaborates on the measurement procedure over time. Paragraph 5.3 describes the measurement procedure at different positions.

5.1 A SPATIAL DESCRIPTION OF ROOM BK01.WEST.050

The measurements reported in this section have taken place at the faculty of Architecture (TUD) in the office meeting room: BK01.West.050 (figure 5.1).

The room has a southwest orientation, a surface of 6,1mx3,55m and a height of 2,8m. A plan and section drawing of the office space is presented in figure 5.2. All walls are painted white. A colored acoustic board reduces reverberation time. In the middle of the room a white table is positioned. Chairs were left out of the experiment and the artificial light was turned of.

The first type of measurement (over time) (paragraph 5.2) took place on position A (figure 5.2). Position A,B,C, with 1,5m; 2,5m; 3,5m distance from the window, show the measurement positions of the second measurement series (different position) (paragraph 5.3). The photographed angle Q will be discussed throughout the measurement.



Figure 5.1 An impression of room BK.01.West.050 photographed with a fish-eye camera.

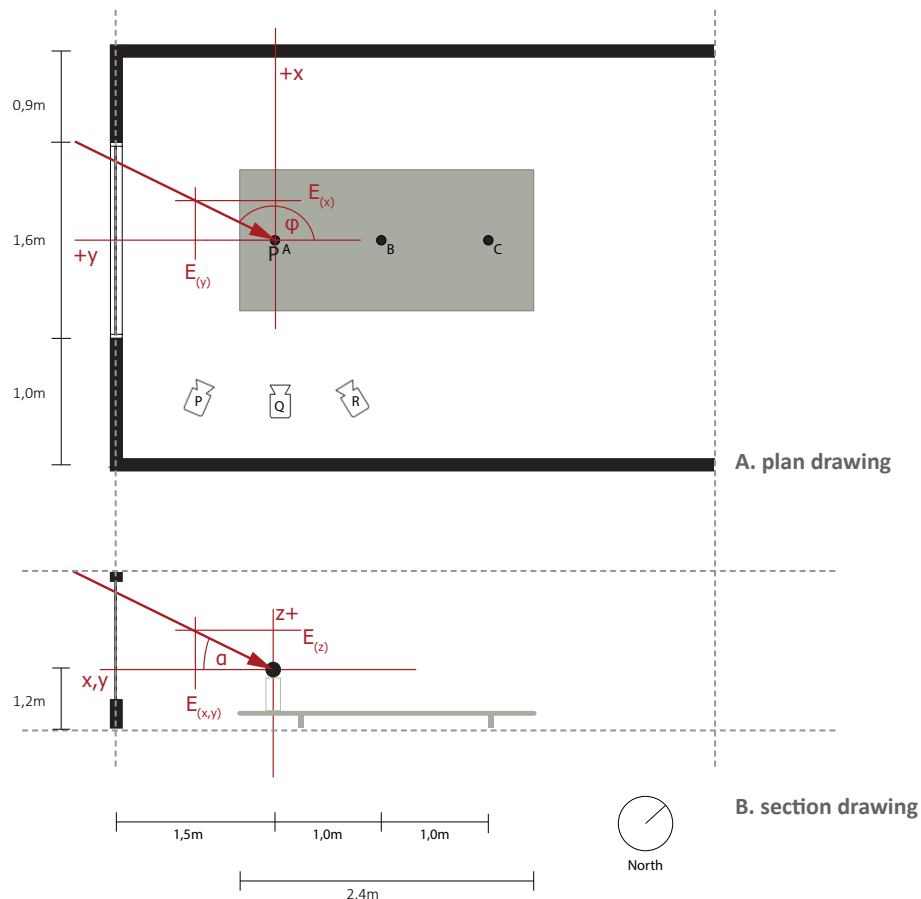


Figure 5.2 (A) The plan drawing of room BK.01.West.050 in the (x,y) -plane with azimuth (ϕ). The angle of the camera view direction is P,Q,R and the position of the cubic illuminance meter and objects is A,B,C.(B) The section of the room in the (x,y,z) -plane with the altitude (α).

5.2 CUBIC ILLUMINANCE METER AND LIGHT FIELD VISUALIZATIONS: OVER TIME

This paragraph describes the measurement procedure of the first type of measurement in which time is a variable to obtain variations in the light field. The aim of the measurement is the verification of the use of the cubic illuminance meter as a tool to measure the light field (on position A, fig. 5.2).

The measurement series was carried out in two parts:

- *First*, a measurement was conducted with the cubic illuminance meter only (every 5 minutes over 20 minutes) so that it did not have to be moved during the measurement.
- *Second*, a measurement series in which alternately, the cubic illuminance meter was used and then the objects were photographed on position A (every 15 minutes over 1,5 hour). The aim was to link the physical data to the appearances of the objects. Furthermore, from this data a web application visualization (by Kartashova) is made.

Paragraph 5.2.1 presents the use of the cubic illuminance meter. Paragraph 5.2.2 presents the light field visualization by objects. Paragraph 5.2.3 presents the web application visualization.

5.2.1 THE CUBIC ILLUMINANCE METER

This paragraph elaborates on the use of the cubic illuminance meter to simultaneously measure the light intensity, light direction and diffuseness. The set-up of the cubic illuminance meter is shown in figure 5.3.

A self-built cubic illuminance meter was fabricated, based on design of Xia (2016): An

MDF cube serves as a base for six KONICA MINOLTA Illuminance Meters, type T-10. The iterative building process is presented in appendix C. The cubic illuminance meter was rotated and attached at a tripod and positioned on a table to have a total height of 1,20m. The rotation of 45-degrees on its y-axis and 35-degrees around the x-axis was applied to lighten as much faces as possible. Figure 5.3 presents the resulting (x'', y'', z'') coordinate system. This is used to calculate the vector components (see page 49).

The measurement procedure of the installed cubic illuminance meter is as follows:

- Position the cubic illuminance meter with plane 1 perpendicular to the y'' -axis and the window is perpendicular to the y -axis (figure 5.2-5.4).
- Connect the cubic illuminance meter (i.e. the KONICA MINOLTA Illuminance meters) to a computer with Microsoft Excel and do a baseline check with the lids of the illuminance meters still on.
- Take off the lids and conduct the measurements needed.
- The output of the cubic illuminance meter for calculating the light intensity and diffuseness will be processed in a spreadsheet, following formulas 4-14, 18-20, 22, 23 (Chapter 3).

An extensive measuring protocol, including the preferred conditions and preparation steps, is described in appendix E1, as well as the items checklist.

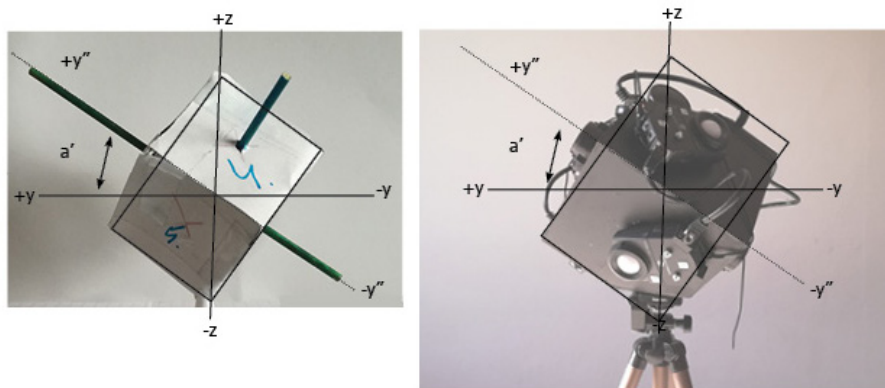


Figure 5.3 Vertical section of the tilted cube (left) and the self-made cubic illuminance meter. The angle a' is the angle at which the u, v , and w axes intersect the horizontal x, y plane. The numbers 4 and 5, in the left image, correspond to the plane 4 and 5 in figure 5.4.

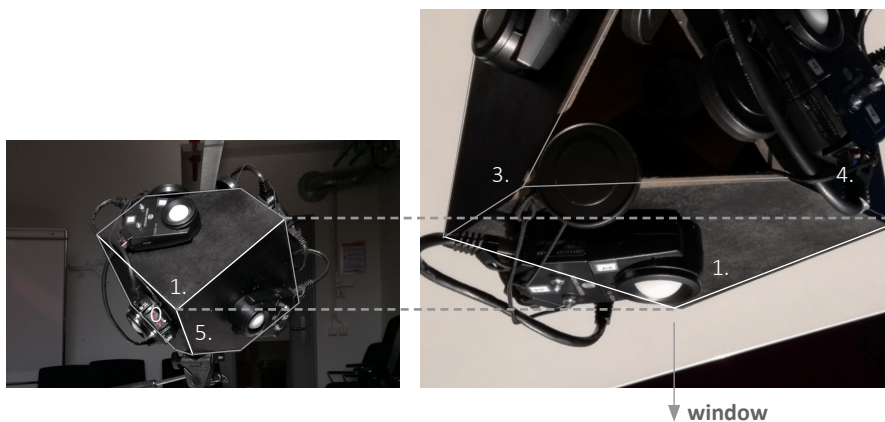


Figure 5.4 Each lux meter is numbered and series connected from 0-5. Each plane corresponds to a Lux meter. Plane 0,1,5 face the window (left), plane 1,3,4 face the ceiling (right).

The procedure of rotation results in a different rotation matrix compared to formula 21 presented on page 32. This is caused by how the axes are defined relative to the window, and that we calculated with a rotation of 35° instead of $35,3^\circ$. And so, when rotating the cube respectively 45-degrees and 35-degrees around the y- and x-axis, we obtain the following transformation matrix (M) that is applied to the cube (appendix C).

$$M = \begin{pmatrix} \cos(-45^\circ) & \cos(-45^\circ)\sin(35^\circ) & \sin(45^\circ)\cos(35^\circ) \\ 0 & \cos(35^\circ) & \sin(35^\circ) \\ \sin(-45^\circ) & \sin(-45^\circ)\sin(35^\circ) & \sin(45^\circ)\cos(35^\circ) \end{pmatrix} = \begin{pmatrix} 0,707 & -0,406 & 0,579 \\ 0 & 0,819 & 0,579 \\ -0,707 & -0,406 & 0,579 \end{pmatrix}$$

We now say that the lightmeters are positioned on what we define the (x'', y'', z'') -axes. For the light unit vector that is measured on these new axes, we notate $e(x'', y'', z'')$, and its x'', y'', z'' - components as $e(x'')$, $e(y'')$, $e(z'')$. To obtain the light unit vector with respect to the familiar (x, y, z) -axes, we use that $e(x, y, z) = M^{-1} e(x'', y'', z'')$, to get the following system of equations;

$$\begin{aligned} e_{(x)} &= 0,707(e_{(x'')} - e_{(z'')}) \\ e_{(y)} &= 0,819e_{(y'')} - 0,406(e_{(x'')} - e_{(z'')}) \\ e_{(z)} &= 0,574e_{(y'')} + 0,579(e_{(x'')} + e_{(z'')}) \end{aligned}$$

5.2.2 VISUALIZATION: LIGHT FIELD DEPICTED BY OBJECTS

The light intensity, light direction and light diffuseness were simultaneously depicted on four objects: a white sphere, a golf ball, a icosahedron and a dodecahedron with pegs (figure 5.5). The appearance of an object always presents the immediate interaction with the light field. To capture this, the objects were photographed with a luminance camera.

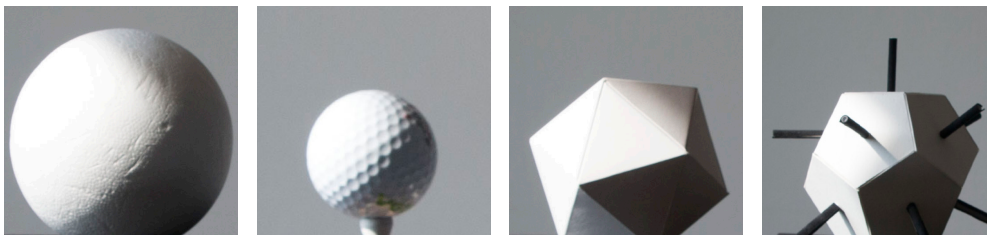


Figure 5.5 The white matt objects photographed in this research, from left to right; sphere, golf ball, icosahedron, dodecahedron with pegs. It will appear that the golf ball is too small for the focus of the camera.

The measurement procedure to photograph the objects was as follows:

- The objects were positioned (one-by-one) on a block on a table with a total height of 1,20m (figure 5.2). The block was covered with black paper preventing disturbing reflectances from the block's material.
- A digital single reflex camera equipped with a normal lens, fastened on a tripod (1,20m height), was positioned at P, Q, R, facing the objects (figure 5.2).
- Three images were taken (underexposed, normal and overexposed), combined into a high dynamic range image (HDR).
- A false-color map was created with *LMK Labsoft Techno Team* software to visualize the dynamic luminance range on objects.

An extensive measuring protocol, including the preferred conditions and preparation steps, for the use of the luminance camera to visualize the light field is described in appendix E2, as well as the items checklist.

5.2.3 VISUALIZATION: A WEB APPLICATION

Besides the immediate visualization of the light field interacting with objects, the illuminance values measured at each face of the cubic illuminance meter can be transformed in a web application visualization. Hence, the light intensity, light direction and light diffuseness can simultaneously be visualized by computer generated arrows and ellipsoids in an light-visualization web app (<http://lightvisualizations.000webhostapp.com> - paper still to be submitted)(figure 5.6).

Therefore, a (*.csv)-file was uploaded containing, for each measurement point, the coordinates (X,Y,Z) and the measured illuminance of each face of the cube. See appendix D for a more extensive description.

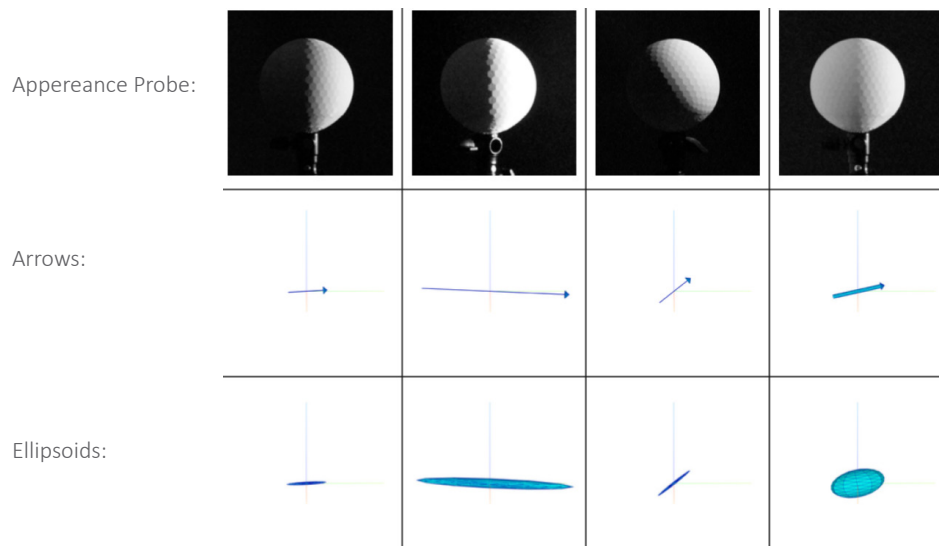


Figure 5.6 The various visualization type of the web application by Kartashova, in relation to the appearances of a white probe as a gauge object.

5.3 CUBIC ILLUMINANCE METER AND LIGHT FIELD VISUALIZATIONS: DIFFERENT POSITIONS

This paragraph describes the measurement procedure of the second type of measurement in which position is a variable to obtain variations in the light field. The aim of the measurement is to gain a better understanding of use of the tools to measure and visualize the light field (on position A,B,C fig. 5.2).

The measurement series was carried out in two parts:

- *First*, a measurement was conducted with the cubic illuminance meter only (on position A,B, C) to limit information loss caused by time differences.
- *Second*, a measurement series has taken place in which both the cubic illuminance meter and the luminance camera were used. The light field was measured with the cubic illuminance meter and, alternately, the objects were photographed (on position A,B,C), to link the physical data to the appearances of the objects. From this data also a web application visualization (by Kartashova) is made.

Paragraph 5.3.1 presents the use of the cubic illuminance meter. Paragraph 5.3.2 presents the light field visualization by objects. Paragraph 5.3.3 presents the light visualization by Kartashova.

5.3.1 THE CUBIC ILLUMINANCE METER

The lower order properties of the light field were simultaneously measured with a cubic illuminance meter with a similar set-up as presented in paragraph 5.2.1. Only the position differs: A,B and C instead of position A only.

5.3.2 VISUALIZATION: LIGHT FIELD DEPICTED BY OBJECTS

The simultaneously visualization by objects was performed in accordance with paragraph 5.2.2. In contrast with the measurement over time (paragraph 5.2) this measurement used only two objects: a white sphere, a white painted hockey ball (figure 5.7). Because it appeared that the golf ball was too small for a sharp focus of the camera.



Figure 5.7 The white matt objects photographed in this measurement; (left) white sphere, and (right) a hockey ball with rough texture.

5.3.3 VISUALIZATION: A WEB APPLICATION

The light field visualization by Kartashova is similar as presented in paragraph 5.2.3.

6

MEASUREMENT RESULTS

This chapter presents the results of the measurement described in chapter 5. In order to find an answer on the main question of this research we executed two types of measurement: (i) a measurement over time and (ii) a measurement with a variation of position. Paragraph 6.1 presents the results of the measurements over time. Paragraph 6.2 presents the results of the measurement at different positions.

6.1 CUBIC ILLUMINANCE METER AND LIGHT FIELD VISUALIZATION: OVER TIME

This paragraph describes the results of the first type of measurement in which time is a variable to obtain variations in the light field. The aim of the measurement is to check if the cubic illuminance meter generates sufficient results with the purpose to gain a better understanding of the light field in a daylit room (on position A, fig. 5.2).

Paragraph 6.1.1 presents the results of the measurement with a cubic illuminance meter only (on October 26 and October 21). Paragraph 6.1.2 shows the results of the the appearances of objects (October 21). Paragraph 6.1.3 presents the web visualization of the cubic illuminance values of the measurement on October 21 (paragraph 6.1.1).6

6.1.1 THE CUBIC ILLUMINANCE METER

This paragraph presents the results of two measurements with a single cubic illuminance meter with time as a variable.

Table 6.1 presents the results of the cubic illuminance meter on October 26 for every minute from 15:30h-15:35h to detect the stability of the measurement tool. It shows the rough data (i.e. illuminance values) and the calculated light intensity (E_{sr}), light direction (altitude (α) azimuth (φ)) and diffuseness ($D_{normalized}$). Appendix F2 gives an example (based upon measurement of october 26) of how the measured illuminances on each face of the cube (numbers in red) are processed into the light intensity, light direction and diffuseness using Microsoft Excel.

Table 6.2 gives the results of the cubic illuminance meter on October 21 for every 15 minutes from 15:00-16:00h. Figure 6.4 shows the graphs of the results presented in table 6.2.

Table 6.1 The measured illuminances on each plane of the cube (left columns in grey) and the calculated lower order properties of the light field, using formula 4-14,18-20, 22, 23, of a measurement in room BK01. West.050 on October 21. Each face corresponds to a plane on the cube, see figure 5.4.

face / time	Output Cubic Illuminance meter						calculated Light Field properties			
	0	1	2	3	4	5	Intensity	Altitude	Azimuth	Diffuseness
	lux	lux	lux	lux	lux	lux	E_{sr}	(α)	(ϕ)	($D_{normalized}$)
15.30h	2886	13117	1431	693	687	3908	4017	16,86	183,49	0,23
15.31h	2821	12685	1384	680	660	3763	3886	16,84	183,28	0,23
15.32h	2738	12209	1335	665	634	3608	3743	16,83	183,1	0,23
15.33h	2624	11479	1258	644	593	3377	3525	16,77	182,76	0,24
15.34h	2754	12121	1326	659	605	3565	3709	16,69	182,81	0,23
15.35h	3035	13626	1487	700	654	4015	4148	16,65	183,09	0,23

Table 6.2 The measured illuminances on each plane of the cube (left columns in grey) and the calculated lower order properties of the light field, using formula 4-14,18-20, 22, 23, of a measurement in room BK01. West.050 on October 26 , 15.30h. Each face corresponds to a plane on the cube, see figure 5.4.

face / time	Output Cubic Illuminance meter						calculated Light Field properties			
	0	1	2	3	4	5	Intensity	Altitude	Azimuth	Diffuseness
	lux	lux	lux	lux	lux	lux	E_{sr}	(α)	(ϕ)	($D_{normalized}$)
15:00h	6537	39642	4941	1413	10367	12023	13419	25.99	198.13	0.32
15:15h	7174	45813	6624	1663	12222	15340	15607	24.73	200.40	0.33
15:30h	6689	42924	6767	1804	6794	12024	14480	23.35	192.22	0.35
15:45h	6759	45212	6979	1800	8674	14782	15285	22.60	196.39	0.34
16:00h	9702	46307	6911	3181	1921	9609	14171	20.71	178.56	0.28

5.1.2 VISUALIZATION: LIGHT FIELD DEPICTED BY OBJECTS

This paragraph presents the luminance images in grey and false-color maps of the measurement on October 21. Figure 6.1 presents the objects photographed at 15:00h and 16:00h. Appendix F3 presents the objects photographed at the other time slots. Figure 6.2 shows the image of the objects in relation to results of the cubic illuminance meter (figure 6.3). The figure contains the series images of probes photographed from angle Q, in a normal mode colour scheme and in a false colour mode with a logarithmic scale of display.

It appeared (discussion in chapter 7) that the cubic illuminance meter was partly covered in shadow until 15:00h. Hence, this part in the graph is neglected during analysis.

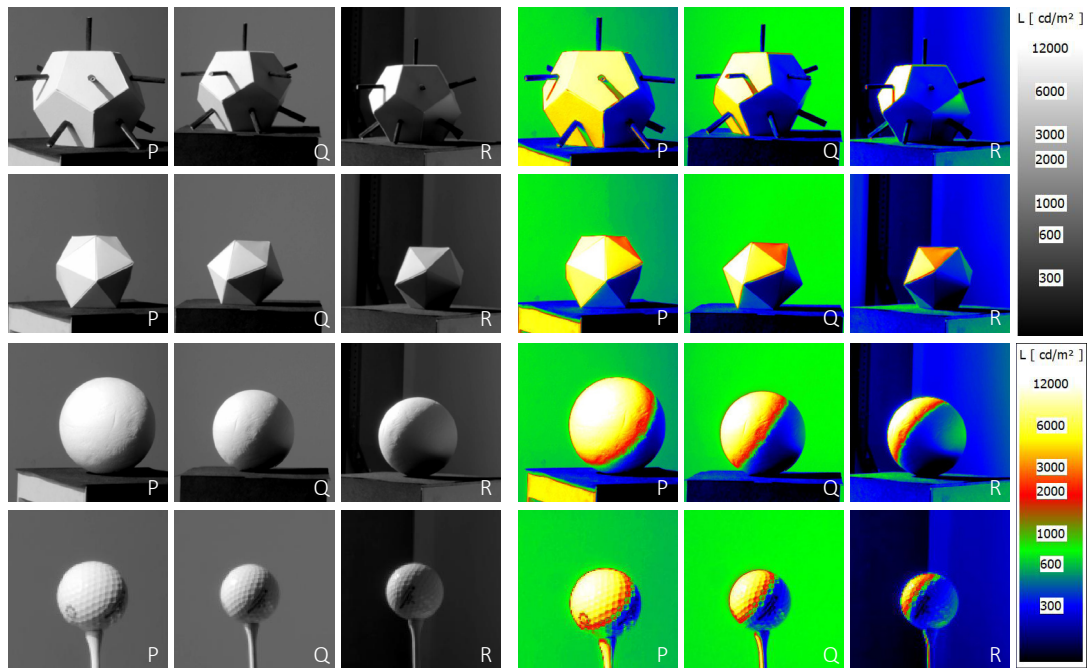


Figure 6.1 The objects photographed from angle P, Q, R at October 21, 15:00h.

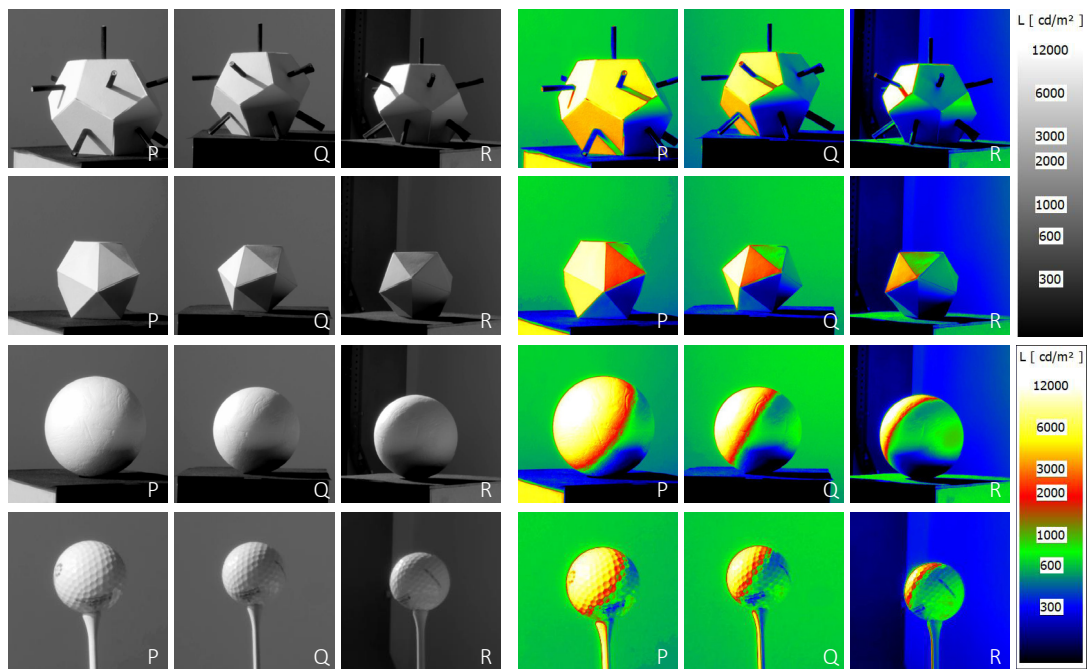


Figure 6.2 The objects photographed from angle P, Q, R at October 21, 16:00h. The left columns show the objects in a grey scale. The right columns present the objects in a false-color scale processed in LMK Labsoft software.

Figure 6.3 Series images of white matt probes photographed from angle Q (figure 4.1) in room BK.01.West.050, from 15:00h-16:00h, on October 21. The top two rows shows similar image. In addition, the top row includes black arrows which represent the measured altitude. The row below present the false color images with a colour scheme of 0-12000 cd/m².

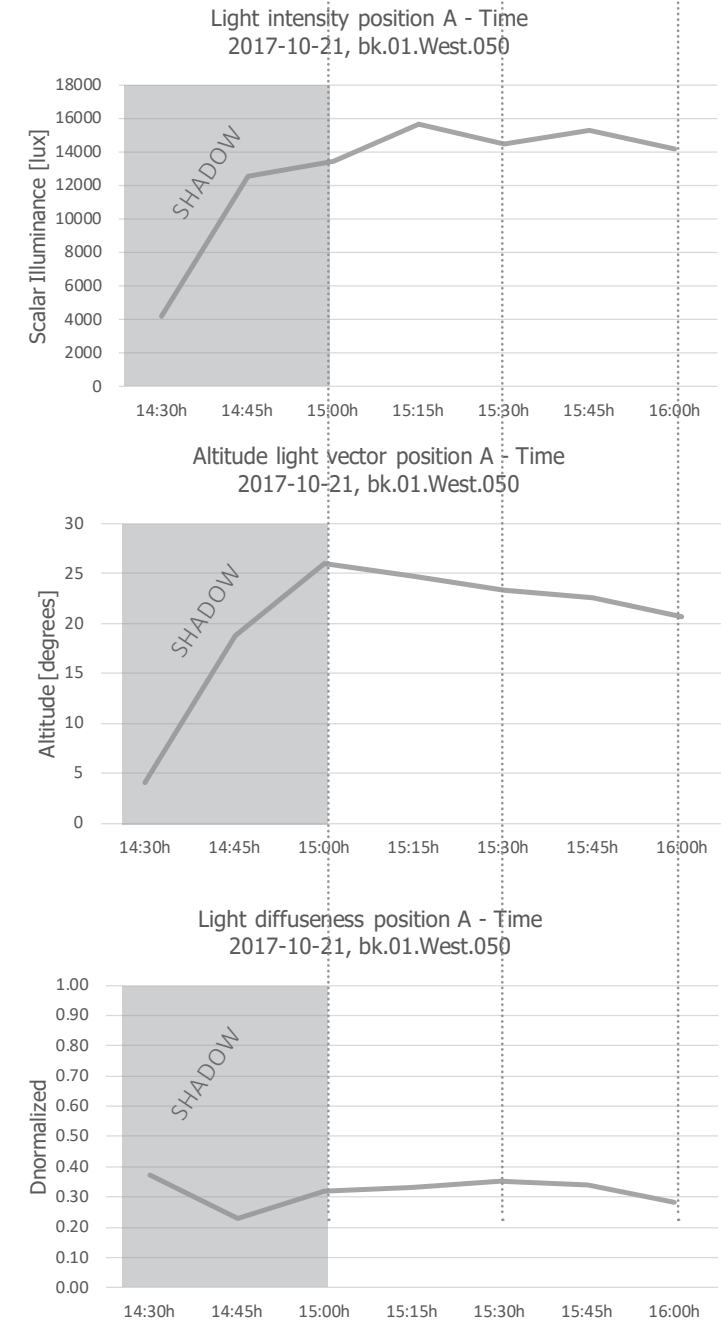
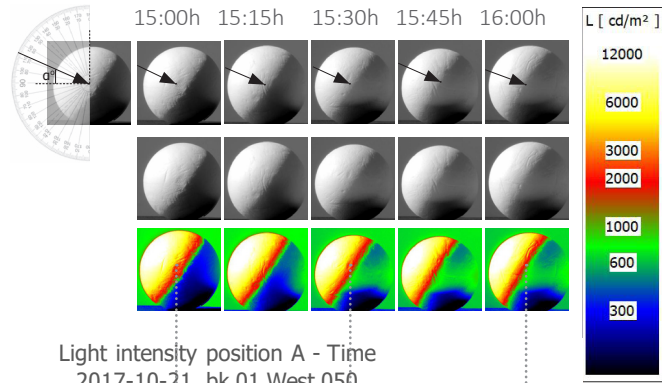


Figure 6.4 From top to bottom; graphical representation of the calculated light intensity, light direction and light diffuseness on position A from 14:30h-16:00h on October 21. The grey part is a measurement error due to shadow casted on some faces of the cubic illuminance meter.

6.1.3 VISUALIZATION: A WEB APPLICATION

The results of the light visualization in tubes and ellipsoids of the measurement on October 21 (table 6.2) are presented in figure 6.5.

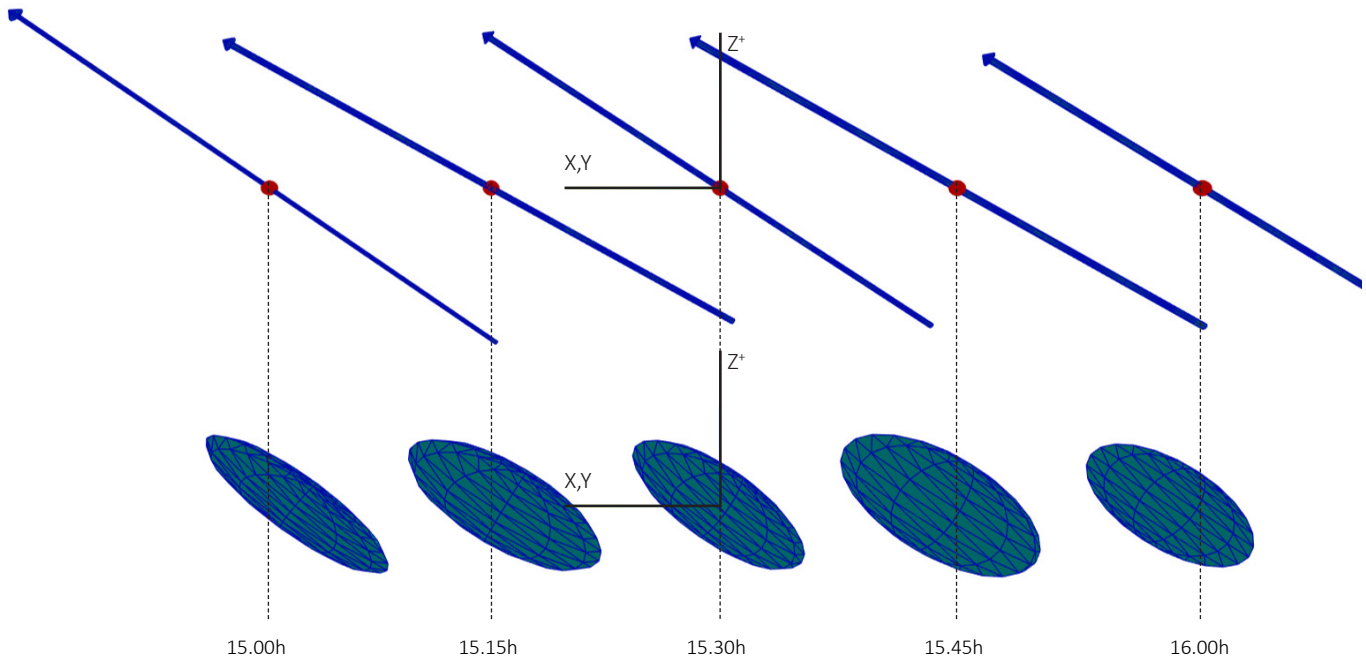


Figure 6.5 Light field visualization of October 21. The visualization includes the light intensity, light direction and light diffuseness in one point represented by an arrow, or ellipsoid (Scale-4 set for a tilted cube).

6.2 CUBIC ILLUMINANCE METER AND LIGHT FIELD VISUALIZATION: DIFFERENT POSTITIONS

This paragraph describes the results of the second type of measurement in which position is a variable to obtain variations in the light field. The aim of the measurement is to check if the cubic illuminance meter generates sufficient results with the purpose to gain a better understanding of the light field in a daylit room (on position A,B,C, fig. 5.2). Different from the results presented in the previous paragraph, only two objects were photographed in this measurement; a probe and a hockey ball.

Paragraph 6.2.1 presents the results of the measurement with a cubic illuminance meter only (on October 26 and December 12). Paragraph 6.2.2 shows the results of the the appearances of objects (December 12). Paragraph 6.2.3 presents the web visualization of the cubic illuminance values of the measurement on December 12 (paragraph 6.1.1).

6.2.1 THE CUBIC ILLUMINANCE METER

Table 6.3 presents the light intensity as the scalar illuminance, the diffuseness ($D_{\text{normalized}}$) and the light direction over time. The measurements took place at October 26, 15.29h in room BK.01.West.050.

Table 6.3 The output of the single cubic illuminance measurements and its final calculation results -a measurement in room BK01.West.050 on October 26 , at position A, B and C, respectively 0,5m; 1,5m; 2,5m distance from the window.

Output Cubic Illuminance meter							Result calculation formula 4-20			
face / position	0	1	2	3	4	5	Scalar	Altitude	Azimuth	Diffuseness
	lux	lux	lux	lux	lux	lux	E_{sr}	(α)	(ϕ)	($D_{normalized}$)
A	2996	13889	1513	715	734	4154	4248	16,95	183,82	0,23
B	2564	10296	1086	558	676	4529	3325	10,7	188,44	0,23
C	2063	8215	427	460	358	4389	2637	7,81	190,28	0,16

Table 6.4 The output of the cubic illuminance measurement that is related to the photographed objects (figure 5.6-5.8) of a measurement in room BK01.West.050 on December 12 , at position A, B and C, respectively 0,5m; 1,5m; 2,5m distance from the window.

Output Cubic Illuminance meter							Result calculation formula 4-20			
face / position	0	1	2	3	4	5	Scalar	Altitude	Azimuth	Diffuseness
	lux	lux	lux	lux	lux	lux	E_{sr}	(α)	(ϕ)	($D_{normalized}$)
A	812	3680	453	377	265	1033	1200	20,27	181,42	0,3
B	862	1576	300	305	147	674	628	3,98	170,67	0,4
C	609	782	145	225	122	477	374	-4,21	168,53	0,44

6.2.2 VISUALIZATION: LIGHT FIELD DEPICTED BY OBJECTS

The appearances of the white probe and hockey ball on position A,B, C at December 12 are presented in figure 5.6. In addition, their relation to the measured cubic illuminance are shown in figure 5.7 in which the black arrow presents the measured altitude (α).

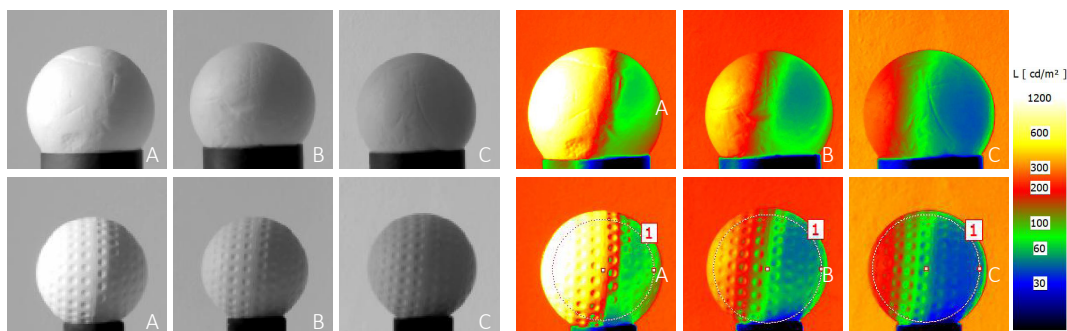


Figure 6.6 The objects photographed from angle Q at December 12 (position A, B or C).

Table 6.5 The luminance level of the golf ball at position A,B or C at December 12 in BK.010.West.050.

	Luminance Hockey Ball		
	Min	Max	Mean
	[cd/m²]	[cd/m²]	[cd/m²]
Position A	44,47	1668	478
Position B	18,36	439,3	133,9
Position C	22,64	239,3	85,18

Figure 6.7 Series images of white matt probes and hocey ball photographed from angle B in room BK.01.West.050, on December 21 , Delft. The black arrow indicates the measured altitude light vector and so similar to the values presented in the graph in 5.8.

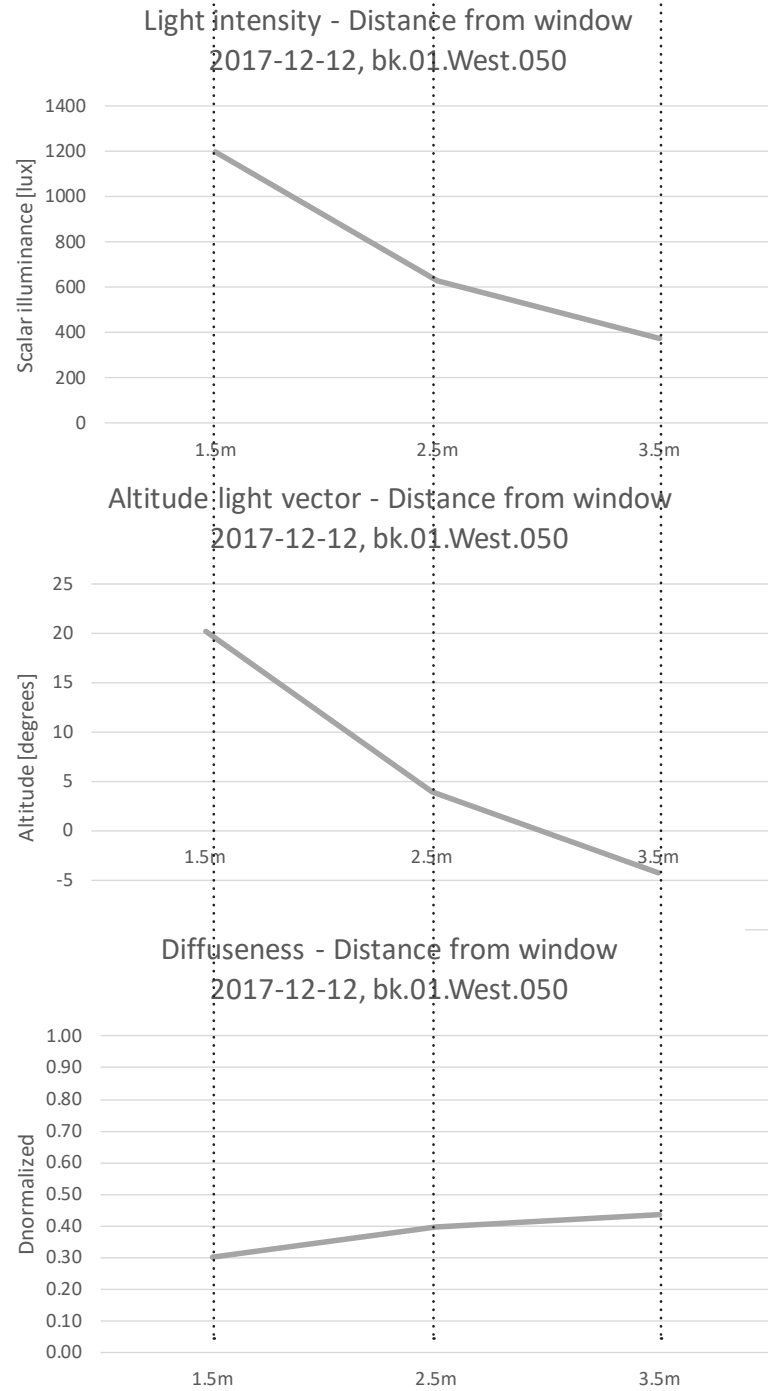
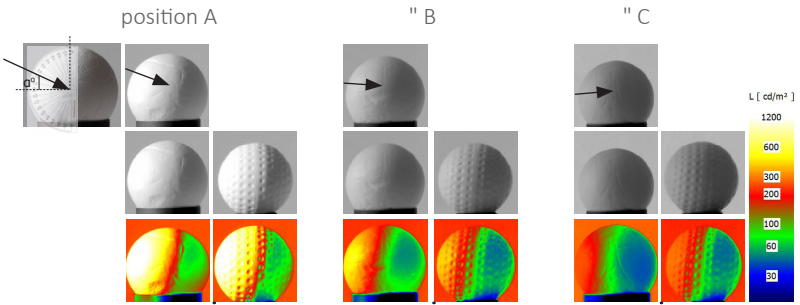


Figure 6.8 Graphically and visually representation of the lower order properties of the light field at a distance of 1,5m; 2,5m; 3,5m from the window.

6.2.3 VISUALIZATION: A WEB APPLICATION

The results of the light visualization in tubes and ellipsoids of the measurement on December 12 (table 6.4) are presented in figure 6.9.

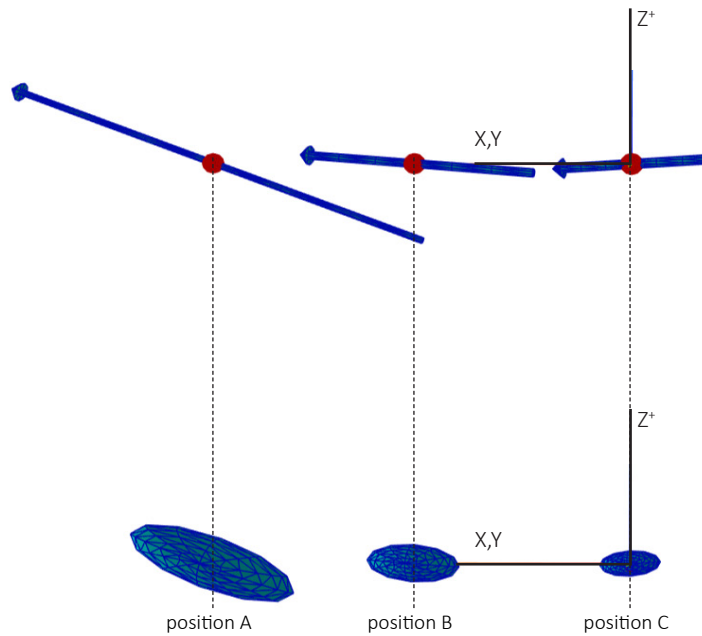


Figure 6.9 Light field visualization by arrows and ellipsoids (scale-1) that present the light intensity, light direction and light diffuseness simultaneously in a point. The results present the measurement of December 12 in BK010.West.050 at position A, B and C.

7

DISCUSSION PART II

The measurements in Part II of this research explored to what extent variations in the light field can be measured with a cubic illuminance meter, and how the physical data can be visualized. Therefore, objects were photographed, and the images were related to data measured with the cubic illuminance meter.

The imposed variations in the light field were examined by two types of measurements: (i) measured the light field over time, every 15 minutes from 14.30h to 16.00h (paragraph 5.1), (ii) measured the light field on three different positions, with 1,5m; 2,5m; 3,5m distance from the window (paragraph 6.2). Both experiments were similarly analysed regarding the lower order properties of the light field: the light intensity, direction and diffuseness.

The results (chapter 6) of the measurements in Part II are discussed simultaneously in the following manner: First, we discuss the use and the set-up of the cubic illuminance meter, and the limitations regarding the measurement. Second, we compare the results from the visualization-by-objects with the result from the cubic illuminance meter to verify the results of the self-built tool. One-by-one the effect of the lower order properties of the light field on the appearances of the objects are examined. In addition, the web application visualization of Kartashova is discussed.

7.1 CUBIC ILLUMINANCE METER

The aim of the measurements in part II was to investigate to what extent we can measure the light field in a daylight scene using a cubic illuminance meter. This question was stated with the notion that in previous research (Cuttle, 2008; Xia, 2016) the cubic illuminance meter was used as a tool to measure the light intensity, direction and diffuseness. In addition, we verified to what extent our self-built model matched the visualizations on the object (paragraph 6.2). Based upon these result and the research of Cuttle and Xia we confirm that the cubic illuminance meter can sufficiently measure the light field in a point in a daylight scene. In this paragraph the use of the tool and its set-up are discussed.

The orientation of the cubic illuminance meter during research was fixed: we found that by rotating the cube 45 degrees around the y-axis and 35 degrees around the x-axis the cube is reasonably similar to attitude 3 by Xia (2016) relative to the light source, and comparable to the orientation Cuttle proposed (2008) in his study. Despite the dynamic

character of daylight this orientation of the cubic illuminance meter prevents the cube from being parallel to the light source or have faces similarly lighted. Certainly, this results could contribute to the study of Xia (2016) who designed the cubic illuminance meter with the same criteria but applied it on a scene with artificial light.

The results of this research showed that by positioning the cube on a line with a grid point spacing of 1,0m, an indication is given of the light field within a daylit space. Therefore, the assumption is made that only a few grid-points are enough to restore the light field, as Mury concluded in his PhD thesis (2009). However, it should be noted that our finding is solely based upon a daylit scene with a single light source, i.e. a single window in the façade.

Another finding is that clear sky types are vulnerable for measurement errors due to collimated light resulting in casted shadows in the scene. More specifically, the cubic illuminance meter represents a point but is in fact larger a larger cube. As a point in 3D space is either completely in shadow or not, we need the cube to be as well. Conversely, when parts of the cube are in the shadow, and other parts are not, measurement errors appear. To illustrate, we consider the pictures taken of the measurement set-up in figure 7.1 where the light cells of the cubic illuminance meter are partly covered in shadow due to the window not being large enough. Therefore we'd analysed the images only from 15:00h on (figure 5.2). Clear sky types have a strong directional component that can cause shadow patterns in an interior setting, making these sky types more vulnerable for such measurement errors.

On the limitation of the measurement with the cubic illuminance meter, it should be noted that it is beyond the research' scope to find a proof for the accuracy of the measured lower order light properties. For example, we cannot verify the accuracy of these results in relation to the orientation, as other studies did (Ashdown & Eng (1998) in Xia, 2016). They found that the sensitivity of the cubic illuminance in a situation with strong directional light could result in a 33% variance of the scalar illuminance. To improve the accuracy of the tool it is recommended to increase the volume of the cubic illuminance meter in subsequent research.

Overall, the experimental procedure allowed us to analyse the light field in a daylit room (no artificial lighting) with a single window, resulting in one-directional lighting. For the analysis of the light direction this is beneficial. However, when multiple light sources are present it is recommended to test the set-up again for its sufficiency.



Figure 7.1 Pictures of the setting in room BK.01.West.050 at (from left to right) 14:26h, 15:25h and 15:56h.

7.2 LIGHT FIELD VISUALIZATION

The discussion regarding the light field's visualization is split into the visualization by objects and the visualization by the web application.

Light field visualization by object

The aim of the measurement is to investigate whether the output of the cubic illuminance meter can be aligned with the appearances of the objects. Furthermore, the images give an impression of what the measured values (E_{sr} , alpha, phi, $D_{normalized}$) represent. Both aspects are discussed in this paragraph. Extended examination to other ways of visualization, that for example work in architectural visualizations, is beyond the scope of this research. Due to testing with daylight conditions, simultaneous adjustments in the lower order properties appear, the individual adjustments will be discussed separately.

This research analyzes the objects objectively based upon grey and false-color illuminance maps that disregard the instantaneous aspect of the visualization. This is in contrast with previous studies (Xia, 2016; Pont, et al., 2007; Koenderink, et al., 2007) in which a gauge object was used as a tool for immediate visualization. Moreover, the camera set-up is time consuming and information loss occurs due to the 2D image processing from a three-dimensional scene. Nevertheless, the false colour images are objective and give more information in relation to the grey coloured images, which is consistent with data obtained from research of Madsen & Donn (2006).

Regarding the light intensity, it is most convincing to argue that there's a correspondence between how the light intensity is depicted by the objects (in cd/m^2) and how it is measured with the cubic illuminance meter (in E_{sr}). The gradual decrease of the light intensity (E_{sr}) measured by the cubic illuminance meter is in accordance with the luminance values from the images from position A, to B, to C (figure 6.8, table 6.5). The differences between luminance values in the false-color images over time (figure 6.3;6.4) are minimal, which aligns with measured light intensity (E_{sr}) as well. Even when we crosslink both measurements and set them to the same luminance scale (figure 7.2) the images are aligned with the corresponding measured light intensities (E_{sr}) (table 7.2).

In addition to this analysis, the variations in the light intensity are responsible for the different levels of brightness (figure 7.2). Whereupon we conclude that a human observer is able to distinct the various levels of light intensity visible on the objects. This agrees with the result of Xia *et al.* (2016-II;III). She suggested in a research in which participants had to fit the luminance of a disk to a surrounded scene, that human observers are good in inferring the light intensity. Our analysis is limited because the visualizations are HDR images and set in a certain scale for comparison. This results in information loss compared to how a human observer perceives the object in a real scene. Besides, we're biased in our analysis since we are aware of the measured light intensity.

Considering the light direction, our results show that the altitude light direction depicted by a white sphere corresponds with the measured light direction with the cubic illuminance meter (represented by the black arrow in figure 6.3 and 6.7), during a clear sky-type. In a simulation workshop of Madsen and Donn (2006) the light direction depicted on simulated spheres in a daylit space, was defined. Also research of Pentland (in Koenderink *et al.* 2007; Xia, *et al.* 2016-II;III) confirmed that observers can estimate the illumination direction from an image.

On all objects the light vector is roughly defined, but a sphere with a rough surface (i.e. hockey training ball) captures the most information. This result is in accordance with a study of Xia *et al.* (2014) who found that the dimples in an object can give additional

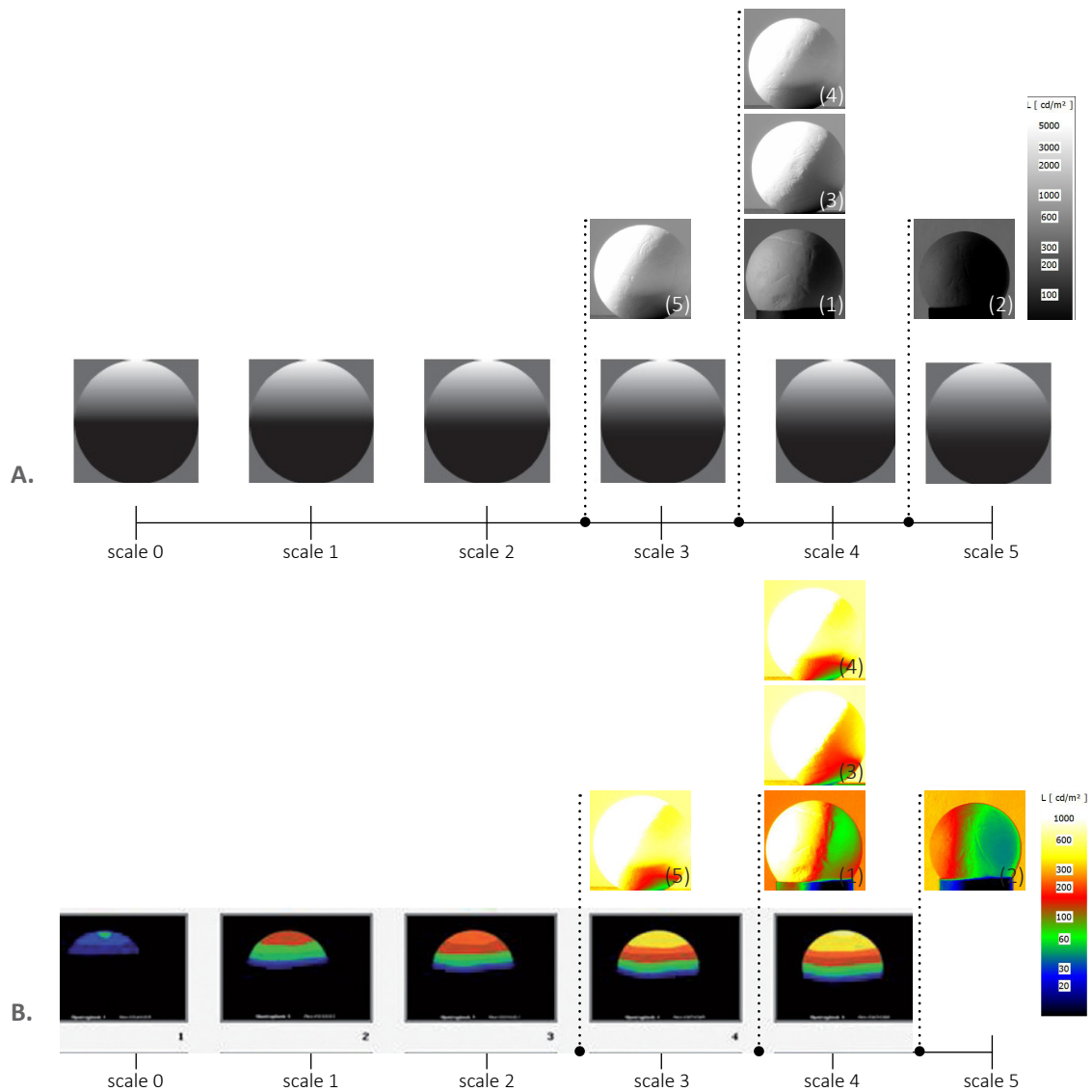


Figure 7.1 (A) A part of Frandsen's Scale of Light (range 0-5) showing the level of diffuseness in grey scale, and **(B)** a part of the same Scale of Light in luminance color. The photographed objects are from the measurements over time (image no. 3-5) and the measurement at different positions (image no. 1, 2)(table 7.1).

Table 7.1 A part of Frandsen's Scale of Light (scale 0-5, ratio 0-0,5) in which the diffuseness values of the images in figure 7.1 are presented corresponding the diffuseness in the original Scale of Light. Image no. 1-2 are from paragraph 5.2 and image no. 3-5 are from paragraph 5.1

			Scale of Light						
			Scale	0	1	2	3	4	5
image no.	position	time	Ratio	0	0,1	0,2	0,3	0,4	0,5
(1)	A	14:00h	-----	-----	-----	-----	0,3	-----	-----
(2)	C	14:00h	-----	-----	-----	-----	-----	0,44	-----
(3)	A	15:00h	-----	-----	-----	-----	0,32	-----	-----
(4)	A	15:30h	-----	-----	-----	-----	0,35	-----	-----
(5)	A	16:00h	-----	-----	0,28	-----	-----	-----	-----

cues about the light field, increasing the amount of illumination cues where observers are sensitive for.

We found that an object with increasing visible faces provides a better estimation about the light direction. The icosahedron (20 faces) improves the readability of the light direction with compared with the dodecahedron: the sharp transitions between the surfaces are visible. The pegs on the dodecahedron give additional information about the light direction which seems difficult to interpret. Xia *et al.* (2016-II;III) found similar results in a real setting in which the dodecahedron (without pegs) was suggested as best compared to shapes derived from a pentagon body. De Bruin-Hordijk *et al.* (2008) suggested that as well.

Although it can be related to common sense that variations in the light field are clear when the objects are photographed perpendicular to the light direction (i.e. parallel to the window), this study wanted to analyse and verify it first. We found that the light altitude is best visible when the object is photographed perpendicular to the incoming light (angle Q in figure 5.2). In this way the view direction is aligned with the x -axis, resulting in a clear (z, x - y)-plane. Furthermore, the appearance of the objects vary when photographed from a diverse angles. This is also expressed by Cuttle (2008): “As the viewer changes direction, the illuminance of the probe can change” (p.215).

We found that the level of diffuseness in the images is difficult to align with the diffuseness measured by the cubic illuminance meter ($D_{normalized}$). On the one hand, the visualizations of image no. 1, 3, 4 in both the grey-scale photograph as the false-color maps in figure 7.1 show different appearances, while they have relatively similar measured diffuseness levels. On the other hand, the correspondence between the images of Frandsen’s Scale of Light and the images in the false-color Scale of Light, do not align the visualizations with the photographed probes. The latter is in accordance with research of De Bruin-Hordijk *et al.* (2008) who showed that shadow images in real scenes can hardly be related to a scale set in a laboratory setting due to interreflections in a real scene. Furthermore, both examinations could be attributed to the different levels of intensity. The comparison we make with the Scale of Frandsen is based upon research of Xia *et al.* (2016-II) who used three levels of diffuseness (21%, 30% and 39%) related to Frandsen’s Scale of Light. She suggested that observers are not able to indicate the level of diffuseness because it largely interacts with the level of intensity. Since we notice a correspondence with the conclusion of Xia *et al.* based upon the levels of diffuseness, the measured levels of diffuseness (0,28% – 0,44%), and the difficulty to examine the diffuseness, we therefore confirm that the level of diffuseness is difficult to align.

On the limitation of the visualization of the light field by images of objects, it should be noted that a combination of possible measurement errors could negatively influence our results: the camera setting (manually setting of levels of exposure), its position and angle.

Light field visualization in the web application

Regarding the web application (Kartashova *et al.* 2016), our results confirm that it is a valuable tool to gain an impression of the light field in a scene when understanding the light field’s properties. Moreover, the visualization is able to give an impression at once of the light field’s situation, rather than comparing different graphs. However, exact values are not presented. For the evaluation of the light direction and intensity, we found that the light field can be visualized best by using the arrows rather than the ellipsoids. The visualization of the diffuseness is in both situations difficult due to the small measured differences.

8

CONCLUSION PART II

In Chapter 5 and 6 the light field has been analysed empirically to research the application of the tool use. Based on the results discussed in chapter 7, we present the conclusions in chapter 8. These conclusions formulate answers to the questions of how to measure the light field and how to visualize the light field. Finally, a number of learning points are set-up that form a base for the case study in chapter 9-12 of this research.

In a number of points an answer is worked out on the question:

How can variations in the light field be measured with a cubic illuminance meter in a daylight scene?

- A self built cubic illuminance meter, is able to simultaneously measure the light intensity, light direction and diffuseness in a point in a daylight scene, when the following rotation is applied:

By rotating the cube 45° around y-axis and 35° around x-axis, way no face is parallel to the light factor, resulting in a $D_{\text{cuttle, normalized}}$ that is less prone for error.

- To measure the light field in a daylight office meeting space, a single gridline is sufficient to restore the light field of a daylight scene.

- The cubic illuminance meter represents a single point in a scene, but is in fact a larger cube. As a point in 3D space is either completely in a shadow or not, we need the cube to be as well. When parts of the cube are in the shadow, e.g. of a windowsill, and other parts are not, measurement errors appear. Clear sky types have a strong directional component that can cause shadow patterns in an interior setting, making these sky types more vulnerable for such measurement errors.

The answers on the following question:

How can variations in the light field be measured with a cubic illuminance meter in a daylight scene?

- A rough textured white object is a valuable tool to give an (immediate) robust impression of the light field in a situation of collimated light for clear sky types. In this situation,

the light direction is strongly visible and the light intensity indicative. The diffuseness however, is not clearly captured due to ambiguity with the intensity. This can be also due to interreflections in the room. For evaluating the light direction, an object with increasing visible faces provides a better estimation of the light direction in a HDR image.

- The angle of making a photograph relative to the light direction has influence on how the object is perceived. Three angles were photographed in which the light altitude is best visible when the object is photographed perpendicular to the incoming light.

- The web application by Kartashova is a valuable tool to gain an impression of the light field in a scene when understanding the light field's properties. When the single points are positioned in a gridline, the light field is clearly visualized. For the evaluation of the light direction and intensity, the visualization using arrows work best.

LEARNING POINTS

Overall, the discussed results form a basis for the case study presented in part III:

- A cubic illuminance will be used to measure the light intensity, light direction and diffuseness.
- A rough textured white ball is used for immediate visualization of the light field to give a visual indication of the light field's situation in the scene.
- Due to time limitations only angle B, perpendicular to the light direction, will be photographed.
- In addition to the immediate light field visualization by using objects, the visualization by arrows generated by the web application by Kartashova is used since it is a valuable tool to gain an impression the light field too.

PART III
RESEARCHING THE
LIGHT FIELD THROUGH A
CASE STUDY

METHOD - CASE STUDY

For the final analysis of this research a case study will be performed in an office room at the faculty of Civil Engineering (Ct2.72), which is known as a visually uncomfortable office meeting space in terms of daylight glare probability. The aim of the case study is to compare the light intensity, light direction and light diffuseness to the discomfort metric: Luminance Contrast Ratio (CR).

Paragraph 9.1 introduces the case study. Paragraph 9.2 elaborates on the in-field measurement that consists of a measurement using: (i) the luminance camera equipped with a fish-eye lens to measure the actual level of visual comfort, (ii) the cubic illuminance meter, (iii) and the luminance camera with normal lens to visualize the objects. Paragraph 9.3 elaborates on the set-up of the validation and calculation model of room Ct2.72 (in 3D modelling program Rhinoceros® 3D (Rhino) using DIVA Radiance as a plug-in).

9.1 PROBLEM DESCRIPTION CASE STUDY

Room ct2.72 is an office room located at the faculty of Civil Engineering, at Delft Technical University. Visual uncomfortable daylight situations are experienced, especially during the morning office hours (9:00-12:00h). When a person is positioned, viewing the window, glare seem to appear (figure 9.1).

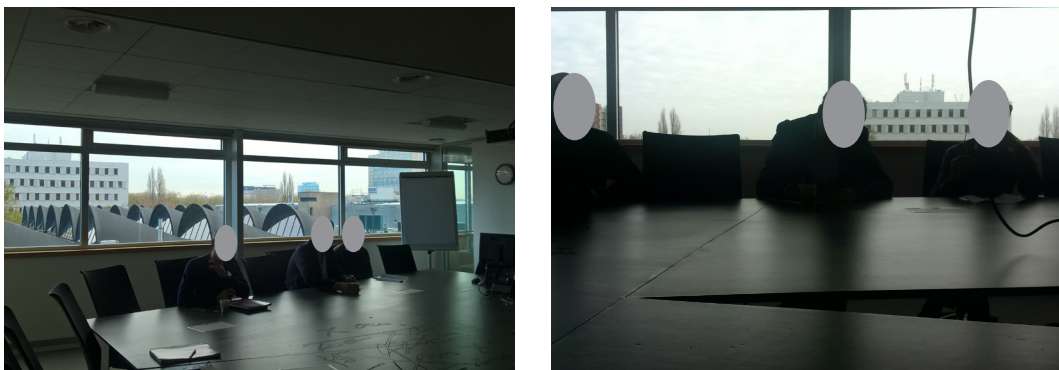


Figure 9.1 An impression of room Ct2.66 (similar to Ct2.72) during use, photographed on November 3rd, 11:05h.

9.2 MEASUREMENT

This paragraph elaborates on the measurement which took place in the morning of November 21 and December 1. Paragraph 9.2.1 describes the spatial design of room Ct2.72. Paragraph 9.2.2 presents the calculation method of the luminance Contrast Ratio (CR) and the DGP. Paragraph 9.2.3 refers to chapter 6 that describes the use of the cubic illuminance meter. Paragraph 9.2.4 presents two visualizations method; one with the luminance camera with the normal lens, and the web application visualization.

9.2.1 SPATIAL DESIGN CT2.72

The assessed office room, is a general meeting space. Figure 9.2 presents a section- and plan drawing. The room is 7,3m wide, 7,2m deep and 2,4m-3,2m high. The orientation is 66 degrees east from north, located in Delft. Walls and ceiling are painted and only the façade wall has windows with double glazing. The main room surface reflectances were obtained by using a luminance disk with a reflection factor of 95,2% and a luminance camera with normal lens. Gridline A and B define the eye-level of a standing and sitting person.

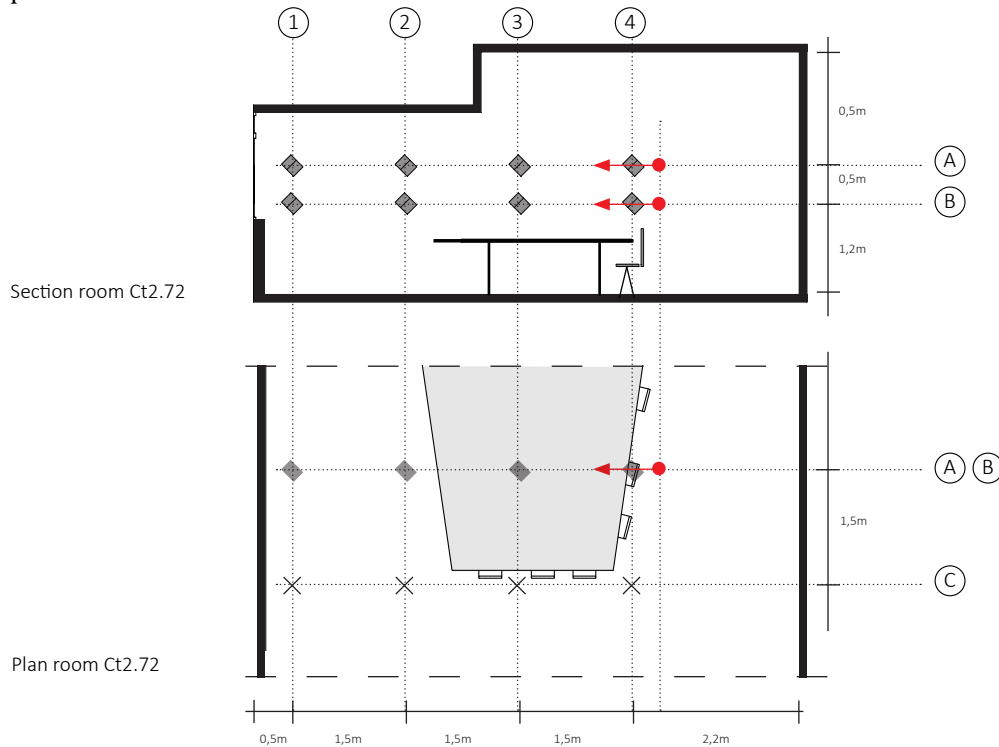


Figure 9.2 Plan drawing and section (left) of room ct2.71 at the faculty of Civil Engineering. (Right) An image of the room with the view direction towards the façade.

9.2.2 VISUAL COMFORT METRICS: LCR AND DGP

In this research the following visual comfort metrics were used; the luminance Contrast Ratio and the DGP, on which we elaborate one by one.

First, the luminances are measured by using a digital camera equipped with a fish-eye lens, i.e. a luminance camera. The camera is positioned on two positions, see the red dots in figure 9.2: on gridline A and gridline B facing the window. The calibrated luminance camera makes a series of 3 images, each with different exposure levels, set manually, combined into a high dynamic range (HDR) image. To calculate the luminance contrast ratio of the scene, a false-color map is created with *LMK Labsoft Techno Team* software. By

using the formulas 1 and 2 (chapter 2) the luminance Contrast Ratio are calculated for the specific view directions.

Second, the DGP is calculated with formula 3 (chapter 2). Therefore a luminance meter is vertically positioned just above the camera lens (the red dots in figure 9.2).

9.2.3 CUBIC ILLUMINANCE METER

The measurement approach of the case study was the same as the approach described in part II of this research. Paragraph 5.1 describes the use of the cubic illuminance meter. The overall proceedings were carried out as follows:

- The experiment was carried out on November 23 and December 1.
- After measuring the Luminance Contrast Ratio (paragraph 9.2.2),
- A cubic illuminance meter measured the light field at each gridpoint (A1-4; B1-4, in figure 9.2)

This sequence was repeated twice: a measurement without a table cover, and, a measurement with a white paper folded over the table. To gain understanding of the effect of adjustments in the room on the light field. The results were processed and used as a basis for a validation model in Rhino/Diva (paragraph 9.3).



Figure 8.3 (left) An impression of a luminance camera on a tripod photographing a hockey ball on a tripod, and (right) the installation of the cubic illuminance meter on a tripod at grid point A1. The left image shows the in white paper folded table as well.

9.2.4 LIGHT FIELD VISUALIZATION

The approach of the light field visualization of the case study was the same as described in part II of this research. Paragraph 6.2 presents the use of a luminance camera equipped with normal lens to visualize object's appearances and the web application by Kartashova. After measuring the cubic illuminance meter at each gridpoint (A1-4; B1-4), the proceedings were carried out as follows:

- Four tripods were set at the proper height (gridline A and gridline B, incl. and excl. table height) at gridpoint A/B1-4.
- A hockey ball positioned on each tripod was photographed from gridline C, perpendicular to the window (figure 9.3).

This sequence was repeated twice: a measurement without a table cover, and, a measurement with a white paper folded over the table.

After the measurement, the HDR images were processed into luminance false-color maps by using *LMK Labsoft software*.

9.3 COMPUTER-GENERATED MEASUREMENTS

After the measurement in room Ct2.72, which will form a base for the simulations, this paragraph elaborates on these simulations in Rhinoceros DIVA. First, the set-up of the validation model is presented in paragraph 9.3.1. Paragraph 9.3.2 elaborates on the method to run the various simulations on November 3 with the aim to improve the level of comfort in Ct2.72.

9.3.1 SET-UP RHINO MODEL - VALIDATION

To create a reliable simulation model of the daylight office space Ct2.72, the room is simulated in Rhino/DIVA using the ray-tracing Radiance simulation parameters as follows:

- A simplified model with the same dimensions as room Ct2.72 was developed (7,3m wide, 7,2m deep and 2,4m-3,2m high; orientation 66 degrees east from north)(figure 8.4).
- The location set for the simulation was Amsterdam, due to limited weather data.
- The main room surface reflectances (ceiling, facade, floor, glazing, table, walls) were selected (table 9.1) based upon the materials available in the Radiance library, on <http://lighting-materials.com> and own settings:
Radiance lighting materials for simulation are defined by 5 values: the R-, G-, B-reflectance, the specularity and the roughness.
- 8 cubes were modelled with a rotation of 45° around the y-axis and 35° around the x-axis with a node in the centre of each face, resulting in 48 illuminance values reported for comparison⁵. During measurement the layer with the cubes was turned of and only the nodes were present for calculation. The cubes were simulated on grid level A.
- The validation was set on 2017-12-01 10:15h, using a CIE Overcast Sky with the following advanced Radiance Parameters: -ab 7 -ad 1500 -as 100 -ar 300 -aa 0.1 (appendix K).
- The output in Excel, the radiance values in R,G,B-setting, were converted using the formula: $luminance\ value = R*0.265 + G*0.67 + B*0.065$ *179
Formula 2-21 were applied to calculate the light intensity, light direction and light diffuseness using Microsoft Excel.
- The fish-eye visualizations were generated from gridline A (red dot figure 9.2) and analysed via the average luminance values given by rectangles (appendix G).

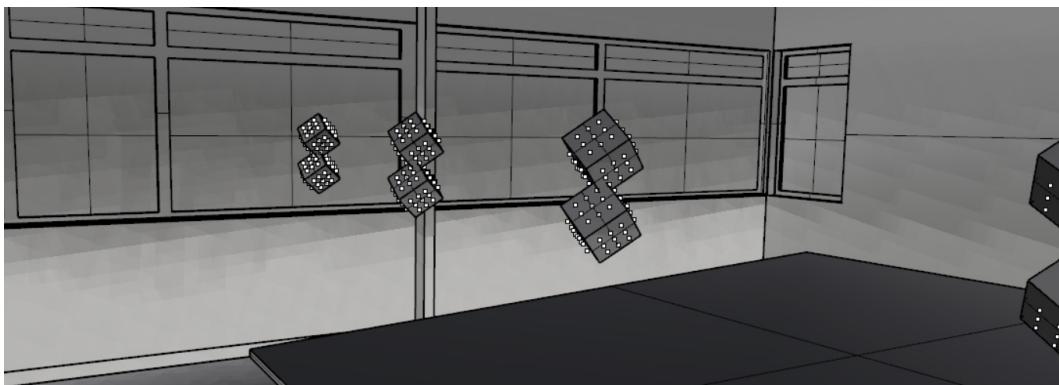


Figure 9.4 Screenshot of the interior, including the cubic illuminance meters, of the Rhino/DIVA model of room Ct2.72.

⁵ Radiance lacks the possibility to centre a single node on a face. Therefore, a grid of 9 nodes has been created on each face of all 8 cubes, resulting in 432 data points. However, only 48 centre points were used in the analysis of the simulation.

The given configuration is the final validated model, referred to as the *reference model*. The configuration of the reference model was chosen from various other models. Within a trial-and-error process, the variables (i.e., surface materials) were changed until the illuminance values on each face of the cube agreed most with the measurement. And so that, subsequently, the light intensity, light direction (i.e. altitude and azimuth) and light diffuseness agreed as well.

Since there is no usual procedure for such model evaluation, we applied the following regarding the statistical analysis: the horizontal illuminance, measured in the window sill, serves as a reference for the light intensity. And so, the error for the light intensity is given by the difference in lux between the simulation and the measurement, relative to the lux measured in the window sill. The error for the light direction is given by the difference in degrees relative to the maximum difference, 180°. Additionally, the vector angle between the vectors is a measure of difference as well. The diffuseness is a normalized quantity, hence the error is described as relative to 1.

Table 9.1 Radiance material configuration used in the reference model of room Ct2.72.

Material	Description Radiance Material	Optical properties
Ceiling	void plastic White_ceiling_panels_85 0 0 5 0.8574 0.8495 0.7980 0.0047 0.0000	85% reflectance
Facade	void plastic OutsideFacade_30 0 0 5 0.30 0.30 0.30 0 0	30% diffuse reflectance
Floor	void plastic GenericFloor_20 0 0 5 0.2 0.2 0.2 0 0	20% reflectance
Glazing	void glass Glazing_DoublePane_ Clear_80 0 0 3 0.87 0.87 0.87	80% visual transmittance, 87% visual transmissivity
Ground plane	void plastic OutsideGround_10 0 0 5 0.1 0.1 0.1 0 0	10 % reflectance
Table	0 0 5 0.0460 0.0456 0.0463 0.0668 0.0000	37 % reflectance
Walls	void plastic GenericInteriorWall_50 0 0 5 0.5 0.5 0.5 0 0	50 % diffuses reflectance

9.3.2 SIMULATION

With the *reference model* as a base (table 9.1), new simulations can be run. In these simulations we adjusted parameters of the reference model in order to make an attempt for improvements in the room regarding the level of visual comfort (table 9.2; figure 9.5). The simulations were run with the date set on November 3, 11:00h, based upon the experienced visual discomfort presented in the photographs of figure 8.1. For the calculations of the cubic illuminance values, we set the *point-in-time illuminance* on 11 03 11.00, with an *CIE Clouded Sky*. The 180 degree fish-eye visualizations are based upon the same date and sky-type.

The differences between the various models (8 in total) consist of either adjustments of the table cover (model B,C: a white matt table or a black matt table) or the lay-out of the room (model D-F: horizontal overhang, triple glazing, horizontal louvers)(table 8.2), or both (model F).

Moreover, the horizontal overhang has a width of 160cm. The horizontal louvers have a size of 2,0x10,0cm over the width of the room, under an angle of 45° (figure 8.5).

Table 9.2 Radiance material configuration used in the various models (B-F) based upon the reference model of room Ct2.72.

Adjusted model no.	Adjustment in:	Adjustment made:
A (reference model)		
B	table	white matt table (total reflectance: 91% specular reflectivity: 0%) 0 0 5 0.9193 0.9187 0.8881 0.0000 0.0000
C	table	black matt table (total reflectance: 4,7% specular reflectivity: 0%) 0 0 5 0.0460 0.0456 0.0463 0.0 0.0000
D	lay-out	horizontal overhang
E	lay-out	triple glazing (visual transmittance: 47% visual transmissivity: 96.2%) 0 0 3 0.5135 0.5135 0.5135
F	lay-out + table	horizontal louvers + white matt table (see model B)
G	lay-out	horizontal louvers
H	table	white shiny desk (total reflectance: 91% specular reflectivity: 6,68%) 0 0 5 0.9193 0.9187 0.8881 0.0668 0.0000

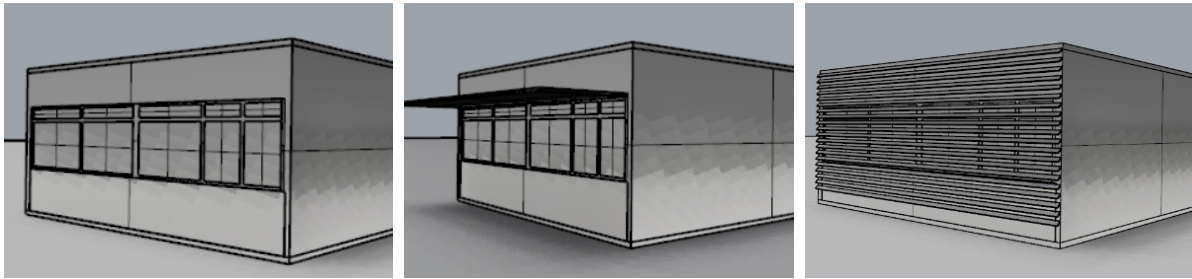


Figure 9.5 Screenshot of various adjusted Rhino/DIVA models of room Ct2.72. From left to right: the reference model; the model with 1,5m horizontal overhang; the model with horizontal louvers

10

RESULTS - CASE STUDY

The results of the case study in office room Ct2.72 are presented in this chapter. Paragraph 10.1 presents the results of the in-field measurement, with the cubic illuminance meter and the luminance camera with fish eye lens, in room Ct2.72 with a clouded sky on December 1. Paragraph 10.2 elaborates on the results of the validation of the simulated model in Rhino/DIVA of room Ct2.72 on December 1. Furthermore, the results of the various adjusted simulations on November 3 are presented.

10.1 MEASUREMENT

This paragraph presents the results of the measurement in room Ct2.72. To increase confidence in the experimental data two series of measurements were performed; on November 21 and December 1. The results of the measurement on December 1 are given in this paragraph. The results of measurement on November 21 are shown in Appendix I.

First, paragraph 9.1.1 presents the measured room surface reflectances. Paragraph 10.1.2 defines the level of visual comfort in terms of the luminance Contrast Ratio and the DGP. Paragraph 10.1.3 shows the results of the cubic illuminance meter and object visualizations are shown.

10.1.1 SPATIAL DESIGN: ROOM SURFACE REFLECTANCES

The measured main room surface reflectances are presented in table 10.1. An example image of the table is presented in figure 10.1. Appendix H elaborates on the other images taken.

Table 10.1 Measured room reflectances by using a disk with a reflectance of 95,2%.

	Mean luminance disk	Mean luminance surface	Reflectance surface
Main room surfaces	[cd/m ²]	[cd/m ²]	[%]
Table	4,8	2,9	58
Ceiling	6,4	12,1	180
Wall	13,3	13,1	94
Floor	8,7	3,9	43

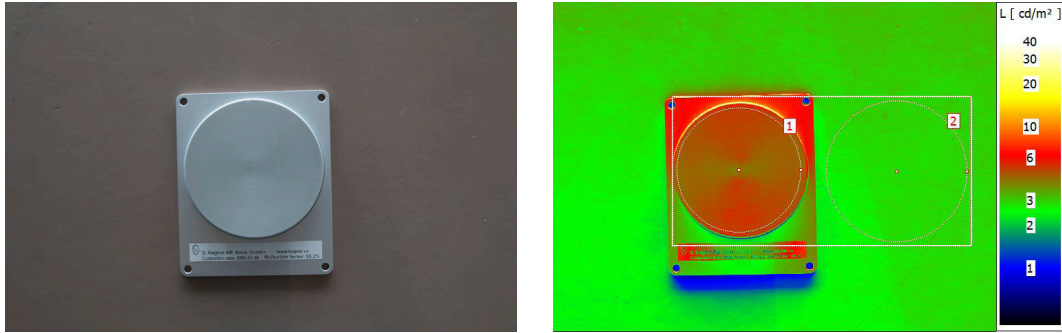


Figure 10.1 (left) A disk with a reflection factor of 95,2% positioned on the table in room Ct2.72. By turning the image into false color map (right) the relative reflectivity can be measured.

10.1.2 VISUAL COMFORT METRICS: LCR AND DGP

This paragraph presents the results of the visual comfort metrics; LCR and the DGP, measured in a setting without a table cover and including a table cover.

The DGP is calculated with formula 3 (paragraph 2.3) at the height of gridline A (=1,41m) and gridline B (=1,18m). The height mimics the height of eye level of a person sitting and standing at the table. The level of DGP is presented in table 10.2

The results of the measured Luminance Contrast Ratios on gridline A and B are given in table 10.3 which corresponds to the images presented in figure 10.2.

Table 10.2 Vertical lux measurement taken above the camera lens during the Luminance Contrast Ratio measurement, on December 1, 10:15h.

	Measurement excl. white table cover		Measurement incl. white table cover	
	E_v [lux]	DGPs _{wienold}	E_v [lux]	DGPs _{wienold}
gridline A (=1,41m)	643	0,22	1189	0,26
gridline B (=1,18m)	983	0,25	1326	0,27

Table 10.3 The results of the luminance ratio (=max/mean) of the measurement on December 1, 10:15h. The table corresponds to the images in figure 9.2.

	Gridline A - Incl. table cover				Gridline B - Incl. table cover			
	Min	Max	Mean	Contrast Ratio	Min	Max	Mean	Contrast Ratio
Ergorama (30°) - circle 2	7,2	647	114,3	1:5,7	6,8	667	139,9	1:4,8
Ergorama (60°) - circle 3	0,7	648,7	52,46	1:12,4	0,6	667	60,63	1:11

	Gridline A - Excl. table cover				Gridline B - Excl. table cover			
	Min	Max	Mean	Contrast Ratio	Min	Max	Mean	Contrast Ratio
Ergorama (30°) - circle 2	3,6	394	76,3	1:5,2	5,4	527,6	116	1:4,5
Ergorama (60°) - circle 3	0,3	399,1	31,9	1:12,5	0,3	527,6	46,4	1:11,4

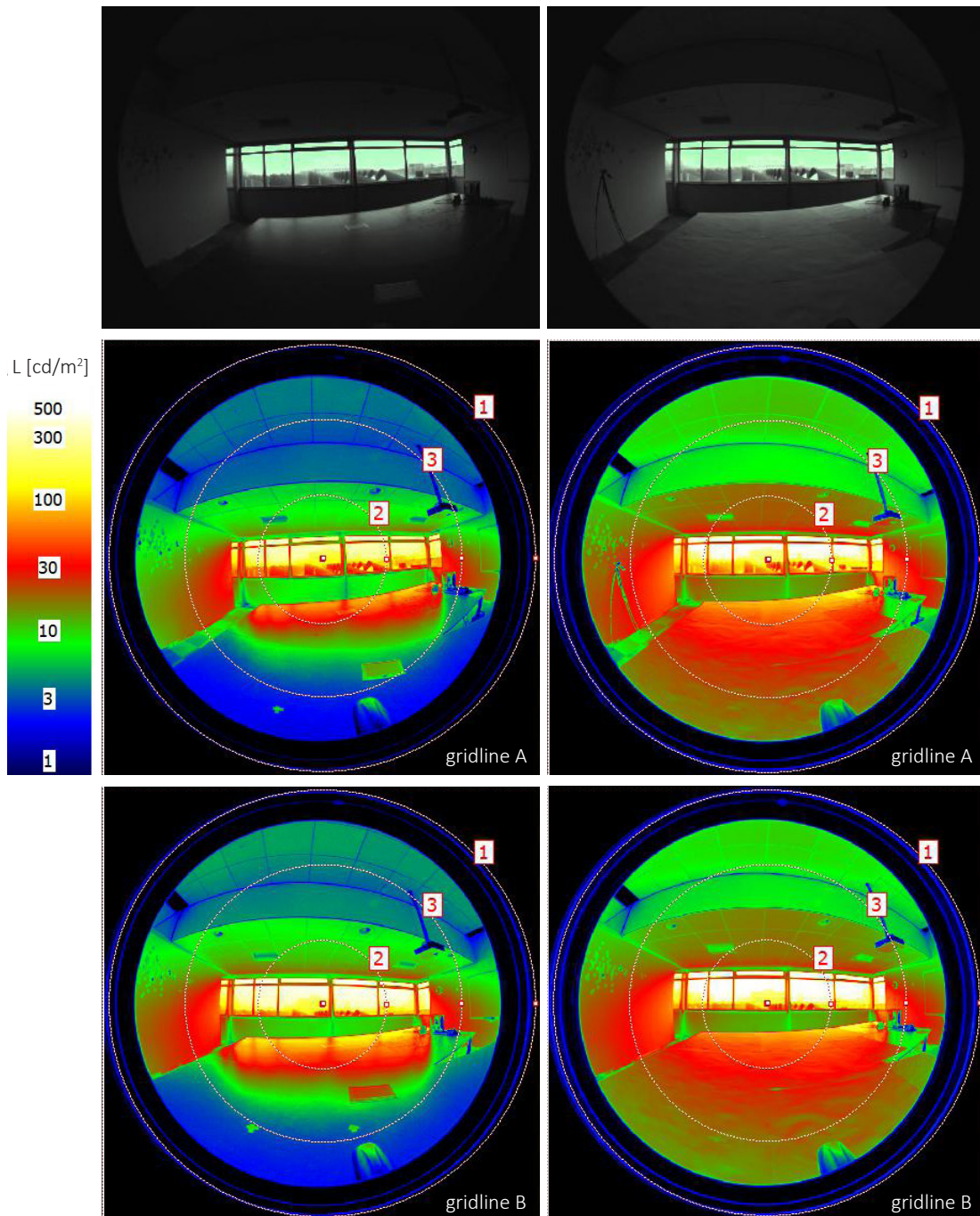


Figure 10.2 HDR images (topline) and false-color luminance maps (2nd and 3rd row) of fish-eye camera images of room CT2.72 on December 1. Gridline A has a height of 1,41m, and gridline B a height of 1,18m. The images left show the office room without table cover, and, right including table cover. Circle 1 represents the ergorama (30°) and cricle 2 the panorama (60°)

10.1.3 CUBIC ILLUMINANCE METER

The calculated light intensity, light direction and diffuseness (formula 4-20) are presented in the graphs in figure 10.3. The raw data of this measurement on December 1, 10:15h is given in the appendix J. The red bar in the figure 10.3 presents the range of observers' preference according to Cuttle (2008).

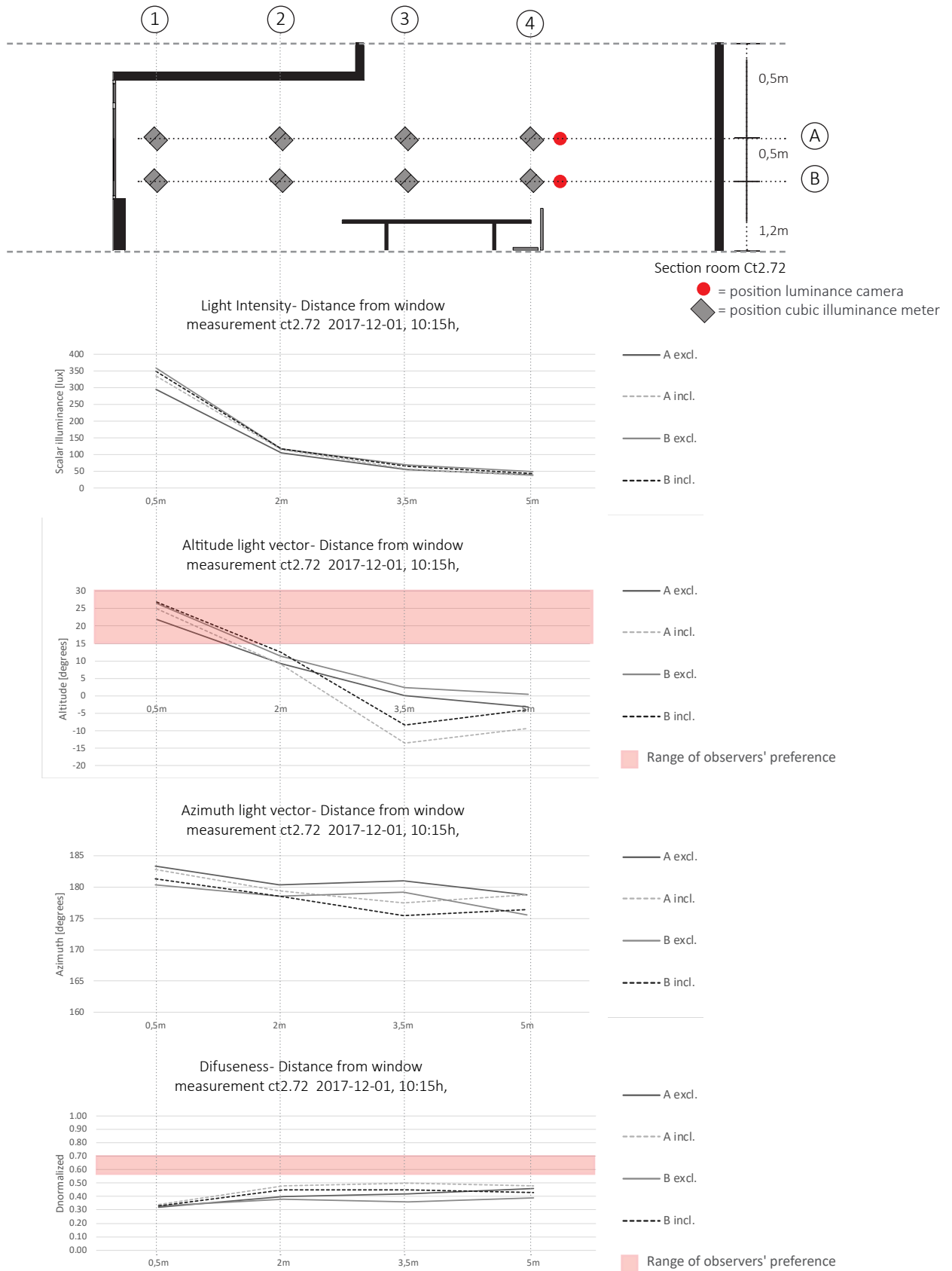


Figure 10.3 The calculated light intensity, light direction (altitude and azimuth) and the diffuseness at a distance of 0,5m-5m from the window (gridpoint 1-4), on gridline A (=1,41m and B (=1,18m). The results are extracted from the cubic illuminance measurement on December 1st, 10:15h in room Ct2.72.

10.1.4 LIGHT FIELD VISUALIZATION

The light visualization is split into the visualization with the web application of Kartashova (figure 10.4) and how the light field is depicted on rough textured white spheres (figure 9.5).

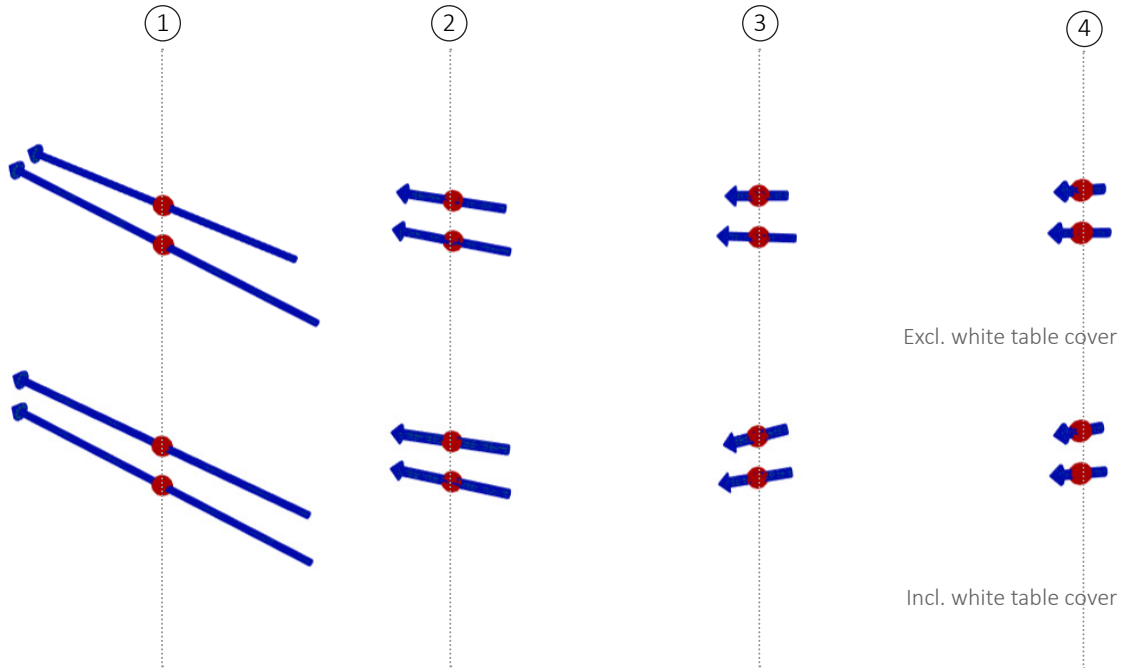


Figure 10.4 A web application visualization in arrows (scale 0) of the measured light field on gridline A and B at position 1-4 in the room ct.72, on December 1, 10:15h with an overcast sky (CIE).

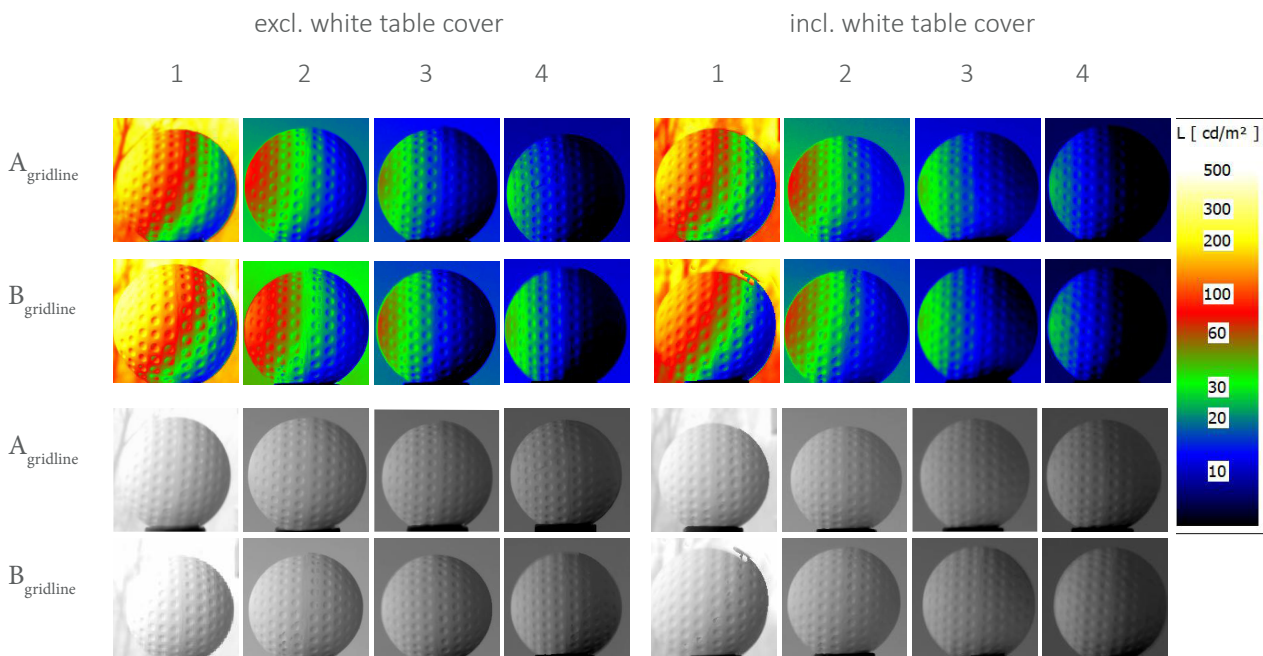


Figure 10.5 A Visualization of objects' appearance in false color images and normal colors. of room CT.72 on December 1, 10:15h. Gridline A has a height of 1,41m, gridline B a height of 1,18. The images left show the office room without table cover, and, right including table cover.of the measured light field on gridline A and B at position 1-4 in the room ct.72, on December 1, 10:15h with an overcast sky (CIE).

10.2 COMPUTER-GENERATED RESULTS

The results from the measurements presented in paragraph 10.1 are used as a basis for the validation of the simulation model. This paragraph presents the computer-generated results. Paragraph 10.2.1. elaborates on the validation of the model of room Ct2.72. Paragraph 10.2.2 elaborates on the simulated results of the validated model.

10.2.1 VALIDATION

To create a reliable Rhino/DIVA simulation model of room C2.72, the model is validated for each cubic illuminance meter over different positions (A1-4; B1-4). This was done using the illuminance values of the measurement on December 1, 10:15h (paragraph 10.1). This will be presented first. Then, an impression of a fish-eye image and a false-color map, resulting in the luminance Contrast Ratio, is given.

The light field

In an iterative process, the room surface materials and the lay-out of the real room were constructed and manipulated in various models, resulting in a validated model referred to as the *reference model*. The material configuration of the reference model is presented in table 9.1 (paragraph 9.3). This reference model has the lowest simulation error of all other run simulations, see yellow bar in figure 10.6. The final result of validation in which the light intensity, the angle between the vectors and the light diffuseness matches best, is presented in table 10.3.

Appendix L presents the raw data of the simulated illuminance values on each face of the cube, as well as the material configurations of the other simulation models.

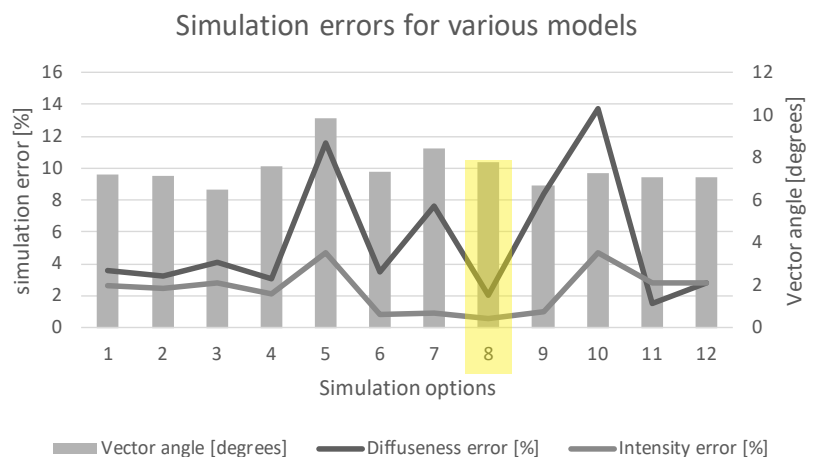


Figure 10.6 Results of comparison between measurement and various simulation models on December 1, 10:15h, each with a different Radiance material configuration. The statistical analysis regarding the error for the light intensity is given by the difference in lux between the simulation and the measurement, relative to the lux measured in the window sill. The vector angle between the vectors is a measure of difference as well. The diffuseness is a normalized quantity, Hence the error is described as relative to 1. All results are stacked in a column, the lowest values (option 8- yellow bar) will be used during further simulations.

Table 10.4 Results of comparison between measurement and simulation on December 1, 10:15h. The statistical analysis regarding the error for the light intensity is given by the difference in lux between the simulation and the measurement, relative to the lux measured in the window sill. The vector angle between the vectors is a measure of difference as well. The diffuseness is a normalized quantity, Hence the error is described as relative to 1.

Comparison measurement simulation .(8)- *the reference model*
calculated intensity, angle between vectors and diffuseness

	Intensity		Angle between vectors	Diffuseness	
	E_{sr} [lux]		[degrees]	$D_{normalized}$	
	Measurement	Simulation		Measurement	Simulation
A1	295	303	2.00	0.32	0.36
A2	106	103	5.71	0.4	0.41
A3	55	53	10.75	0.42	0.38
A4	40	40	11.18	0.46	0.45
B1	360	364	1.26	0.33	0.36
B2	117	123	16.04	0.38	0.38
B3	70	63	7.05	0.36	0.34
B4	49	46	8.06	0.39	0.39
Difference		0,57 %	7.76		2,02%

Luminance Contrast Ratio

The reference model is the result of the validation based upon the measured cubic illuminances. The result of the 180° fish-eye visualization (gridline position A) is presented in figure 10.7 as well as the luminance false-color map. The result of the luminance CR give in table 10.5.

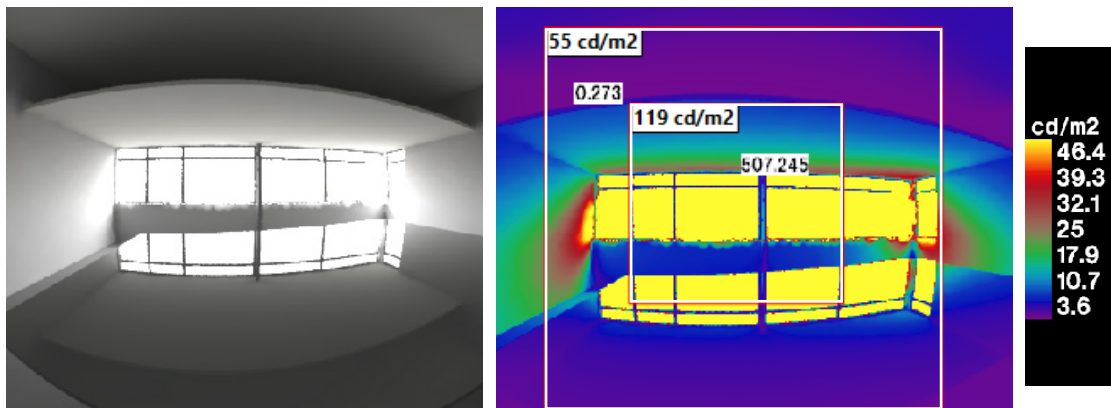


Figure 10.7 180 degrees fish eye visualization of the simulation model of Ct2.72, on gridline A. With (left) the impression of the modelled room and (right) the luminance false-color map. The squares on the false-color image present the ergorama (inner square) and the panorama (outer square) of the field of view. The values define the average, minimum and maximum luminance (cd/m^2)(table 10.5).

Table 10.5 Comparison between the Luminance Contrast Ratio (=max/mean) of the measurement and the simulation on December 1, 10:15h..

	Measurement 12 01 10.15h Overcast sky (CIE)			Simulation 12 01 10.15h Overcast sky (CIE)		
	mean	max	Ratio	mean	max	Ratio
	[cd/m^2]	[cd/m^2]		[cd/m^2]	[cd/m^2]	
Ergorama (30°)	71	290	1:4,1	119	507	1:4,3
Panorama (60°)	37	290	1:7,8	55	507	1:9,2

10.2.2 SIMULATION

The validated model forms a base for subsequent simulations. The various simulations are adjustments of the reference model. This paragraph presents the results of the simulation runs on November 3, 11:00h (Clouded Sky). The light field simulation of November 3, 11:00h (Clear Sky) are presented in appendix M.

First, the level of visual comfort is presented for each of the different models on the basis of the luminance CR visualized in Rhino/DIVA (figure 10.8A, 10.8B). The results of raw data to calculate the luminance CR are presented in table 10.6 and summarized in figure 10.9. In figure 10.8A an extra visualization is added (model A'') in which imaginary people are modelled, with a high luminance of 745,5 cd/m² and a low level of 3,5 cd/m² resulting in high contrasts.

Second, regarding the light field, the light intensity, light direction (altitude, azimuth) and the diffuseness levels of gridpoint A1-4 and B1-4 are presented in separate graphs in figure 10.10. The level of observers' preferences is indicated with a red bar. A visualization by the web application of Kartashova is presented in figure 10.11A (model A-E) and figure 10.11B (model F,G).

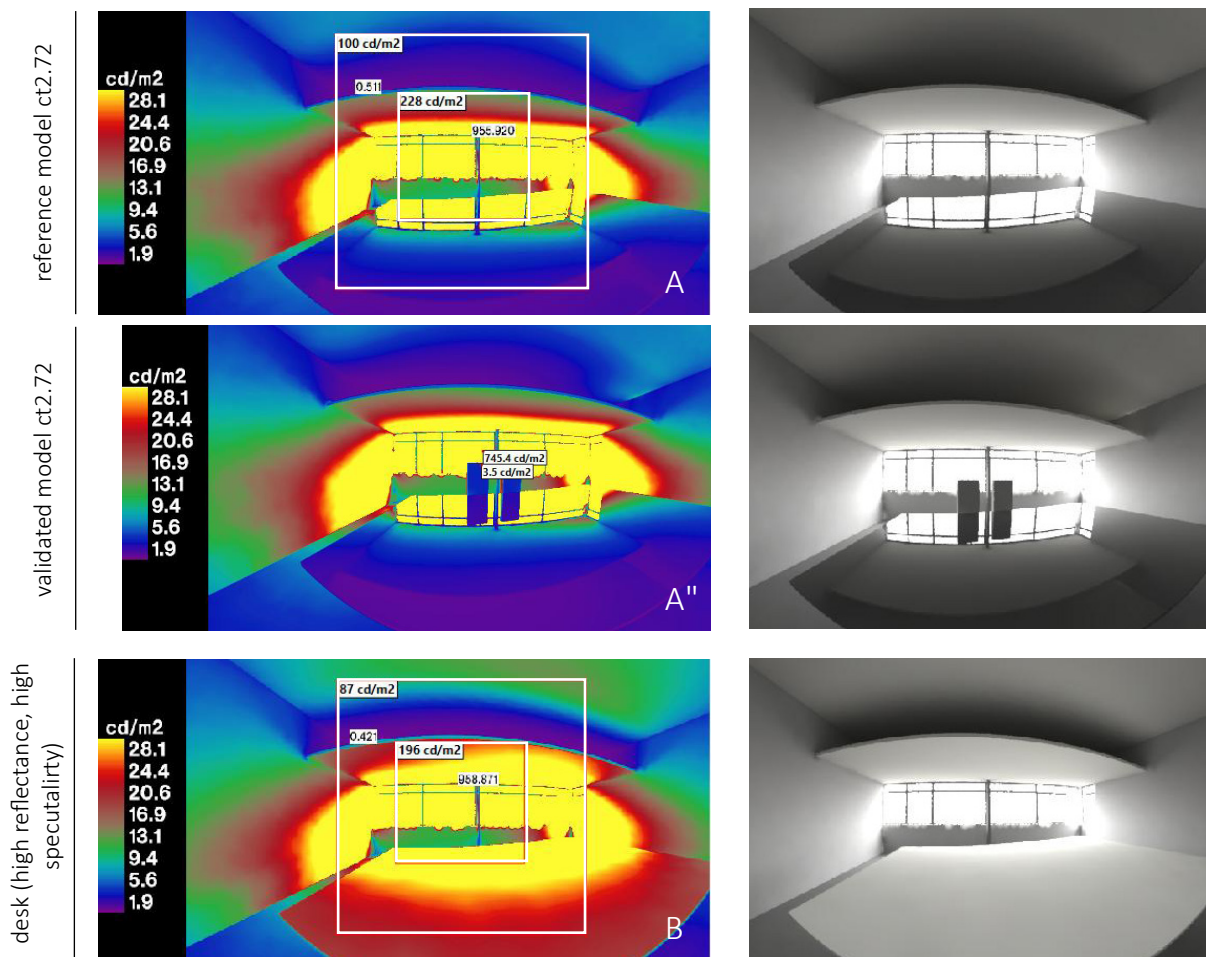
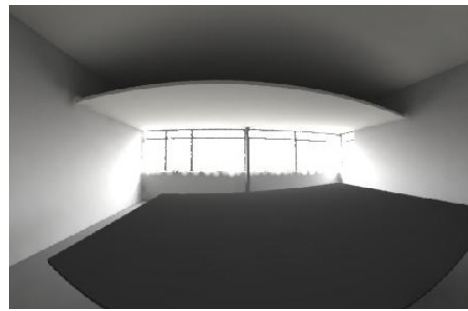
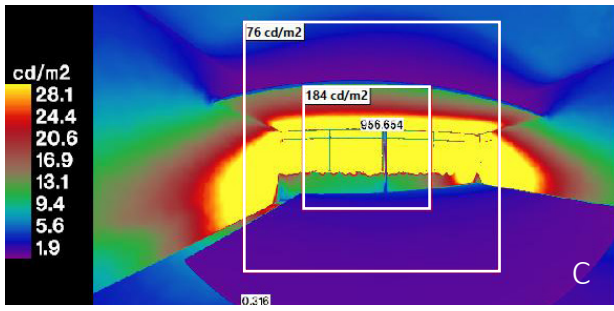
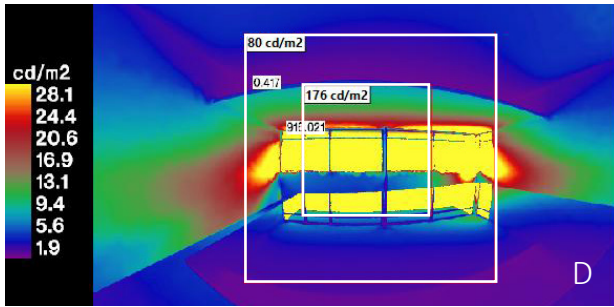


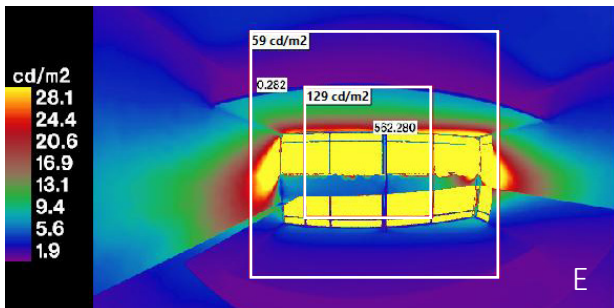
Figure 10.8 (top)(left) The false colour images of the simulations in overcast sky (A-E) and clear sky (A''-E'') on November 3, 11:00h in office room Ct2.72. The images present the following (material) adjustments: A presents the reference model in which (A'') people are added. Model (B) presents a white matt desk, (C) has a matt black desk, (D) is including a horizontal overhang of 1,5m width. Model (E) shows the model with triple glazing with 45% light transmittance instead of double clear glass with 80% light transmittance; (F) presents horizontal louvers and (G) horizontal louvers including a matt white table, (H) is a white shiny table cover.



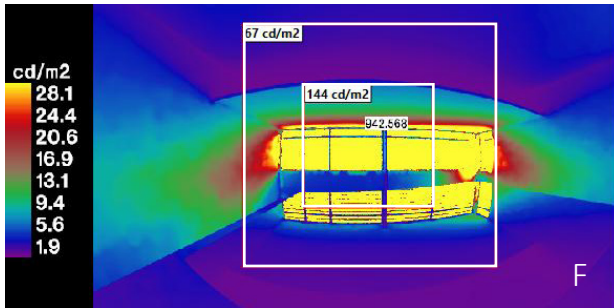
desk (low reflectance, high specularity)



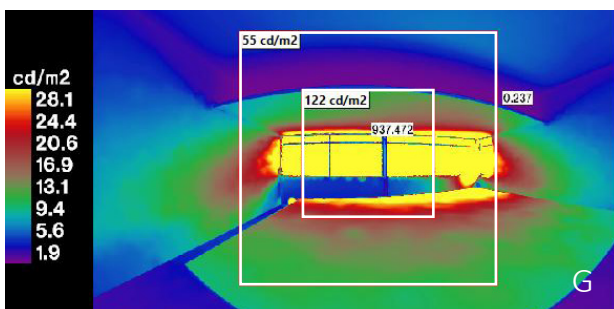
horizontal overhang



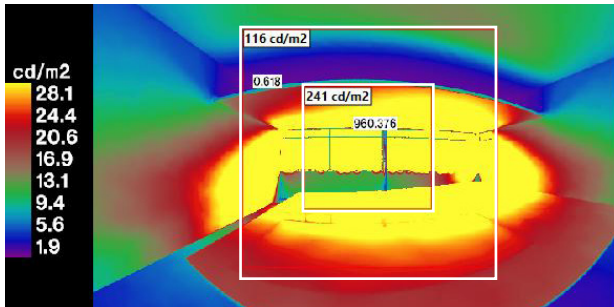
Light Transmittance 47% instead of 80%



horizontal louvers



horizontal louvers + white desk



white shiny desk

Table 10.6 Luminance Contrast Ratio measured in various simulations models (A-G) with overcast sky on November 3, 11:00h. The tables are related with the images in figure 9.8.

image A	reference model ct2.72 (black shiny table)		
	mean	max	Ratio
	[cd/m ²]	[cd/m ²]	
Ergorama (30°)	228	956	1:4,2
Panorama (60°)	100	956	1:9,6

image E	light transmittance 47% instead of 80%		
	mean	max	Ratio
	[cd/m ²]	[cd/m ²]	
Ergorama (30°)	129	562	1:4,4
Panorama (60°)	59	562	1:9,5

image B	white matt table		
	mean	max	Ratio
	[cd/m ²]	[cd/m ²]	
Ergorama (30°)	196	959	1:4,9
Panorama (60°)	87	959	1:11

image F	horizontal louvers		
	mean	max	Ratio
	[cd/m ²]	[cd/m ²]	
Ergorama (30°)	144	942	1:6,5
Panorama (60°)	67	942	1:14,1

image C	black matt table		
	mean	max	Ratio
	[cd/m ²]	[cd/m ²]	
Ergorama (30°)	184	957	1:5,2
Panorama (60°)	76	957	1:12,6

image G	horizontal louvers + white desk		
	mean	max	Ratio
	[cd/m ²]	[cd/m ²]	
Ergorama (30°)	122	937	1:7,7
Panorama (60°)	55	937	1:17

image D	horizontal overhang		
	mean	max	Ratio
	[cd/m ²]	[cd/m ²]	
Ergorama (30°)	176	916	1:5,2
Panorama (60°)	80	916	1:11,5

image H	white shiny desk		
	mean	max	Ratio
	[cd/m ²]	[cd/m ²]	
Ergorama (30°)	241	960	1:3,9
Panorama (60°)	116	960	1:8,3

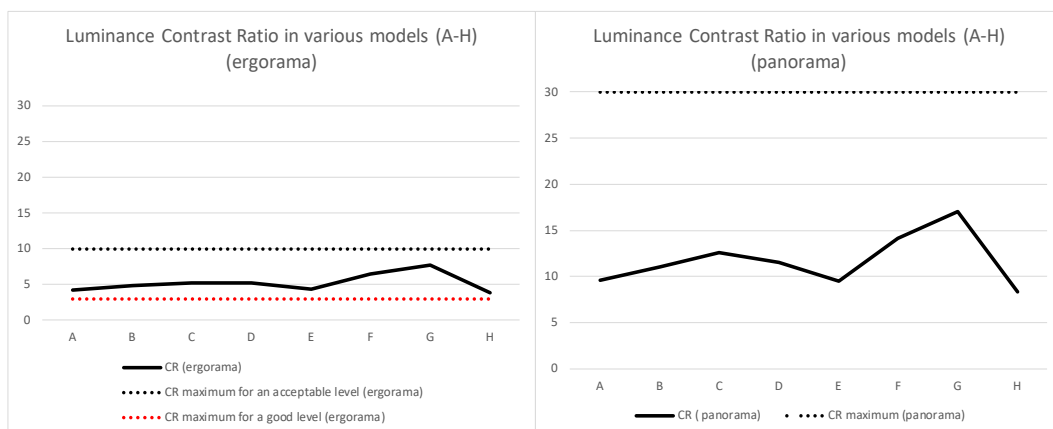


Figure 10.9 The measured and recommended Luminance CR for models (A-H) with overcast sky on November 3, 11:00h. A summary of figure 10.8 and table 10.6.

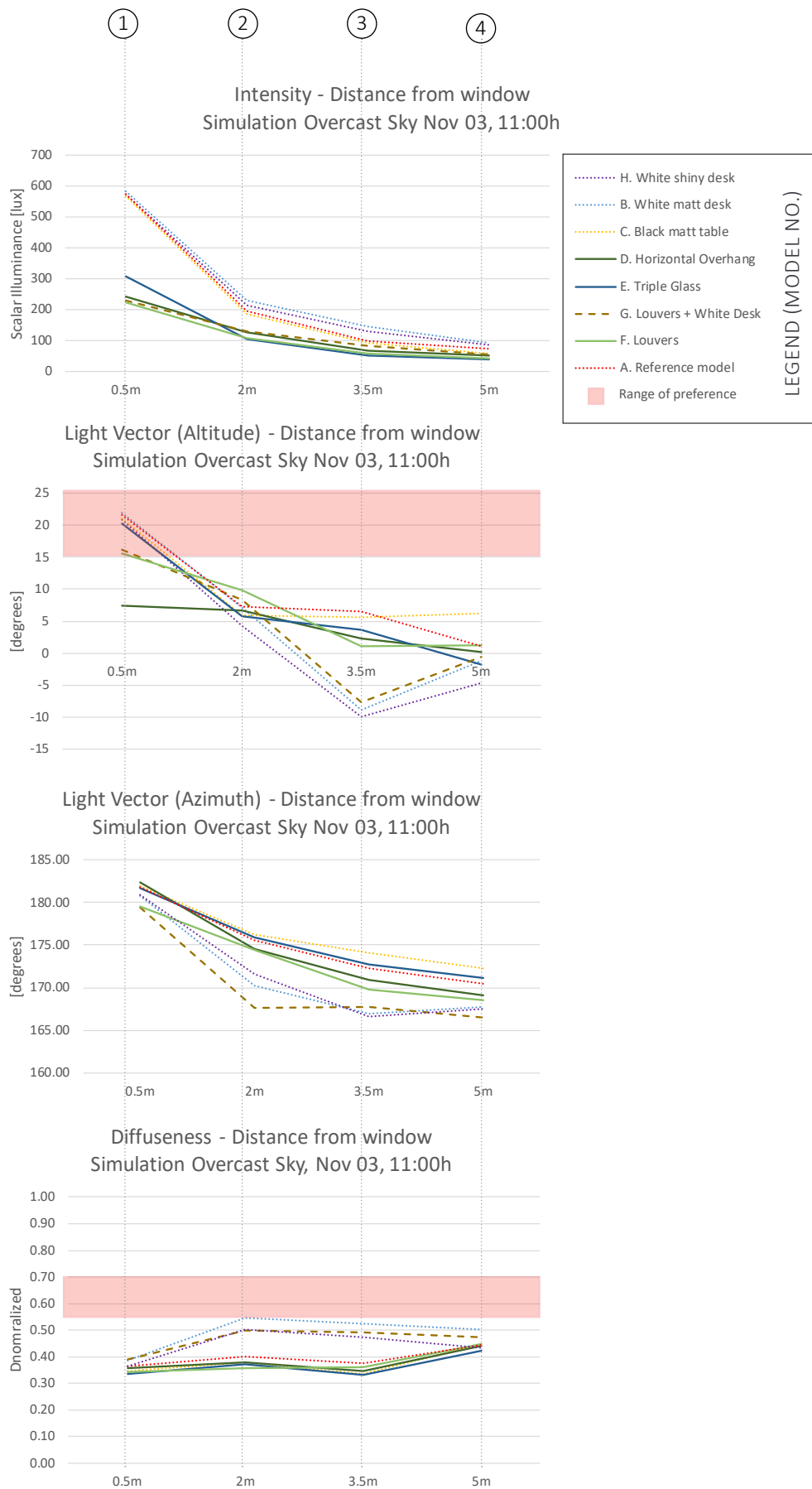


Figure 10.10 Light intensity, light direction (altitude, azimuth) and light diffuseness in simulations with overcast sky on November 3, 11:00h.

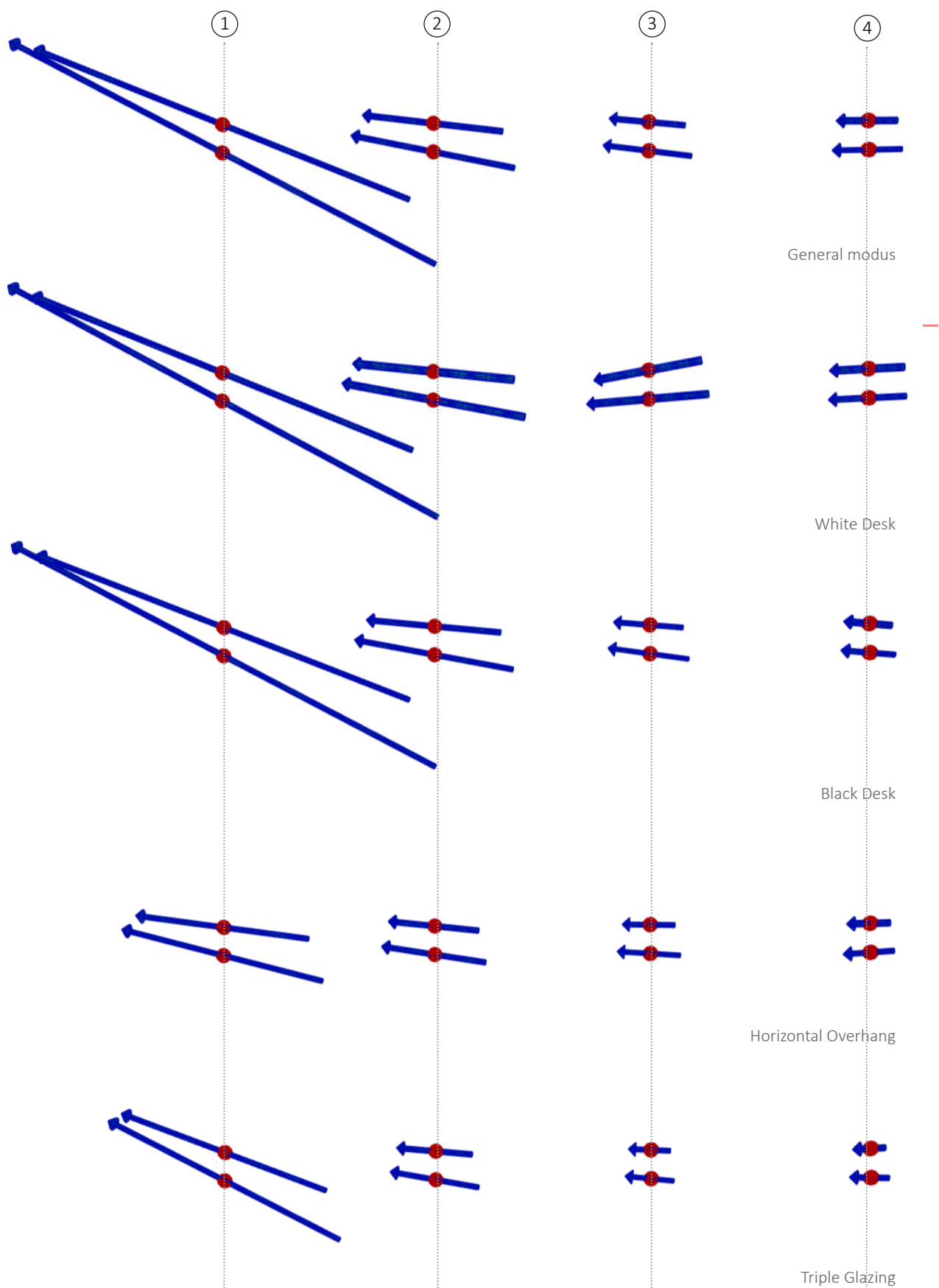


Figure 10.11 A visualization by arrow (scale 0) of the simulations on November 3 with an overcast sky (CIE) on gridline A and B at position 1-4 in the room ct2.72.

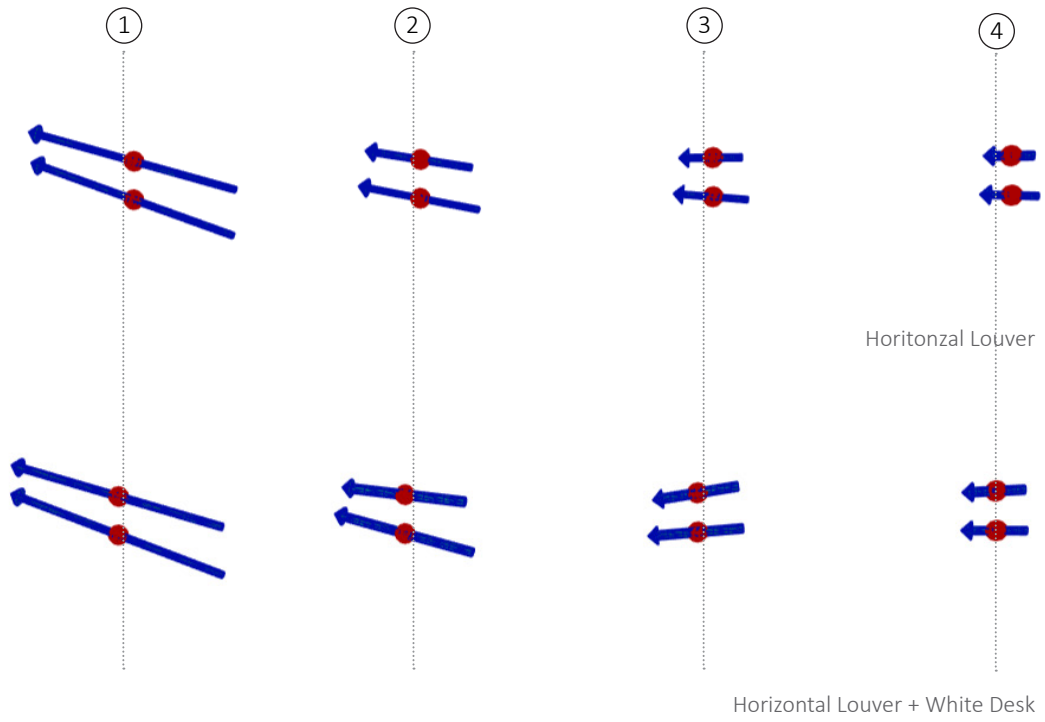


Figure 10.12 A visualization by arrow (scale 0) of the simulations on November 3 with an overcast sky (CIE) on gridline A and B at position 1-4 in the room ct2.72.

11

DISCUSSION PART III

Visual discomfort in daylight scenes is expressed in many different performance-based metrics, all view dependent. The building codes falls short on one universal accepted method to describe discomfort glare. Lately there has been an increased research interest in the three-dimensional analysis of light revealing its spatial quality. This analysis, of describing light in terms of light intensity, light direction and diffuseness in a scene, could be a way to predict visual uncomfortable situations in a daylight office space.

In this research, we conducted light field measurements and simulations, luminance Contrast Ratio- and DGP measurements, in a visual uncomfortable daylight office space (Ct2.72) to identify a potential relation and make improvements in the office space.

Due to the large amount of data processed in the measurements and simulation, the evaluation and interpretation of the results are subdivided. Paragraph 11.1 discusses the results from the in-field measurement on December 1. Paragraph 11.2 elaborates on the findings of the digital model subdivided in the evaluating of a validation model, and the results from various simulation models on November 3. The conclusions (chapter 12) are extracted from the findings of the measurement and simulations on December 1 and November 3, but assumed as generic.

11.1 MEASUREMENT

The aim of the measurement in room Ct2.72 was three-fold: (i) to determine the level of visual discomfort in terms of DGP and CR, (ii) to examine (the variations) in the light field, and (iii) to form a base for the validation of the simulation model. Furthermore, the aim of the measurement was to find a relation between (i) and (ii) to identify the potential difference between the analysis of light field and the luminance CR on the level visual comfort. All aspects are discussed one by one for the measurement without table cover and with table cover.

First, we found that there is no conformity between the levels of discomfort, determined by the luminance Contrast Ratio (CR) and the simplified Daylight Glare Probability (DGPs). Because room Ct2.72 is experienced as visual uncomfortable, we expect a high degree of DGPs and a low CR level. However, the level of DGP indicates an *imperceptible*

glare situation. The CR presents the opposite: The highest recommended ratio of 1:3 is exceeded in the ergorama, suggesting an uncomfortable scene, which is aligned with the experiences. The acceptable level for the luminance CR of 1:10:30 is not exceeded. And so, we find an ambiguity about the actual level of visual comfort. This is in line the absence of consensus in the lighting practice about one standard metric measuring visual comfort (Jakubiec, 2014). The imperceptible range of the DGP can be clarified with findings of Carlucci et al. (2015) who stated that the DGPs lacks a proper description when the observer faces a glare sources. Furthermore, our finding links to the discussion of Cuttle (2010) who claims that performance-based metrics are often not performance based at all.

An alternative explanation for the mismatch between the experienced level of discomfort and the measured values is the absence of people in the field of view during measurement. We'll further elaborate on this aspect in paragraph 11.3.

Furthermore, an interesting finding is that the perceived level of comfort (in luminance CR) is quite stable when the dark table cover is adjusted by adding a white paper cover (table 10.3). Despite the unchanging luminance Contrast Ratio, we examine a variation in appearance of the table. Moreover, the false-color map of the scene with a white covered table (figure 11.1 and table 11.1) presents a more acceptable luminance ratio of the level of 1:2,5. However, this is not passed on to the final luminance CR and the DGP. We attribute this to the strict view dependency of both metrics that does not follow the dynamic view directions of observers.

Second, we examined the light field physically and visually (i.e. using the cubic illuminance meter, and the luminance camera to photograph objects). We found that the diffuseness level is too low and the directionality too high resulting in disturbing contrasts, present on the white rough textured spheres. Moreover, the combination of a low diffuseness level and frontal directional lighting have a negative effect on the perceived spatial quality, as is in line with the experienced level of discomfort in room Ct2.72. To that end, the light field analysis provides information about the light distribution other than luminance and illuminance distributions. Our finding that the combination of directionality and a low diffuseness results in an uncomfortable scene, replicates the findings of an interview series conducted by Cuttle (2010) upon which the level of observers' preferences is based. Also Ganslandt and Hofman (1992) and Xia (2016) explain that certain ratios of diffuseness and directionality (although not defined) could prevent the presence of disturbing shadows.

Furthermore, we found that the effect of the adjusted table cover is clearly visible in the analysis of the light field regarding the altitude light vector. As a result of a higher

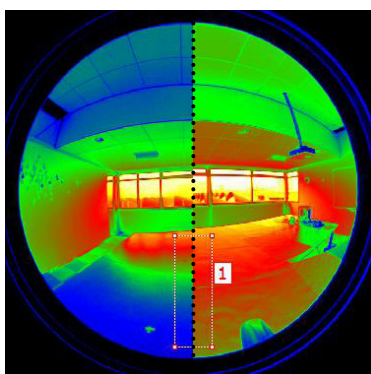


Figure 11.1 A part of the false-color map of room Ct2.71 excl table cover (left) and incl. table cover (right).

Table 11.1 Luminance values for the rectangle given in figure 10.1 in room Ct2.72 excl. white table cover and incl. white table cover.

Rectangle 1	excl white table cover	me incl. white table cover an
min [cd/m ²]	1,6	11,4
mean [cd/m ²]	11,8	31,1
max [cd/m ²]	77,8	79,1
ratio (=max/mean)	1:6,6	1:2,5

reflectance the average light direction variates.

Third, the conducted measurement is assumed as reliable working as a base for the simulation model. To minimize the measurement errors, we conducted two measurements (November 23, December 1) of which the first functioned as a test measurement. However, random errors due to the positioning of the cubic illuminance meter, and the time in-between each measurement point couldn't be prevented. A systematic error occurred when a ring was not removed from the fish-eye lens. This had been corrected in the analysis by taking a larger 180 degrees circle during the CR analysis in the luminance coloured HDR image (figure 9.2). Also problems appeared processing the images in LMK Labsoft: all false-color images had to be re-processed which was very time-consuming. Additionally, the accuracy of the measured surface reflectance appeared sensitive to the angle of photographing. This resulted in a overestimated surface reflectance of the interior ceiling. This has taken into account during the validation (paragraph 10.2). It is suggested to gain more experience working with the tools before during measurement, to minimize the above errors in future work.

Overall, we can conclude that the measurement and visualization set-up in room Ct2.72 was very time-consuming and complex. Extensive knowledge about the use of the tools and a proper preparation time was required. The measurements had to be conducted with precision and with the assistance of someone else. The availability of the measurement instruments and the office meeting space resulted in limited time and tools. And the results gained during the Overcast sky-type may not be valid for a clear sky-type situation. Therefore, a simulation model was validated which we will discuss in the next paragraph.

11.2 COMPUTER-GENERATED RESULTS

The digital results are discussed in two-fold. Paragraph 11.2.1 presents the discussion on the validation. Paragraph 11.2.2 elaborates on the adjustments in the simulations based upon the reference model.

11.2.1 VALIDATION

The aim of the validation model was to verify the accuracy of the simulation, which is in fact an imitation of a real daylight scene. Assuming a proper measurement (paragraph 11.2) the validated model, i.e. the reference model, functioned as a base for further simulations as discussed in paragraph 11.3. This paragraph elaborates on the validation process.

Reflecting, the validity of a simulation using the Radiance-based DIVA program is limited in the location setting (Amsterdam instead of Delft), and the amount of inter-reflections and rays sent out of a point. The simulated room (Ct2.72) is a basic example of the real scene. The predicted values are a rough estimation of the daylight situation in the room. In this research the DIVA software is assumed as reliable. It is beyond the scope of the research to analyse the accuracy of the raytracing software.

The final validated model has a low error between the simulation and the measurement in the calculated light intensity, light direction and diffuseness (respectively 0,57%; 7,76%; 2,%). Despite the absence of an usual validation procedure for measurements of the light field, only a small simulation error is allowed to achieve simulations that accurately display the measured values. The measurement was conducted on December 1, 10:15h with an overcast sky type. And so, the simulation was run on December 1, 10:15h with a

CIE overcast skytype. However, the determined simulation does not guarantee that the model agrees in another setting (i.e. different date/ sky condition). It could have been an option to compare the results of the measurement on November 24 (appendix I) with the reference model, but because this measurement was a test measurement this option is not executed.

An uncertainty within the validation process is the unlimited amount of values that can be changed and used in the simulation. Choosing the right *reference model* is difficult because you are not sure about if there's a better option to come.

The choice for what in the end became the reference model was partly based upon the low errors between simulation and measurement, but also on the appearance of the table cover in the visualization by Rhino/DIVA. An important finding was that the light field is largely influenced by both the specular and the diffuse reflectivity⁶, what seemed to be overlooked when measuring the room surface reflectance by using a disk (paragraph 10.1.1). The measured total reflectance of the table cover was 57%, but a Rhino visualization of the table with a 57% total reflectance did not match the appearance of the table in the real scene. It is suggested that this is due to the difference between diffuse and specular reflectivity that makes not only a difference between bright/dark but also between matt/shiny. So, despite the variety of default materials in the Radiance library, a new material had to be created in order to get the proper table cover; low reflectance, high specularity. This chosen material for the table in the reference model is assumptive and based upon appearance.

11.2.1 SIMULATION

Based upon the experienced level of visual comfort in figure 9.1 on November 3, 11:00h, (Overcast Sky) a reference model was simulated. We found that the visual uncomfortable setting in the reference model was caused by a combination of low diffuseness and a strong directionality of light (paragraph 11.1). To be able to formulate an answer on the question "How can scene adjustments improve the level of visual comfort?", the level of diffuseness and directionality should be altered.

In an attempt to do so, various models were created with adjustments relative to the reference model. These adjustments in the simulations (8 in total) consist of either adjustments of the table cover (model B,C: a white matt table or a black matt table) or the lay-out of the room (model D-F: horizontal overhang, triple glazing, horizontal louvers), or both (model F) (table 9.2).

First, we elaborate on the influence of the scene adjustments on the lower order properties of the light field (figure 10.10, 10.11A-B), and second, we consider the luminance CR (table 10.6, figure 10.8A-B). We'd assumed that the level of >3472 lux, needed to reach a *disturbing* level on the DGP, would not be reached, and left this out of the research (formula 4)(table 2.1).

Light Field

Many office rooms have interior surfaces with high reflectance to increase the level of daylight in the depth of the scene, and it is generally known that bright surfaces could cause glare. The black shiny table in room Ct2.72 is the opposite of both these advices.

⁵ The reflection of light can be subdivided in two types: (i) specular reflection is a one angle reflection from a smooth surface, and (ii) diffuse reflection is as light is reflected from a rough surface scattering to many angles.

As described in previous paragraphs the level of discomfort is caused by low diffuseness and strong directionality. Because diffuseness is considered as the vector/scalar ratio (formula 22) the chosen adjustments attempt to influence the light vector and the scalar illuminance.

The adjustments are subdivided as follows: (i) Adjustments are based upon influencing the light direction in the room (improvement of the table material), (ii) in the scene (horizontal louvers), or (iii) the effect of a lowered light intensity in the room (horizontal overhang, glazing).

Considering the effect of the adjustments on the light field, we find that none of the adjustments provide a level in which the diffuseness and the light direction lay in the range of observers' preference. This is aligned with the level of visual comfort defined by the luminance CR. In contrast with the results of the luminance CR, the degree of visual comfort does see improvement considering the level of diffuseness in some of the models relative to the reference model. This will be discussed later on.

Our simulated results show that the adjustment into a white table cover increases the level of comfort (figure 10.10). Moreover, the level of diffuseness in a scene is influenced by the reflectance (both specular and diffuse) . This can be explained by the formula of diffuseness, i.e. Vector/Scalar ratio (formula 22, chapter 3). With a decreasing angle of the light vector (figure 10.10 – graph 2) and a relative steady intensity (scalar), the diffuseness in gridpoint 3 increases. The decrease of the angle of the light vector is caused by an increased reflectance of the table surface.

Another finding shows that the adjustments of the horizontal overhang, horizontal louvers and a lowered light transmittance in glazing decrease the intensity significantly at gridpoint 1. This is not reflected in the level of the diffuseness. We attribute this to the fact that sun blinds mainly stop the direct sun and therefore do not provide a solution for visual improvement during clouded sky. However, the simulations did not detect any evidence for this. This could be an interesting starting point for further research. The analysis of the clear sky simulation (appendix M) shows that these adjustments influence the light near by the window, but do not affect the situation further in the room.

Luminance Contrast Ratio

Regarding the luminance contrast ratio, a number of observations have been made. An important finding is that in all created models (model B-H) the level of visual comfort has not improved, considering the luminance CR for the view direction of an observer facing the window (positioned at grid point 1): the ratio did not get lower than 1:3. Instead, in some models the luminance CR even deteriorated.

This goes along with the finding that the experienced discomfort in the room is not caused by glare but originates from a high contrast between a person and the adjacent background. Moreover, the visual discomfort is experienced when the room is in use, so when people are around (see figure 9.1). This is overlooked during the simulations because these were executed without people in it. To analyse the assumption made, model A' consist of the reference model with simulated rectangles that represent human observers. In addition, figure 11.2 and table 11.1 confirm the finding in a real-scene (photographed on February 15, 9:15h in room Ct6.75).

Regarding the improvement of the table material, we assume that the maximum luminance stays the same. And so, we need a higher mean luminance in the ergorama. We find that a white matt table cover (figure 10.8 model C) has a adverse effect on the level of comfort

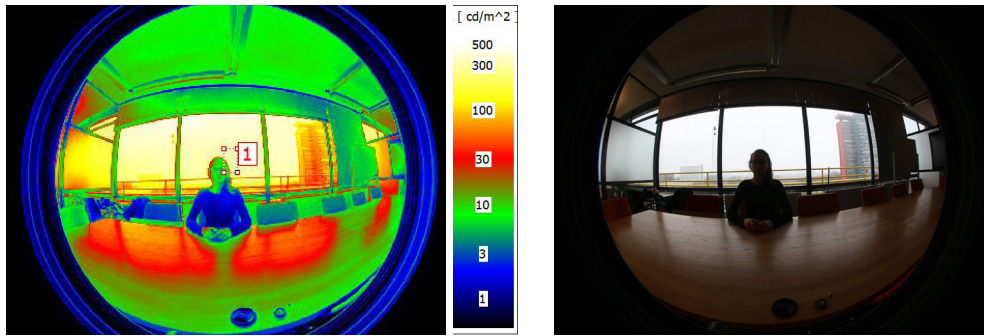


Figure 11.2 An impression of the effect of high contrasts that occur when a person is positioned in front of a bright background (exterior) in the field of view. Left shows the false color map, the right image shows the original normal exposed photo (photographed on February 15, 9:15h in room Ct6.75).

Table 11.2 Luminance values for the rectangle given in figure 10.1 in room Ct2.72 excl. white table cover and incl. white table cover.

Rectangle 1	
min [cd/m ²]	5,1
mean [cd/m ²]	279,8
max [cd/m ²]	367,1
ratio (=max/min)	1:71,9

Table 11.3 Luminance contrast ratio for the various models in which the reflectivity of the table cover has been adjusted. The data is part of table 9.6 in chapter 9.

	Model A (reference model)	Model H	Model B	Model C
	shiny black table	shiny white table	matt white table	matt black table
Ergorama ratio (=max/mean)	1:4,2	1:3,9	1:4,9	1:5,2
Panorama ratio (=max/mean)	1:9,6	1:8,3	1:11	1:12,6

while the white shiny (model H) cover improves the level of comfort in the ergorama relative to the reference model (table 11.3). Considering the panorama, the effect is opposite. We expect to need a higher total reflectivity, and so we adjust the black shiny table (total reflectance low, specular reflectance high) cover with a white matt table (total reflectance high, specular reflectance low) (model B). However, a lower mean luminance is measured within the ergorama. It suggests that besides the total reflectance attention should be paid to the *specularity* (as it is called in DIVA Radiance).

The horizontal louvers in the room produce an altering light direction causing less reflections on the table. This results in a deteriorated luminance CR as well. The effect on the luminance Contrast Ratio by the adjustment of glazing is negligible. Both the max and mean luminance values have been halved, resulting in a stable luminance CR.

CONCLUSION PART III

This chapter presents the answer on the questions stated in the introduction: "What is the difference between the analysis of the light field and the analysis of the Luminance Contrast Ratio on the measured level of visual comfort?" and "How can scene adjustments influence the level of visual comfort in a room?".

In a number of points an answer is formulated on the question:

What is the difference between the analysis of the light field and the analysis of the Luminance Contrast Ratio on the measured level of visual comfort?

- Visual comfort is view dependent and examined by various view-dependent metrics, i.e. $DGPs|_{wienold}$ and luminance CR. These metrics are limited in the assessment of visual comfort regarding the field of view, because they do not measure anything outside the chosen viewing direction. Conversely, the analysis of the light field has the advantage of providing view-independent spatial information.

- The analysis of the light field gives information about the light distribution in a space other than luminance and illuminance distributions.

High contrasts are a result of strong directional lighting in combination with a low diffuseness. Visual comfort is related to how we perceive a space or an object. High contrasts that can cause an object (e.g. human) to be perceived as dark. By using a cubic illuminance meter, these parameters can be measured, contributing to the analysis of visual comfort.

- Regarding the complexity and time of processing the measurements we conclude that no distinct difference can be determined. The analysis of the light field is time-consuming when using a single cubic illuminance meter. The in-field measurement results have to be processed afterwards. An analysis using the common visual comfort metrics is time consuming as well.

- The analysis of a scene with the luminance Contrast Ratio is based upon a visualization of the scene. In contrast, the analysis of the light field by using a cubic illuminance meter

is based upon numerical measurements with the possibility of a visualization of the light field itself. This could result in difficulties regarding improvements in the scene since the disturbing factor (i.e. light source or material property) is not apparent.

Subsequent, answers are formulated on the following question:

How can scene adjustments influence the level of visual comfort in a room?

Considering room Ct2.72, we could verify that the room is experienced as uncomfortable caused by high contrasts. Based upon the analysis of the light field these high contrasts are due to a combination of strong directional light and low diffuseness in the view direction of the human observer. To make improvements in the level of visual comfort the level of diffuseness should be improved and the directionality lowered. It should be noted that despite the attempts to make improvements in the level of visual comfort, it has not been possible to get the degree of visual comfort to an acceptable level. And so, the emphasis in this question lay on the *influence* of adjustments, rather than *improvements*.

- Scene adjustments should affect the light intensity and light direction in order to influence the diffuseness level and/or the directionality of the light. To increase the level of diffuseness when the intensity remains stable, an increased light vector is needed. And so, with a stable light vector a lowered intensity is required.

- An overhang, decreased light transmittance in glazing, and louvers lower the intensity but influence the light direction too. Resulting in unchanging diffuseness levels. It is recommended to research the level of visual comfort by adding sky light, since a strong horizontal light direction is prone for low levels of visual comfort.

- Adjustments in the total surface reflectance should be subdivided into the diffuse and the specular reflectance of a surface.

The diffuse reflectivity of the table should be increased and the specular reflectivity should be decreased compared to the reference model to improve the level directional-to-diffuseness lighting.

- Adjustments of the surface reflectance (i.e. the diffuse and the specular reflectance) have contrasting effect on the properties of the light field and the luminance Contrast Ratio, caused by the differences in limitation of a view dependent metric

- Beyond the scene's adjustment, the level of comfort could be improved by changing the position of the observer:

The main occupants' view direction is related to the positioning of the table, resulting in the experience of high contrasts when facing the window. It is suggested that the table is turned a quarter turn so that the changing of seating position results in an improved visual comfort. Considering this situation regarding the light field, the diffuseness level stays intact but the angle to the glare source differs. Therefore, it should be noted that the strong directionality of the light close to the window can still cause discomfort due to casted shadow covering half of the faces, when people are facing each other (appendix N).

FINAL CONCLUSION & RECOMMENDATIONS

Based upon the answers on the subquestions, as presented in the conclusions of Part I, II and III, this chapter elaborates on the answer on the main research question. Furthermore, recommendations are formulated providing a base for further research.

13.1 CONCLUSION

The central question of this research is:

To what extent is the analysis of the light field an effective alternative to predict visual comfort in a daylit office meeting space?

The answer on the question is formulated as follows:

The analysis of the light field with a cubic illuminance meter is a promising candidate to determine the light quality regarding visual comfort. In contrast with the luminance Contrast Metric, the light field analysis provides information about the lighting conditions in a space other than luminance and illuminance distributions. Furthermore, the analysis is view-independent, and the light field is very sensitive for adjustments in room surface properties (i.e. material reflectivity and roughness). With this additional information the analysis of the light field can improve the lighting qualities in a space. It could open doors to renewed choice of surface materials, and help with the positioning of people in an office space.

However, the analysis of the light field with the cubic illuminance meter lacks a visualization of the situation. So knowledge about the actual disturbing source is not clearly apparent. The measuring tool is time-consuming in practice and takes time to understand, although current measurement methods can also be time consuming. Besides, the research to acceptable levels of diffuseness and preferred angles of the light vector are still minimal so that application still requires further research.

Overall, it remains challenging to set up a well-lit meeting space when daylight is present due to the strong horizontal component of the available light. But it is at least convenient to learn more about the three-dimensional aspects of light to improve one's surroundings.

13.2 RECOMMENDATION

The previous sub-conclusions and discussion highlighted the final conclusions of this research. It has identified a relation between visual comfort and the lower order properties of the light field. The conclusions are limited because they are based upon findings in a case study evaluating a single observers' position in room Ct2.72. To make the conclusion more universal, it is strongly recommended to test the relation between visual comfort and the light field at different observers' view directions and in other spaces and lighting conditions as well.

Further recommendations are;

- A suggested research approach is to have use multiple case studies in which glare is the actual problem. On the one hand, human observers should participate for a more perception based approach (in addition to research of Cuttle (2008)). On the other hand, other visual comfort metrics could be included to extend the comparison of the light field with visual discomfort.

- In addition, the advantage of using a simulation model can be expanded. It's validity should be checked for different sky types and dates.

- It is recommended to design a simple device⁶ that can measure the light field, and to create a reliable simulation set-up. Because, simulation-based research can provide large amount of data within a relatively short period of time. In contrast, the practical set-up of a light field measurement with a single cubic illuminance in a daylight scene is time consuming and expensive. At the same time daylight is highly dynamic, resulting in inaccurate measurements.

- In addition, when a self-built cubic illuminance meter is used in a measurement, a smaller size of cube is recommended to improve the accuracy of the measurement.

- Knowledge about the light field should be added in the architectural education to grow awareness of the differences and the application of directional light and diffuseness. This could result in a link between an architectural notion of light and a practice-based approach. In addition, effects of window-to-wall ratio and room depth on the properties of the light field could be studied too.

- Considering the light field visualization of Kartashova it is suggested to make it possible to fixate the view-point in order to compare different results with each other. Besides, the analysis of the light field could be improved by option to compare the results with the observers' level of preferences.

- Regarding the application of the research it is at least recommended to prevent the use of dark and shiny desk covers in an office room.

⁶ Xia et al. (2016-III) suggested the use of a smartphone or app to measure the light field's properties.

REFERENCES

- Adelson, Edward H., and James R. Bergen. 1991. "The Plenoptic Function and the elements of early vision." In *Computational Models of Visual Processing*, by M. Landy and J. A. Movshon, 3-20. Cambridge, MA: MIT Press.
- Banham, R. 1984. *Architecture of the well-tempered environment*. Chicago: University of Chicago Press.
- Bell, Paul A., Thomas C. Greene, Jeffery D. Fisher, and Andrew Baum. 2001. *Environmental Psychology*. Orlando: Harcourt College Publishers.
- Berson, D., Dunn, F., & Takao, M. (2002). Phototransduction by retinal ganglion cells that set the circadian clock. *Science*.
- Bommel, W., & Beld, G. (2004). *Werkverlichting: Visuele en Biologische kwaliteiten*. Nederland: Philips Lighting.
- Bouwbesluit. 2017. "www.bouwbesluitonline.nl." Bouwbesluit 2012 Hoofdstuk 3 Afdeling 3.11 Daglicht. april 23. <http://www.bouwbesluitonline.nl/Inhoud/docs/wet/bb2012/hfd3/afd3-11>.
- Boyce, P. 2013. Lighting quality for all. ARROW@dit.
- Chamilothori, Kynthia, Jan Wienold, and M. Andersen. 2016. "Daylight patterns as a means to influence the spatial ambience: a preliminary study." 3rd International Congress on Ambiances. Volos.
- Cuttle. 1971. "Lighting Patterns and the Flow of Light." *Lighting Research and Technology* 171-189.
- Cuttle. 2008. *Lighting by Design*. Oxford: Architectural Press.
- Cuttle. 2010. "Towards the third stage of the lighting profession." *Lighting Res. Technol.* 73-93.
- Cuttle, K., and J. Mardaljevic. 2012. "A Guiding Light." *CIBSE Journal*, december: 14-16.
- Cuttle. 2014. "A practical approach to cubic illuminance measurements." *Lighting Research and Technology* 31-34.
- De Bruin-Hordijk, G.J., H.I.J. Hellinga, and S. Pont. 2008. "Die Kennzeichen des Schattens und die Zehn-Stufen Skala." In *proceedings of Licht* 338-343.
- Frandsen. 1989. "The Scale of Light- A new concept and its application." 2nd European Conference on Architecture. Paris: School of Architecture Copenhagen. 12-15.
- Frandsen. 1987. "The Scale of Light." *International Lighting Review* 108-112.
- Galasiu, A.D., and J.A. Veitch. 2006. "Occupant preferences and satisfaction with the luminous environment and control systems in daylit offices: a literature review." *Energy and Buildings* 38 728-742.
- Galatioto, A., and M. Beccali. 2016. "Aspects and issues of daylighting assessment: A review study." *Renewable and Sustainable Energy Reviews* 66 852-860.
- Ganslandt, Rudiger, and Harald Hofmann. 1992. *Handbook of Lighting Design*. Ludenscheid: Druckhaus Maack.
- Gershun, A. 1939. "The Light Field." *Journal of Mathematics and Physics*.
- Glickman, G., & et al. (2003). Inferior retinal light exposure is more effective than superior retinal exposure in suppressing melatonin in humans. *J Bio Rhythm*.
- Gurney, J. 2010. *Color and Light: A guide for the realist painter*. Riverside: Andrew McMeel Publishin.
- Iacomussi, P., M. Radis, G. Rossi, and L. Rossi. 2015. "Visual comfort with LED lighting." *Energy Procedia* 729-724.
- Jakubiec, J. A. 2014. *The use of visual comfort metrics in the design of daylit spaces*. PhD Thesis, Massachusetts: MIT.
- Kartashova, T., D. Sekulovski, H. de Ridder, Susan F. te Pas, and Sylvia C. Pont. 2016. "The global structure of the visual light field and its relation to the physical light field." *Journal of Vision* 1-16.
- Kelly, Richard. 1952. "Lighting as an Integral Part of Architecture." *College Art Journal*, Vol. 12, No.1 24-30.
- Koenderink, Pont, van Doorn, Kappers, and Todd. 2007. "The visual light field." *Perception advance online publication*.
- Lam, William A.C. 1992. *Perception and Lighting as formgivers for architecture*. New York: Van Nostrand Reinhold.
- Lam, William. 1986. *Sunlighting as Formgiver*. Van Nostrand Reinhold.
- Madsen, M. 2010. "Light-Zone(s): as a Concept and Tool." *ARCC Journal Volume 4* 50-59.
- Madsen, M., and M. Donn. 2006. *Leicester: 5th Radiance Workshop*.
- Mills, E, and N. Borg. 1999. "Trends in recommended lighting levels: An International Comparison." *Journal of the Illuminating Engineering Society* 155-163.
- Mury, A.A. 2009. *The Light Field In Natural Scenes*. Delft: TU Delft.

- Mury, AA, SC Pont, and JJ Koenderink. 2007. "Light field constancy within natural scenes." *Appl Opt.* 7308-16.
- Pallasmaa, Juhani. 2012. *THE EYES OF THE SKIN architecture and the senses*. West Sussex: Wiley.
- Pont, S.C. 2009. "Ecological optics of natural materials and light field." *SPIE-IS&T* 724009-12.
- Reinhart, Christoph. 2014. *Daylighting Handbook I*. USA: Christoph Reinhart.
- Rockcastle, S., and M. Andersen. 2013. *Annual Dynamics of Daylight Variability and Contrast A Simulation-Based Approach to Quantifying Visual Effects in Architecture*. London Heidelberg New York Dordrecht: Springer.
- Rockcastle, S., and M. Andersen. 2015. "Human perceptions of daylight comparison in architecture: a preliminary study to compare quantitative contrast measures with subjective user assessments in hdr renderings." *Proceedings of the 14th IBPSA*.
- Rockcastle, Siobhan, and Marilyne Andersen. 2014. "Measuring the dynamics of contrast & daylight variability in architecture: A proof-of-concept methodology." *Building and Environment* 81 320-333.
- Schirillo. 2013. "We infer light in space." *Psychon Bull Rev* 905–915.
- Simons, R. H., and A. R. Bean. 2001. *Lighting engineering : applied calculations*. Oxford: Architectural Press.
- Skarlatou, A. Z. 2010. *Light Effects in the Design Process*. London: Faculty Built Environment University College.
- Steane, M. A., and K. Steemers. 2004. *Environmental Diversity in Architecture*. Taylor and Francis.
- Torres, S., and V.R.M Lo Verso. 2015. "Comparative analysis of simplified daylight glare methods and proposal of a new method based on the cylindrical illuminance." *Energy Procedia* 699-704.
- Vogels, I. 2008. *Atmosphere Metrics: a tool to quantify perceived atmosphere*. Eindhoven: Philips Research Europe.
- WELL. 2016. *The WELL Building Standard*. New York: Delos Living LLC.
- Xia, L., Pont, S.C., Heynderickx, I.2014. The visual light field in real scenes. *i-Perception*, 5, 613-629
- Xia, L., Pont, S.C., Heynderickx, I.2017. Testing separate and simultaneous adjustment methods for lighting intensity, direction and diffuseness. *i-Perception*
- Xia, L., Pont, S.C., Heynderickx, I.2016-I. Effects of scene content and layout on the perceived light direction in 3D spaces. *Journal of Vision*.
- Xia, L., Pont, S.C., Heynderickx, I.2016-II. Light diffuseness metric, Part 1: Theory. *Lighting Research and Technology*. 1477153516631391, 2016.
- Xia, L., Pont, S.C., Heynderickx, I.2016-III. Light diffuseness metric, Part 2: Describing, measuring and visualising the light flow and diffuseness in threedimensional spaces. *Lighting Research and Technology*, 1477153516631392, 2016.
- Xia, L. 2016. *Perceptual metrics of light fields*. PhD Thesis, Delft: TU Delft.

APPENDICES

A THE DESCRIPTION OF LIGHT & PHOTOMETRIC QUANTITIES

The description of light

Light in itself is invisible for human beings. In terms of radiation, the emission of energy in the form of waves, light is electromagnetic and visible to the human eye in case the wavelengths range from 380-780nm in the electromagnetic spectrum, see figure A.1. Shorter wavelengths, <380nm, are known as UV while the infrared ranges >780nm. In case the wavelengths between 380-780 nm are absorbed by the retina in the eye, three types of photoreceptors possibly react: the cones, rods and an in 2002 identified third photoreceptor called the Retinal Ganglion cells positioned in the lower part of the retina (Glickman & et al., 2003). Every photoreceptor has its own spectral sensitivity and the cones and rods enable human to collect information about motion, faces, objects and everything one can see. Besides this visual impact, the photoreceptor retinal Ganglion cells initiate the non-visual, biological, impact of light influencing our alertness and even sleep quality, regulating the 24-hours body clock (circadian rhythm) (Berson, Dunn, & Takao, 2002) (Bommel & Beld, 2004).

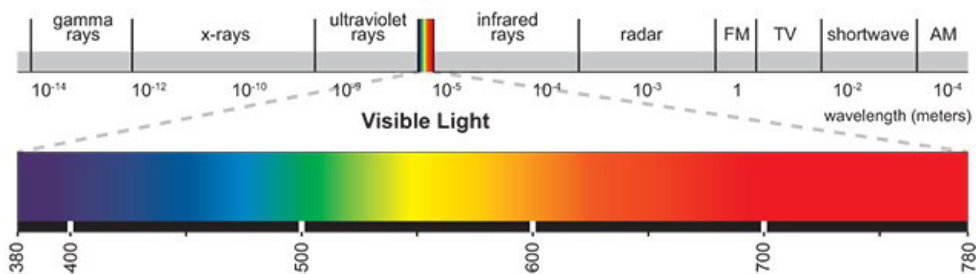


Figure A.1 Light is electromagnetic and visible to the human eye in case the wavelengths range from 380-780nm in the electromagnetic spectrum

The photometric quantities of light

Light is measured in different quantities: the SI photometry measures, see figure A.2. The Luminous flux (Φ) describes the amount of visible light per unit of time in Lumen (lm). The luminous intensity (I) defines the luminous flux per unit of solid angle in candela (cd), $1 \text{ cd} = 1 \text{ lm/sr}$. The Illuminance (E) is the luminous flux incident on a surface lux (lx), $1 \text{ lx} = 1 \text{ lm/m}^2$. The Luminance (L) is the ratio between the light incident on a surface emitted in a certain direction in candela per square meter (cd/m^2).

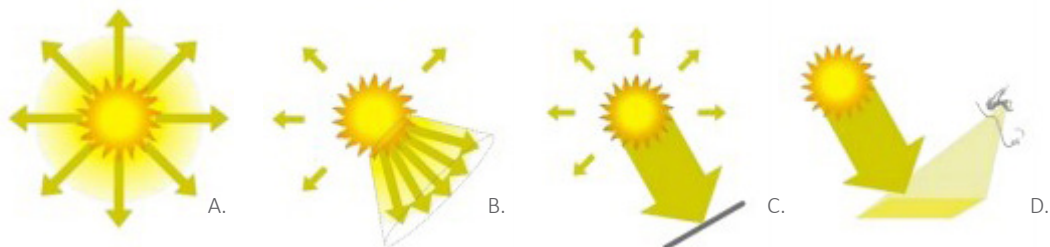


Figure A.2 The photometric quantities of light, with the luminous flux (A), the luminous intensity (B), the illuminance (C) and the luminance (D).

B THE LIGHT FIELD: SPHERICAL HARMONICS REPRESENTATION

The light field can be described up to the second order SH-representation. This is visualized in figure B.1 and mathematically defined as follows:

$$f(\vartheta, \varphi) = w_0 \cdot Y_0^0(\vartheta, \varphi) + w_1/w_0 \cdot (a_1 Y_1^{-1}(\vartheta, \varphi) + a_2 Y_1^0(\vartheta, \varphi) + a_3 Y_1^1(\vartheta, \varphi)) + w_2/w_0 \cdot (b_1 Y_2^{-2}(\vartheta, \varphi) + b_2 Y_2^{-1}(\vartheta, \varphi) + b_3 Y_2^0(\vartheta, \varphi) + b_4 Y_2^1(\vartheta, \varphi) + b_5 Y_2^2(\vartheta, \varphi))$$

The formula presents the mathematical series that describe a function that is a sum of its frequency components: The higher orders are based upon the strength component w_0 .

Formerly, a plenopter device (12 faces) was used to calculate up to the second order. The plenopter contained nine free parameters, defined by the strength of the orders (w_0 , w_1/w_0 and w_2/w_0) and the weight of the components (i.e., a_1 , a_2 , a_3 ; b_1 , b_2 , b_3 , b_4). A cubic illuminance meter has 6 faces and makes it possible to calculate the 0th and the 1st order of the light field representation.

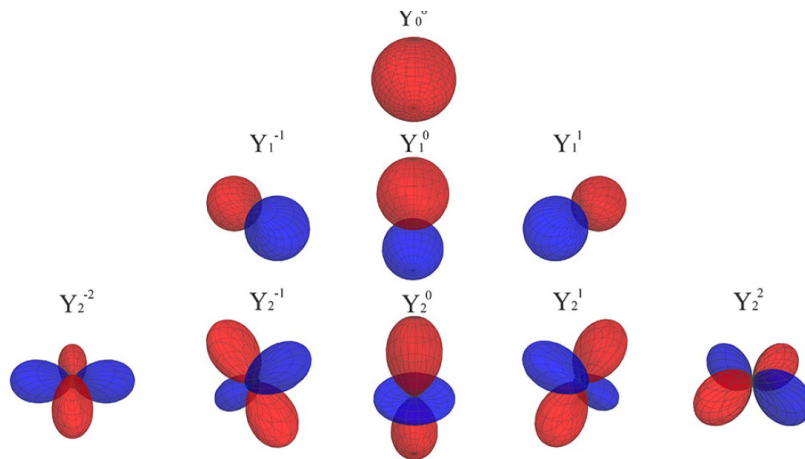


Figure B.1 A plot of spherical harmonic basic functions. Y_0^0 represents the 0th order (monopole) that describes the average radiance from all directions. The second row, containing Y_1^{-1} , Y_1^0 , Y_1^1 shows the 1th order (dipole) that represents the light vector. The third row presents the 2nd order.

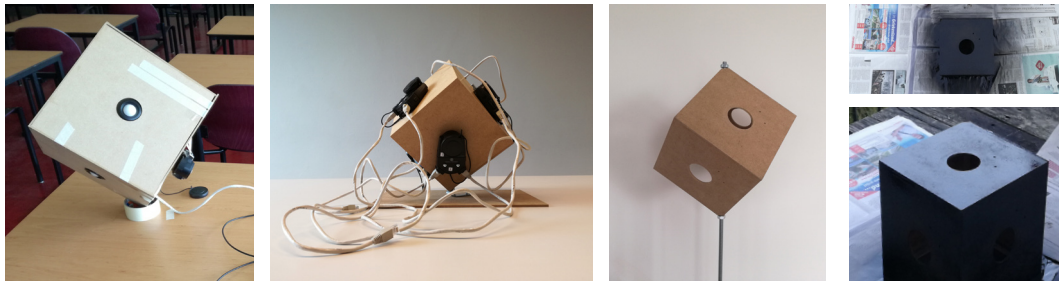
C THE CUBIC ILLUMINANCE METER

The making off: The cubic illuminance meter

The cubic illuminance meter is developed in an iterative process to improve the size, the joints, the cables and the way the luxmeters were fixed on the cube, see figure C.1.

The final design consist of a 17x17cm mdf (4mm thickness) cube with small holes for the $\Phi 4$ mm bolts. The bottum is flattened to fixate the cube to the tripod. The top of the cube is flattened to be able to lay a spirit level on top.

At the outside faces of the cube 6 Lux meters, series connected with each other and a laptop, are fixated.



the making of the cubic illuminance meter



Figure C.1 The top row presents the iterative process of the making off the cubic illuminance meter. The final design of the cubic illuminance meter fixated on a tripod is presented in the line below. The flat top side of the cube makes it possible to orient the cube using a spirit level.

Rotation of axes: Orientation of the cubic illuminance meter

The cubic illuminance meter is rotated 45-degrees around the y-axis and 35 degrees around the x-axis (figure C.2). A transformation matrix defines the rotation of the axis in figure C.3.

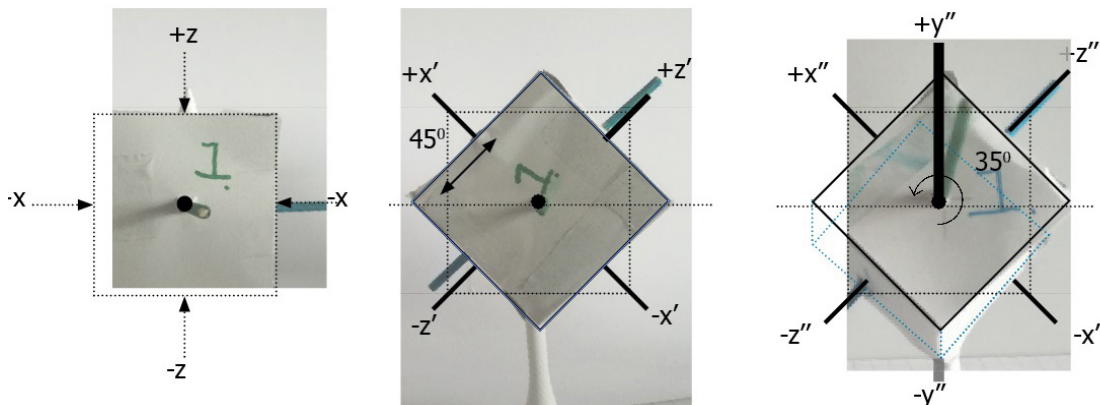
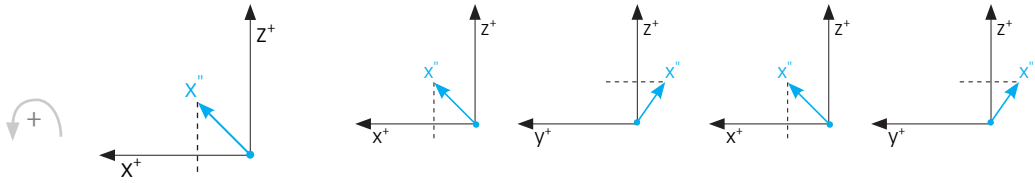
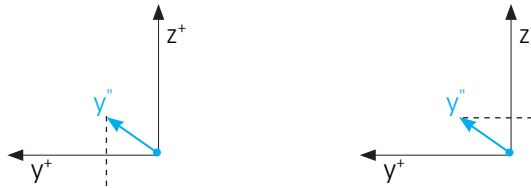


Figure C.2 The orientation of the axis of the cube that serves as a base for the cubic illuminance meter.

$$e_x'' = \cos(-45) \cdot e_x + \cos(-45) \cdot \sin(35) \cdot e_y + \sin(45) \cdot \cos(35) \cdot e_z$$



$$e_y'' = 0 \cdot e_x + \cos(35) \cdot e_y + \sin(35) \cdot e_z$$



$$e_z'' = \sin(-45) \cdot e_x + \sin(-45) \cdot \sin(35) \cdot e_y + \sin(45) \cdot \cos(35) \cdot e_z$$

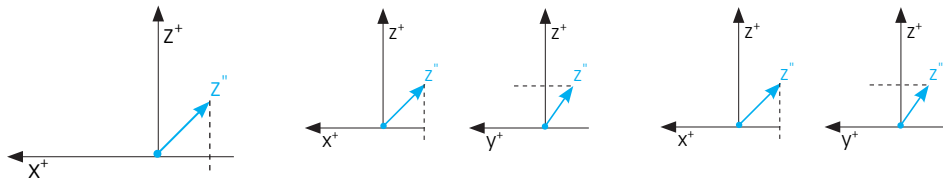


Figure C.3 The transformation matrix is obtained according the following transformation.

$$M = \begin{vmatrix} \cos(-45^\circ) & \cos(-45^\circ) \cdot \sin(35^\circ) & \sin(45^\circ) \cdot \cos(35^\circ) \\ 0 & \cos(35^\circ) & \sin(35^\circ) \\ \sin(-45^\circ) & \sin(-45^\circ) \cdot \sin(35^\circ) & \sin(45^\circ) \cdot \cos(35^\circ) \end{vmatrix}$$

$$= \begin{vmatrix} 0,707 & -0,406 & 0,579 \\ 0 & 0,819 & 0,574 \\ -0,707 & -0,406 & 0,579 \end{vmatrix}$$

D LIGHT VISUALIZATION BY KARTASHOVA

To create a computer generated impression of the light field, a (*.csv)-file is uploaded in the online application of Kartashova (<http://lightvisualizations.000webhostapp.com> - paper still to be submitted). This file contains, per measurement point, the coordinates (X,Y,Z) and six measurements values (face 0-5). It is important to note that the numbering of the faces of the cube in this study do not correlate with the numbering of the faces in the visualization tool, see figure C.1. Therefore, precision is required to generate the final file.

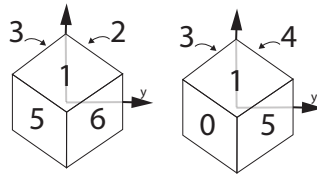


Figure D.1 (Left) image presents the faces of the cube Kartashova used in her application. (Right) the numbering of the cube used in this study.

For evaluating the images with the arrow or ellipsoids understanding of their attitude is required. Both the arrow and ellipsoids are able to represent multiple properties through variation of size. The long axis corresponds to the light vector. Therefore it is important to note that the light vector points to the direction where the light comes from. This is done so that people do not confuse the light vector – average light direction, summary of all light rays passing through a point – with rays – single rays of light.

The size of the object is aligned with the mean illuminance. The level of diffuseness is displayed through the proportion between the short and long axes. For example, fully diffuseness has no direction in it, so is represented by a sphere (Kartashova, et al. 2016).

E MEASUREMENT PROTOCOL

E1. CUBIC ILLUMINANCE METER: ITEMS NEEDED & PROTOCOL

The items needed for a full-scale measurement are written down below:

- Painting tape
- Centimetre roll
- 1 Lux measuring tool for measuring in horizontal plane, or outside luminance
- Cubic illuminance tool
 - o 6 Lux measuring tools
 - o 6 USB cables to series connect the Lux measuring tools
 - o A pre-made cardboard/wooden box
 - o Tripod
 - o Computer program KONINCA MINOLTA (plug-in Excel)
 - o Laptop (needs to work without adapter too)
 - o Cable to connect Lux measuring tool to laptop
 - o 12 bolts $\Phi 4\text{mm}$
 - o 1 bolt fit for a tripod

The measurement protocol is presented in table E.1

Table E.1 A measurement protocol for the use of a cubic illuminance meter.

	Activities
Conditions	1. The measurement should take place during daytime
	2. The measuring should take place in a room where direct sunlight can enter
Measuring spots	3. Mark measuring spots in the window pane to position a single Lux Tool for horizontal Lux measurements.
	4. Mark the position of the tripod where the cubic illuminance meter should be placed and define the (x, y, z)- axes in the room. Take the y-axis in the length of the room, like in figure 2 (plan drawing).
Preparation	5. Fixate the Lux measuring tools with screws on the side planes of the wooden box and keep the covers on. Then, fixate the cube to a tri-pod.
	6. Rotate the cube first 450 degrees about the y-axis and 350 around the x-axis, see figure 4 [orientation], resulting in a x''-, y''-, z''-coordinate system.
	7. Adjust the tripod in height. The middle of the box should stand at 1,20m in height.
	8. Check which Cubic Illuminance Meter corresponds to which axis, in the following matter:
	9. Connect the 6 Lux measuring tools in series with each other, the de-vice and the Laptop.
	10. For a baseline check, open the program of KONICA MINOLTA, meas-ure and check whether all the Lux Meters work.
Measurement	11. Take of the protective covers of the 6 Lux meters.
	12. Measure the Lux level in the horizontal plane with the single Lux tool in the window pane- if possible do this at the same time as the following steps
	13. Measure the illuminance levels with the Cubic Illuminance meter in the computer program KONICA MINOLTA/excel.
	14. In case the measurement is completed, clean up the cables, Lux measuring tools and box again safely.

Cubic illuminance meter: Error analysis test-measurements on May 15

To try out the self-made cubic illuminance meter, a small test was set-up at CiTG3.99 between 12:00 – 15:00. Unfortunately, due to deficiencies the test isn't entirely completed. In table D.2 a list of the mistakes made and the possibilities to prevent this next time.

Table E.2 An error analysis of a test measurement with the cubic illuminance meter on May 15.

Mistakes	Solution
The Lux measuring instrument had to be fixated in the cubic box with tape, resulting in shifted instruments.	Holes should be drilled in the cubic box, since the Lux measuring tools have holes for screws too.
The protective covers of the Lux measuring tools were situated inside the box while, for calibrating the tools, the covers needed to be outside the cubic box.	Place the Lux measuring tools outside the cubic box in order not to forget the protective covers.
To read the results of the 6th Lux measuring tool (not series connected) a hole was made in a side plan of the box, but it was wrongly situated.	Place the Lux measuring tools outside the cubic box in order not to forget the protective covers.
The Lux measuring tools weren't checked beforehand, while the box was already closed	Write a measuring protocol and check it during the measurements in order not to forget this step.
The numbers of the Lux measuring tools weren't written down, so it was unclear which results belonged to which measuring tool.	""
There hasn't been made a null calibration (nulmeting) of 6th Lux measuring tool	""
Photographs couldn't be made since the camera menu was too confusing to understand.	Learn how to work with the camera – ask someone to explain this beforehand the measuring day.

**E2. OBJECT VISUALIZATION WITH LUMINANCE CAMERA:
ITEMS NEEDED & PROTOCOL**

The items needed for a full-scale measurement with a luminance camera are written down below:

- Painting tape
- Measurement
- 1 Lux measuring tool for measuring in horizontal plane, or outside luminance
- Calibrated illuminance Camera with settings according to:
- Fish-eye lens
- Normal lens
- Computer program LMK Labsoft
- Tripod
- Objects: white sphere, black sphere, golf ball, triangle



Table E.3 A measurement protocol of visualization by objects using a luminance camera

	Activities
Conditions	1. The measurement should take place on a sunny day, during day-time
	2. The measuring should take place in a room where direct sunlight can enter
Measuring Spots	3. Mark a measuring spot with painting tape in the window pane to position a single Lux Tool.
	4. Mark a measuring spot with painting tape on the table to position the objects.
	5. Mark measuring spots on the floor for the tripod of the camera.
Preparation	6. To keep the data organized, create computer folders for every position/time.
	7. Fixate the camera with the normal lens on the tripod at the level of the objects (1,20m) and be sure the needed requirements are set.
	8. Position an object on the tripod
Taking a (series) picture	9. Position the camera at a marked spot. Focus the camera on the object and make a shot (which contains 3 pictures)
	10. Repeat the above operations (4-5) at the other marked spots. For the marked spots in room BK01.West.050, see figure XX.
	11. After the one single objects is photographed from the different angles, check the single horizontal lux meter in the window, write down the measured Lux.
	12. Turn off the camera and take out the Memory Card. Drag the images to the right computer folder.
	13. Repeat the above measurements (3-10) for another object.
	14. In case of BK.01.West.050: repeat the above measurements (XX-XX) every 15 minutes
	15. In case of BKXXX: repeat the above measurements for the other object positions.

F MEASUREMENT RESULTS

F1. MEASUREMENT RESULTS: SEPTEMBER 15

During processing the results of a measurement on September 15, it appeared that the artificial light was turned on as well. However, the results were processed as presented in figure F.1 and table F.1, whereupon a short discussion was written.

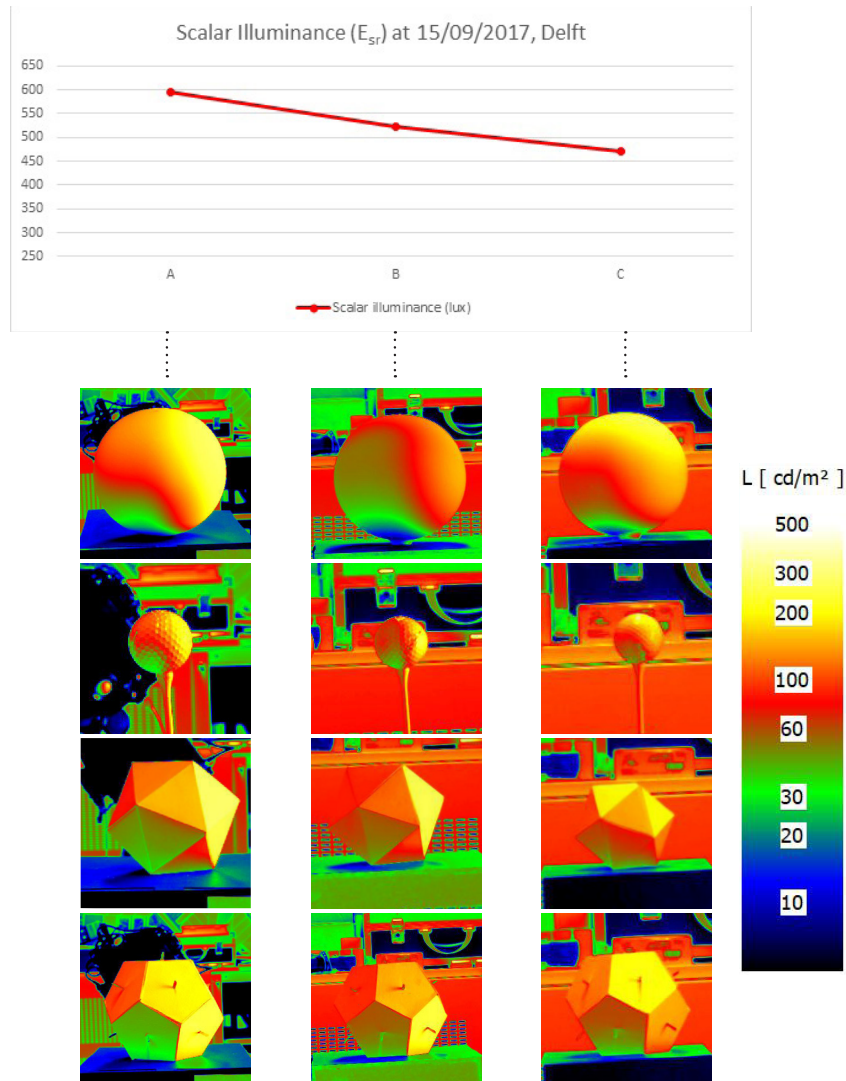


Figure F.1 False-color HDR images of the objects photographed in room 01+West240 at September 15.

Table F.1 The output of the cubic illuminance meter and the calculated intensity, direction and diffuseness measured in room 01+West240 at September 15.

	Output cubic illuminance meter						Results			
	lux	lux	lux	lux	lux	lux	Intensity	Altitude	azimuth	difuseness
	0	1	2	3	4	5	E_{sr}	[degrees]	[degrees]	
A	441	1311	503	169	639	240	596	23.23	177.54	0.51
B	428	1042	295	232	449	452	524	28.2	190.2	0.61
C	381	941	581	192	159	681	472	68.63	164.87	0.52

Observation and discussion (measurement September 15)

In the observation with the *naked eye* a shading pattern, due to reflected light, is seen on all objects, just as expected. However, from every viewing position, the objects appear differently, due to the vector component. According to the vector/scalar ratio of 1,96 corresponding to the *moderately strong* flow of light, the directional effect appears strong on the objects. However, due to the different directions of daylight and artificial light, the flow is experienced as more *weak flow*.

The images taken perpendicular to the window have indeed the least *flow of light*, however the difference is very vague because of the fact that the artificial lighting is switched on too. The cubic illuminance face 1 (closest by the window) corresponds to the observation that the view direction parallel to the window has the most *flow*.

Since the cubic illuminance meter has 6 faces, one could argue that a tilted cube is missing in the object results. The dodecahedron and the icosahedron show the higher order components of the SH representation of the light field. Although the golf ball could be defined as a polyhedron with many more faces too. The icosahedron seems to give more precise information when one uses just the eye to characterize it's interaction with the light field. However, the HDR image, showing the luminance which corresponds to the perceived brightness of humans, of the white probe seems to be read easily too.

Besides the *shading pattern*, Cuttle defined a *shadow pattern*, which appeared on the dodecahedron with pegs. The other objects don't have a shadow caster and therefore no shadow on itself. Thus, they aren't able to show any *sharpness*. The *sharpness* due to the pegs is vague because of the *indirect* daylight in the room. The *sharpness* can be seen with the HDR images too. There is no relation with the cubic illuminance measures of Xia. In the hypothesis there was sharpness expected on the icosahedron. However, it doesn't show any sharpness but the flow is more distinct. The more faces an object has, the more distinct the light appears.

Figure E.1 shows the different view directions and its influence on the perceived light direction with different *flows of light*. Because the vector/scalar ratio stays the same, it shows its dependency on the view direction. Because the *scalar illuminance*, the average illuminance of the probe, is constant (596lx) thus, the vector component seem to have large influence on the object.

The effect of high contrast in the field of view isn't taken into account. Although this has large effect on the images taken and analysed with the naked eye.

F2. MEASUREMENT RESULTS: OCTOBER 26

During processing the results of a measurement on October 26, it appeared that a meter didn't work properly. This came forth after the analysis of the light direction. However, the results were processed as follows.

Figure F.2 present both the results of the light intensity (in terms of scalar illuminance (E_{sr})) measured with a cubic illuminance meter, and the visualization of the interaction of the light field with the objects. The figure presents only the white sphere, photographed from angle Q parallel to the window, in normal color and a false colour mode. In total, four objects were photographed from three different angles on every position. The measurement took place on October 26, at respectively 15:16h, 15:21h, 15:26h. The light direction is measured with the cubic illuminance, resulting in unit vectors. These unit vectors can be related to object's appearance by expressing them in terms of its altitude and azimuth.

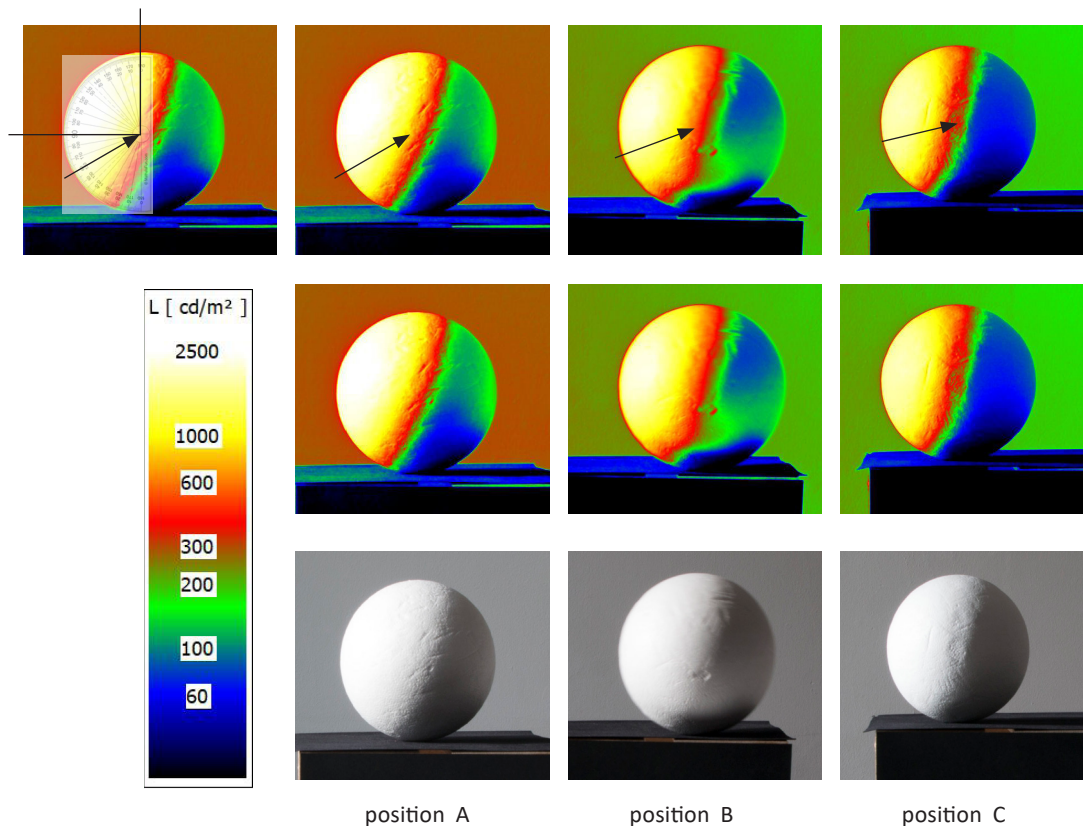


Figure F.2 The objects photographed with the luminance camera at position A, B and C in room BK.01. West.050 – October 26st , 14.30h. The black arrow presents the measured light altitude which presents the error shown in table F.2

Table F.2 The output of the cubic illuminance meter and the calculated intensity, direction and diffuseness measured in room BK.01.West.050 – October 26st , 14.30h. The red values show the measured error.

	Output cubic illuminance meter						Results			
	lux	lux	lux	lux	lux	lux	Intensity Esr	Altitude [degrees]	azimuth [degrees]	Diffuseness
A	1732	1573	774	560	369	1476	1024	-28.12	168.7	0.55
B	1573	1573	787	438	1017	1563	1118	-20.64	196.86	0.67
C	1181	1573	264	333	244	1563	787	-14.38	186.05	0.36

Table F.3 The output of a cubic illuminance measurement and its calculation results of a measurement in room BK01.West.050 on October 26 , 15.30h - as processed in Excel.

Output of the cubic illuminance measurement – October 26st , 15.30h, Delft							
Illuminance data input (lux)				Illumination components (lux)			
				Light vector		Symmetric component	
E(x''+)	693	E(x''-)	3908	E(x'')	-3215	~E(x'')	693
E(y''+)	13117	E(y''-)	1431	E(y'')	11686	~E(y'')	1431
E(z''+)	687	E(z''-)	2886	E(z'')	-2199	~E(z'')	687
Vector and Scalar data (lux)				Diffuseness ratio			
E	12318	~E	937	E /Escalar	3,07		
Escalar	4017			Dnormalized	0,23		
Unit vector				Vector direction			
e(x'')	-0.261	e(x)	-0.06	Azimuth (degrees)			
e(y'')	0.949	e(y)	0.96	α	16,86		
e(z'')	-0.179	e(z)	0.29	Altitude (degrees)			
e(x'',y'',z'')	1.00	e(x,y,z)	1.00	ϕ	183,49		

F3. MEASUREMENT RESULTS: OCTOBER 21

In the measurement of October 21 four objects were photographed from three different angles every 15 minutes for 1,5 hour, from 14:00-16:00. Figure G.1 presents the images photographed from angle Q in two different luminance false-color scales. Figure F.3 present images are from 15:00h, 15:30h and 16:00h, only. Afterwards it appeared that the objects were partly covered in shadow from 14:30-15:45.

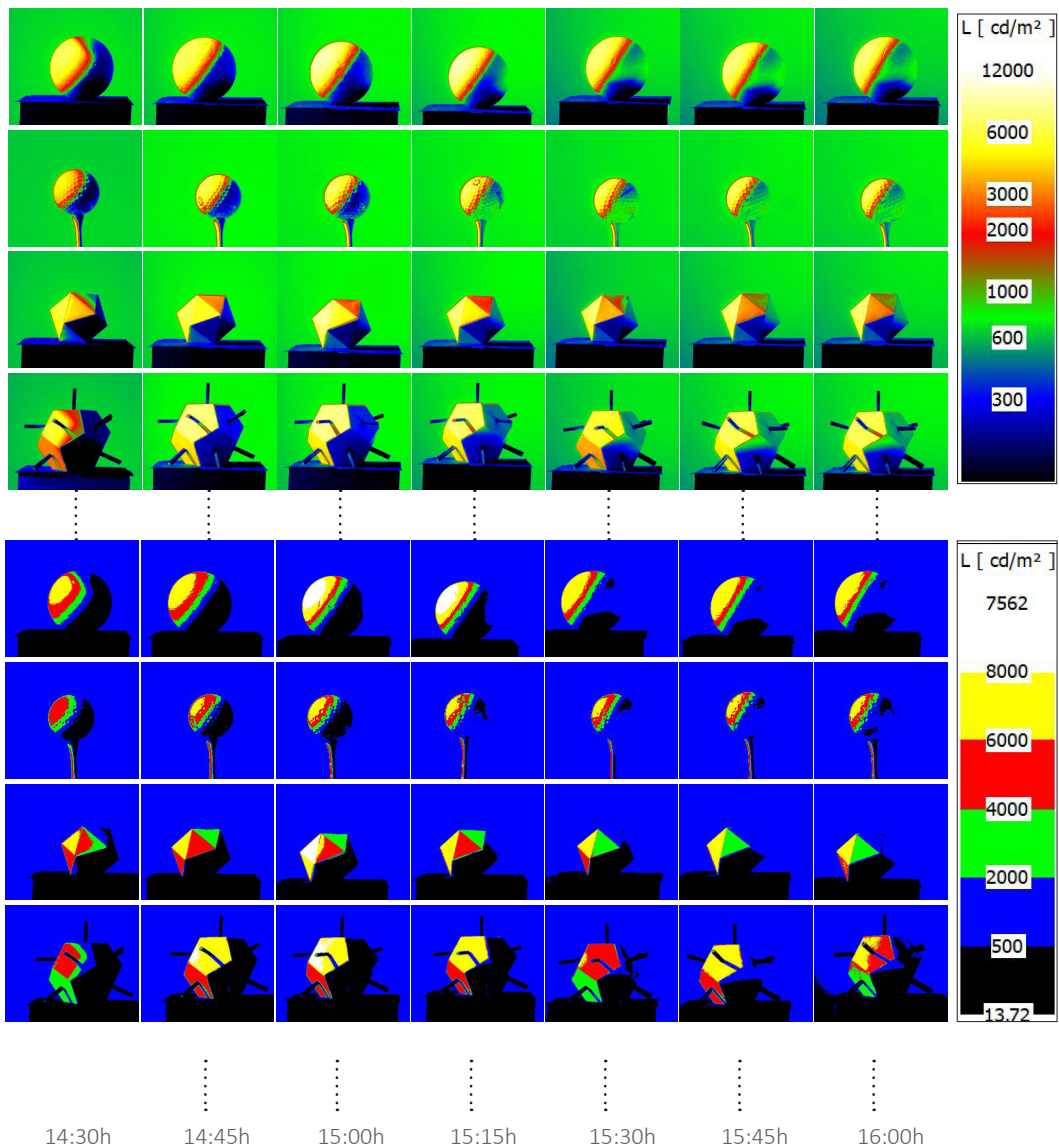


Figure F.3 The objects photographed with the luminance camera at position A in room BK.01.West.050 – October 26st , for every 15 minutes from 14.00h on. Two different false-color scales are presented.

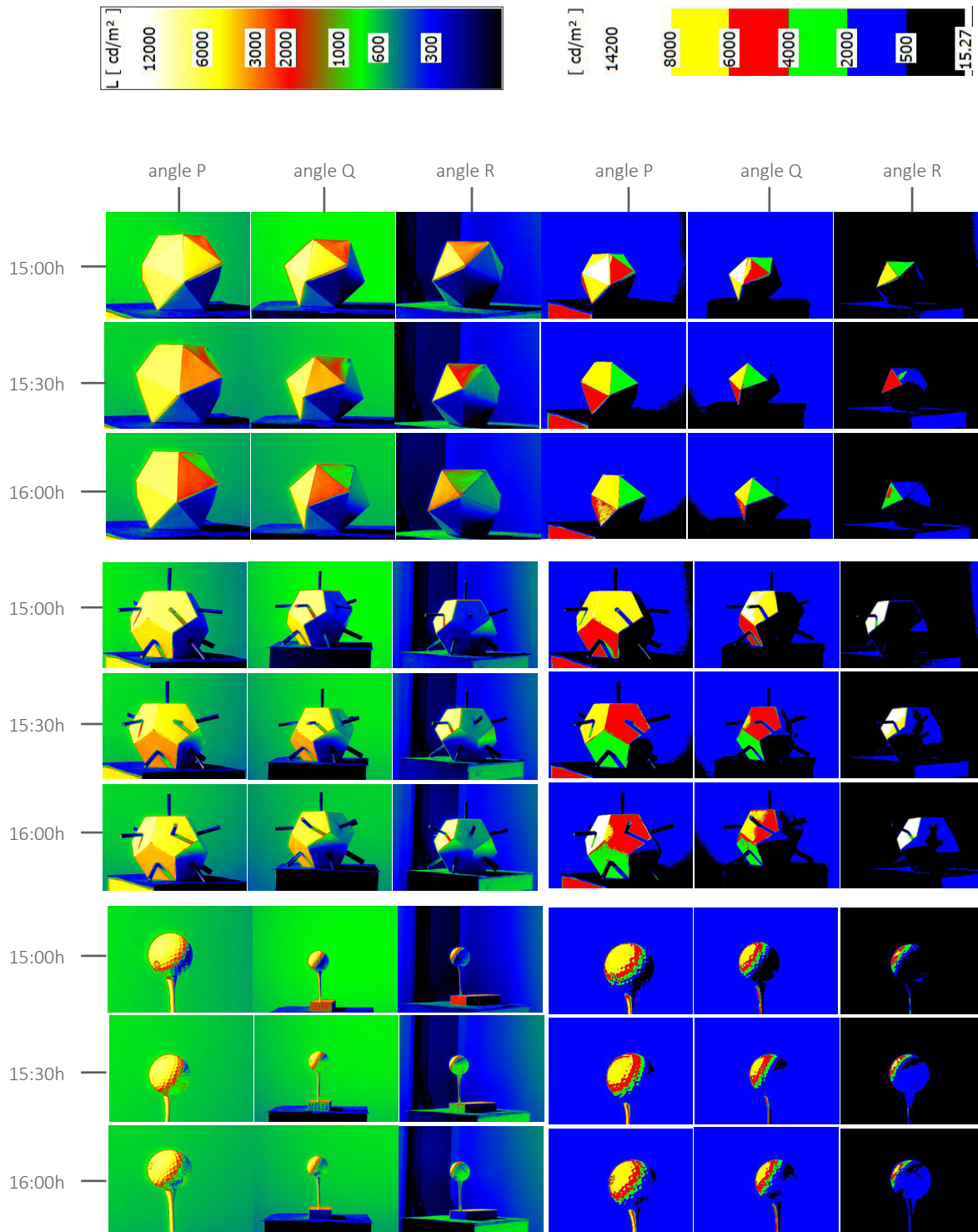


Figure F.4 The objects photographed with the luminance camera at position A in room BK.01.West.050 – October 26st (15:00h, 15:30h, 16:00h). Two different false-color scales are presented.

G FISH EYE

The HDR images taken with a camera equipped with fish-eye lens are processed into luminance false-color maps, as presented in figure H.1. The wide angle of view presents the field of view of a human observer. The software (LMK labsoft) in which the images are processed, has the option to 'measure' the minimum, mean and maximum luminance values in the image within a square or circle. This is used during the analysis of the photographs, i.e. for the luminance contrast ratio.

The fish-eye view is a visualization option in the Rhino/Divia software too. However this program is limited. The maximum and minimum luminance value of the whole image can be given rather than the maximum and minimum values of a selected area. Furthermore, the mean luminance value of a selected area is limited to a square size field. Therefore, during analysis we copy the average area of the in-field taken photograph and mimic this in the simulated visualization of Rhino/Divia.

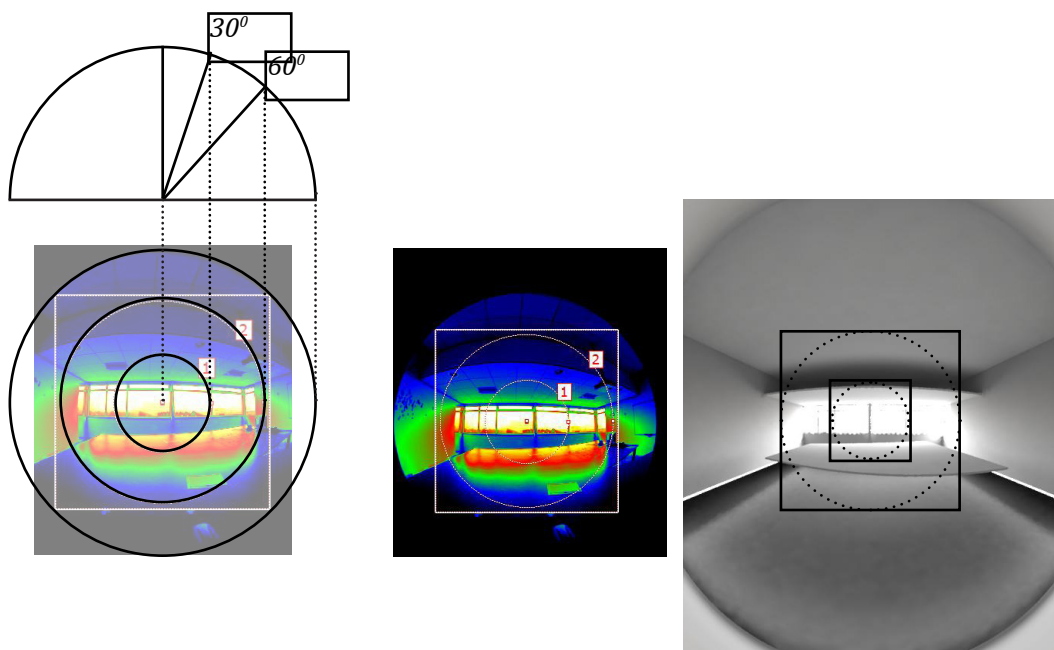


Figure G.1 The wide angle of view of a fish-eye image (left). The selected area in the photographed is mimicked with a square-sized area in the simulated visualization of Rhino/Divia. This is used for the analysis of the luminance Contrast Ratio.

H ROOM SURFACE REFLECTANCE

The main room surface reflectance are determined by the luminance ratio between the disk (95,2% reflectance) and the room surface. The normal and false-color images are presented in figure H.1.

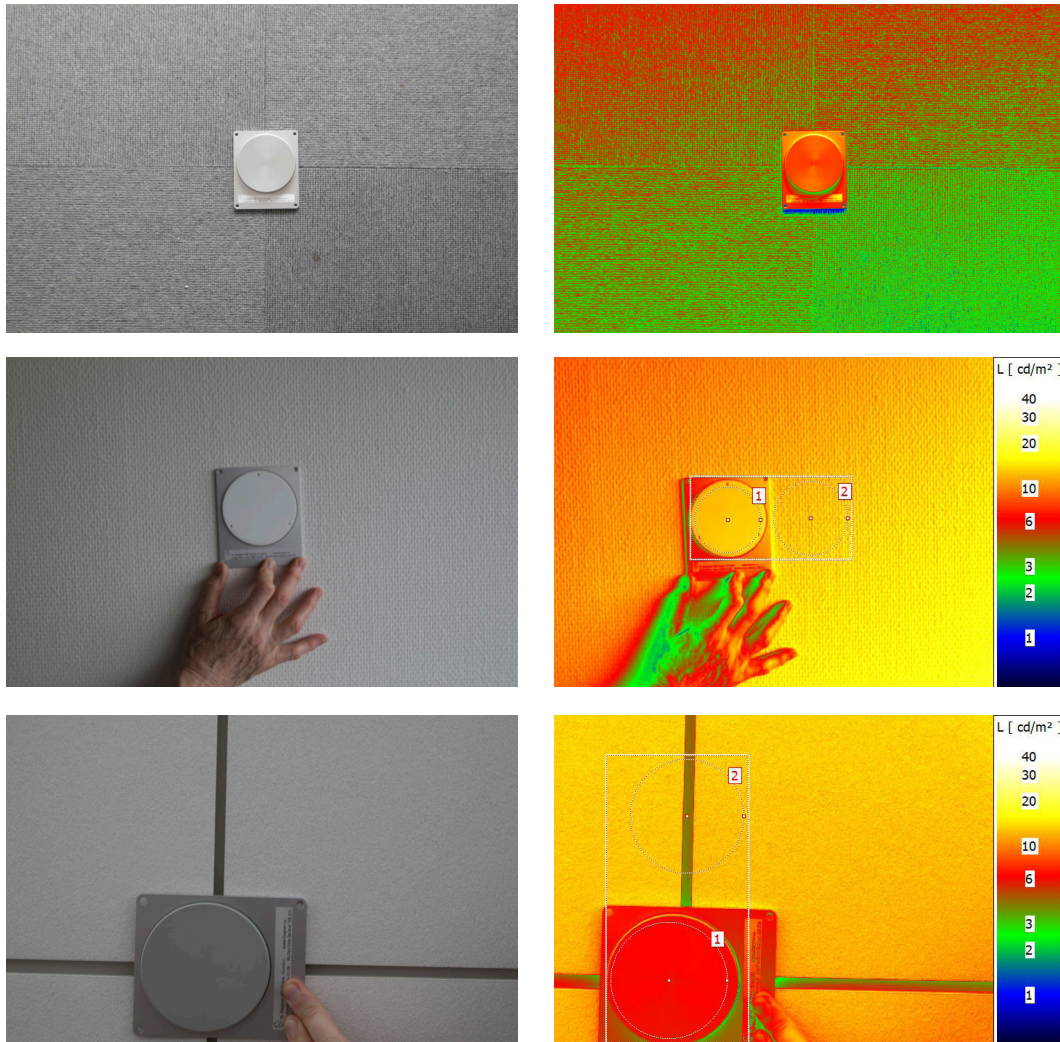


Figure H.1 The room surface reflectance of the main room surfaces. From top to bottom: floor, wall, ceiling.

Table H.2 Measured room reflectances by using a disk with a reflectance of 95,2%.

Main room surfaces	Mean luminance disk [cd/m ²]	Mean luminance surface [cd/m ²]	Reflectance surface [%]
Table	4,8	2,9	58
Ceiling	6,4	12,1	180
Wall	13,3	13,1	94
Floor	8,7	3,9	43

I RESULTS CASE STUDY: NOVEMBER 21

A false color image in LMK software captures the average and maximum values of an area (ergorama/panorama), see figure I.1 and table I.1, in which the resulting luminance ratio (= maximum/mean) are presented. During the experiment the vertical lux is measured by using a single lux meter, positioned just above the camera lens.

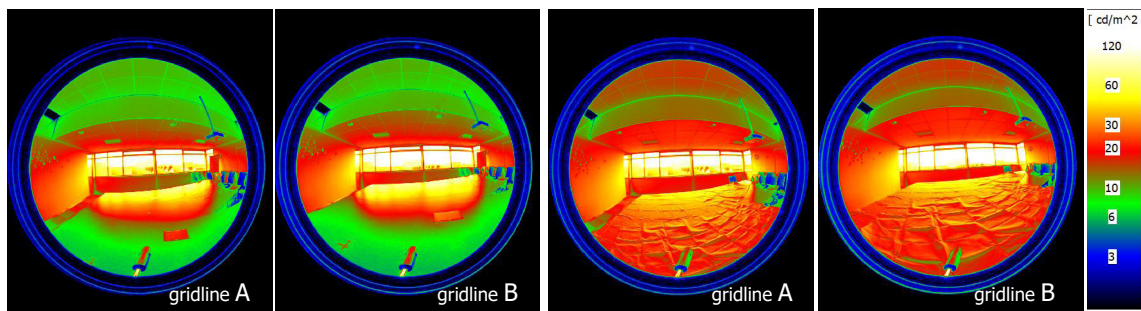


Figure I.1 False-color luminance map of room CT.2.72 on November 21. Gridline A has a height of 1,60m, gridline B a height of 1,20m. The images left show the office room without table cover, and, right including table cover.

Table I.1 Luminance contrast ratio (=max/mean) in ergorama (30°) and panorama (60°) as output from LMK Labsoft on false colour images from a measurement on November 21, 10.00h. In addition, Vertical lux measurement taken above the camera lens during the Luminance Contrast Ratio measurement.

		without table cover		with table cover	
		Ergorama	Panorama	Ergorama	Panorama
Position		30	60	30	60
A (=1,60m)	contrast ratio	1:5,2	1:10,5	1:5,1	1:10,0
B (=1,20m)	contrast ratio	1:4,3	1:9,0	1:4,3	1:8,6
A	Vertical lux	618		573	
B	Vertical lux	451		750	

The horizontal lux meter measured 467, 470 and 449 lux at, respectively, the start of the cubic illuminance measurement and the start and end of photographing the object. Table I.2 presents the calculated lower order properties of the light field, resulting from the cubic illuminance measurement. The objects photographed are presented in figure I.2

Table I.2 The calculated lower order properties of the light field with and without a white table cover, in room Ct2.72 on November 21, 10.00h.

hor.lux start measurement	467					
hor.lux end measurement	470					
time	10:00h					
	incl. tablecover	excl. tablecover	incl. tablecover	excl. tablecover	incl. tablecover	excl. tablecover
Grid position	scalar	scalar	dnormalized	dnormalized	altitude	altitude
a1	165	167	0.35	0.33	24.79	27
a2	50	50	0.67	0.44	-14.84	15
a3	40	29	0.52	0.46	-3.92	7
a4	27	22	0.53	0.52	-1.35	5
b1	210	173	0.35	0.33	30.19	30
b2	73	61	0.49	0.37	14.25	16
b3	45	40	0.48	0.42	1.44	10
b4	31	26	0.49	0.47	5.28	8

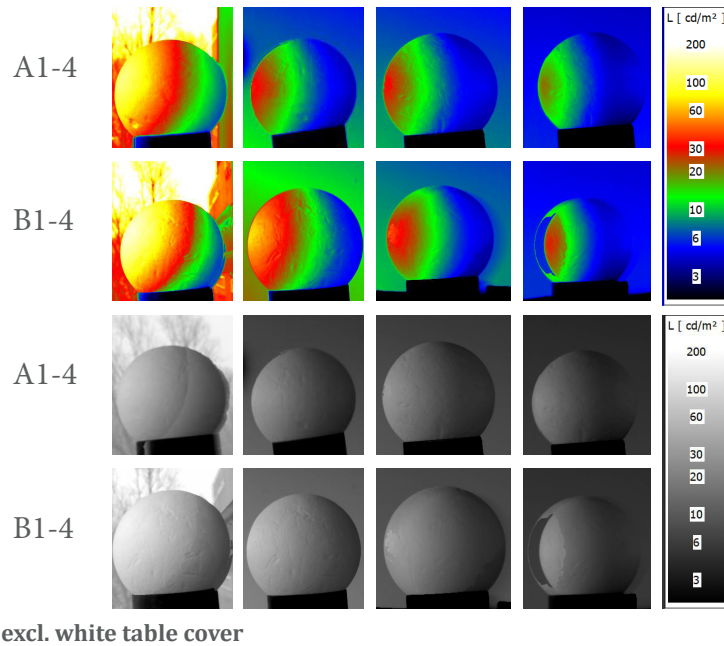


Figure 1.2 Visualization of object's appearance in false color images and normal colors. of room CT2.72 on November 21. Gridline A has a height of 1,60m, gridline B a height of 1,20m. The images show the office room without table cover. The blurry images are caused by a instable tripod.

J RESULTS CASE STUDY: DECEMBER 1, 10:15h & 11:30h

Table J.1 and table J.2 present the calculated results of the cubic illuminance measurement at 10:15h and 11:30h, both with and without white table cover.

Table J.1 The calculated lower order properties of the light field with and without a white table cover, in room Ct2.72 on December 1, 10:15h.

10:15h	Meting I (excl. tafelkleed + bol fotografie)				Meting I (incl. tafelkleed + bol fotografie)				
Coordinates	Escalar	Altitude	Azimuth	Diffuseness	Escalar	Altitude	Azimuth	Diffuseness	
	[lux]	[degrees]	[degrees]	dnormalized	[lux]	[degrees]	[degrees]	dnormalized	
(0,5; 1,41)	a1	295	22	183.33	0.32	335	24.95	182.75	0.34
(2; 1,41)	a2	106	9.21	180.35	0.4	115	9.04	179.34	0.48
(3,5; 1,41)	a3	55	0.08	180.99	0.42	57	-13.51	177.49	0.5
(5; 1,41)	a4	40	-3.22	178.71	0.46	38	-9.25	178.8	0.48
(0,5; 1,18)	b1	360	26.5	180.36	0.33	349	26.96	181.33	0.33
(2; 1,18)	b2	117	11.33	178.59	0.38	118	12.5	178.54	0.45
(3,5; 1,18)	b3	70	2.43	179.14	0.36	65	-8.37	175.41	0.45
(5; 1,18)	b4	49	0.5	175.57	0.39	44	-3.98	176.39	0.43

Table J.2 The calculated lower order properties of the light field with and without a white table cover, in room Ct2.72 on December 1, 11:30h.

11:30h	Meting II (excl. tafelkleed)				Meting II (incl. tafelkleed)				
Coordinates	Escalar	Altitude	Azimuth	Diffuseness	Escalar	Altitude	Azimuth	Diffuseness	
	[lux]	[degrees]	[degrees]	dnormalized	[lux]	[degrees]	[degrees]	dnormalized	
(0,5; 1,41)	a1	496	22.44	185.42	0.33	473	23.61	180.53	0.33
(2; 1,41)	a2	175	8.83	182.02	0.39	160	9.17	175.97	0.48
(3,5; 1,41)	a3	89	-0.39	179.31	0.43	92	-14.31	175.75	0.49
(5; 1,41)	a4	60	-2.59	176.1	0.46	58	-9.51	177.72	0.47
(0,5; 1,18)	b1	751	27.06	182.47	0.34	551	28.29	181.89	0.34
(2; 1,18)	b2	216	12.43	182.1	0.38	185	13.68	176.87	0.44
(3,5; 1,18)	b3	100	2.62	178.66	0.36	98	-8.86	177.41	0.44
(5; 1,18)	b4	70	0.8	177.69	0.39	65	-4.23	176.53	0.41

Table J.3 The measured vertical illuminances for the measurement on 10:15h.

	without table cover	with table cover
	Vertical lux	Vertical lux
gridline A (=1,41m)	643	1189
gridline B (=1,18m)	983	1326

K RADIANCE

K1. RADIANCE: SIMULATION PROTOCOL

The following protocol describes a simulation in DIVA Radiance, a plug-in of the 3D modelling program Rhinoceros® 3D (Rhino).

- Create a model in Rhino
- o Create a model in Rhino similar to room Ct2.72, pay attention to the orientation
- o Set the reflectance
- o Position a tilted cube with faces of 17x17cm, similar to the cubic illuminance meter, on the position of the simulation.
- o Number each face of the cube in Rhino
- Set the DIVA Radiance location and calculation nodes
- o Set the Location to Amsterdam. The weather data is taken from the website of EnergyPlus (https://energyplus.net/weather-location/europe_wmo_region_6/NLD//NLD_Amsterdam.062400_IWEC)
- o Set the Nodes for the scene – analysis point within the Rhino file that sense the amount of illuminance. For each measurement point six faces should be place for each side of the cube.
- o Pick planar surface (for example, side 1 of the cube)
- o Distance of sampling nodes off planar surface in model units (meters): XX
- o Distance between calculation nodes:
- o Set the Metrics to run the Diva simulation
- o Set Daylight Grid-Based > Point-in-Time Illuminance
- o Under Advanced Parameters the Radiance Parameters the complexity of the scene is set with the ambient bounces, change this to -ab 4.
- o Run the simulation
- o A Load Diva Metrics Dialog box appears, set the Lighting test to Illuminance values.
- o Set a color scheme and select label all notes.

K2. RADIANCE: ADVANCE PARAMTERS

The advanced parameters used in the final simulation model are presented in table K.1. It includes also the explanation of the different parameters.

Table K.2 The advanced parameters used in the final Radiance simulation calculation.

Ambient bounces	Ambient division	Ambient sampling	Ambient accuracy	Ambient resolution
7	1500	100	300	0,1
Ambient bounces	This parameter describes the number of diffuse inter-reflections which will be calculated before a ray path is discarded			
Ambient division	The ad-parameter determines the number of sample rays that are sent out from a surface point during an ambient calculation			
Ambient Samplin	An ambient sampling parameter greater than zero determines the number of extra rays that are sent in sample areas with a high brightness gradient			
Ambient Accuracy	The combination of these two parameters with the maximum scene dimension provides a measure of how fine the luminance distribution in a scene is calculated. According to page 385 in Rendering with Radiance, the combination of aa=0.1, ar=300 and a maximum scene dimension of 100m yields a minimum spatial resolution for cached irradiances of: The simulation resolution will be $(100m \cdot 0.1) / 300 \approx 3cm$. This is sufficient if the facade/roof openings through which the daylight enters the building feature no details below 3 cm. The formula reveals that it is advantageous to keep your scene dimensions as small as possible.			
Ambient resolution				

L VALIDATION MODEL

The final simulation model is validated with the measurements, see table M1.M2.. Figure L1 presents the differences between the measurement and simulation in terms of altitude and azimuth. M4 presents the simulations made in which option 8 is the final chosen model, i.e. the reference model.

Table L.1 Comparison of the errors for the vector angel (in degrees) and the diffuseness (in %) for a selection of the individual simulations run. The red dot indicates the chosen simulation.

face/ position	Measurement						Simulation					
	0	1	2	3	4	5	0	1	2	3	4	5
	(lux)	"	"	"	"	"	"	"	"	"	"	"
a1	245	815	30	103	147	262	269	793	38	139	152	274
a2	131	253	24	49	54	129	141	244	26	61	47	126
a3	78	119	16	26	28	78	82	124	14	26	19	63
a4	59	81	13	21	20	57	47	71	13	17	15	36
b1	273	984	31	151	176	256	253	953	38	167	189	266
b2	143	289	23	53	56	131	153	311	27	68	49	132
b3	101	167	16	28	31	94	89	158	15	20	29	68
b4	76	112	13	23	21	65	54	92	12	19	17	39
						average	128			average		130

Table L.2 Comparison of the errors for the vector angel (in degrees) and the diffuseness (in %) for a selection of the individual simulations run.

face/ position	absolut difference measurement- simulation					
	0	1	2	3	4	5
	(lux)	"	"	"	"	"
a1	24	-22	8	36	5	11
a2	10	-9	2	11	-7	-2
a3	4	5	-1	0	-9	-15
a4	-12	-9	-1	-4	-5	-21
b1	-20	-31	7	16	13	10
b2	10	22	4	15	-6	1
b3	-12	-9	-2	-8	-2	-27
b4	-22	-19	0	-4	-4	-26

Table M.3 Comparison of the errors for the vector angel (in degrees) and the diffuseness (in %) for a selection of the individual simulations run. The red dot indicates the chosen simulation.

	Comparison measurement simulation .(2) calculated light direction			
	Altitude		Azimuth	
	α [degrees]		ϕ [degrees]	
	Measurement	Simulation	Measurement	Simulation
A1	22	21.82	183.33	180.99
A2	9.21	7.56	180.35	175.33
A3	0.08	2.21	180.99	172.30
A4	-3.22	3.31	178.71	172.53
B1	26.5	27.88	180.36	181.73
B2	11.33	12.34	178.59	174.67
B3	2.43	7.23	179.14	176.82
B4	0.5	8.05	175.57	172.51

Table L.4 Comparison of the errors for the vector angel (in degrees) and the diffuseness (in %) for a selection of the individual simulations run. The red dot indicates the chosen simulation.

Options (1-6) simulation- validation (correct model)							
Option		.	.(2)	.(3)	.(4)	.(5)	.(6)
Optical properties / Material							
Ceiling		high_refl_90%	panels_85%	"	"	"	high_refl_90%
Floor		gen_fl_20	"	"	"	"	"
Wall		generic_50%	"	"	"	plaster_80%	generic_50%
Glazing		80clear	"	"	"	"	Tvis70
Table		wood_desk_32%	"	desk_54%	hosp_10%	"	wood_desk_32%
Groundplane		outsidegroun_20%	"	"	"	"	"
Column		Generic_50%	"	"	"	"	"
comparison measurement- simulation							
light intensity	%	2,62	2,53	2,64	1,51	4,66	-0,37
altitude	%	0,4	0,35	0,34	1,08	1,96	0,29
azimuth	%	-2,8	-2,93	-2,28	-2,03	-0,79	-3,03
vector angle	degrees	7,18	7,16	6,49	7,6	9,82	7,31
diffuseness	%	3,5	1,9	3,7	-0,5	11,6	3,5

Options (7-12) simulation- validation (correct model)							
Option		.(7)	.(8)	.(9)	.(10)	.(11)	.(12)
Optical properties / Material							
Ceiling		high_refl_90%	panels_85%	generic_70%	gen_80%	high_refl_90	gen_80%
Floor		generic_20%	"	carp	"	"	"
Wall		generic_70%	generic_50%	plaster_80%	"	gen_50%	"
Glazing		Tvis70	clear80	Tvis70	80	Tvis70	"
Table		hosp_10%	wood_36%	hosp_10%	wood_desk_32%	"	desk_54%
Groundplane		outsidegroun_20%	outside_10%	outside_20%	"	10%	"
Column		Generic_50%	"	"	"	"	"
comparison measurement- simulation							
light intensity	%	0,20	-0,16	2,64	4,72	-2,83	-2,85
altitude	%	1,56	0,75	0,34	0,23		0,03
azimuth	%	-1,45	-2,09	-2,28	-2,52		-2,64
vector angle	degrees	8,45	6,97	6,49	7,28	7,06	7,06
diffuseness	%	7,6	0,8	3,7	13,7	1,5	2,8

M SIMULATION NOVEMBER 3

M1. SIMULATION NOVEMBER 3, 11:00H CLOUDED SKY

The raw data of the simulated cubic illuminance values from the various simulations based upon the reference model presented in the graphs in figure 9.10 are shown in table M.1-3.

Table M.1 The cubic illuminance values and the calculated lower order properties of the light field from the simulations in paragraph 9.2.2 of the various adjusted models (model A-C).

REFERENCE MODEL (image A)										
face/ position	Simulated Illuminance Values Cubic Illuminance meter						Calculated lower order properties of the light field			
	0	1	2	3	4	5	intensity	altitude	azimuth	diffuseness
	(lux)	"	"	"	"	"	E_{sr}	(α)	(ϕ)	($D_{normalized}$)
a1	500	1485	71	261	292	531	572	21.57	181.84	0.36
a2	266	455	41	109	87	237	196	7.31	175.52	0.40
a3	146	239	23	49	40	108	99	6.59	172.23	0.37
a4	115	162	28	37	33	81	73	1.16	170.48	0.44
b1	481	1806	72	318	341	513	682	27.24	181.42	0.36
b2	290	573	43	124	96	253	233	11.70	175.32	0.38
b3	173	294	22	41	57	124	117	7.65	175.58	0.34
b4	139	206	27	40	17	93	84	0.32	167.30	0.33

MODEL (image B): white matt desk										
face/ position	Simulated Illuminance Values Cubic Illuminance meter						Calculated lower order properties of the light field			
	0	1	2	3	4	5	intensity	altitude	azimuth	diffuseness
	(lux)	"	"	"	"	"	E_{sr}	(α)	(ϕ)	($D_{normalized}$)
a1	516	1486	91	286	299	530	584	21.88	180.82	0.39
a2	299	476	110	154	112	240	230	7.10	170.18	0.54
a3	234	271	79	88	59	176	144	-8.82	166.94	0.52
a4	144	177	36	56	44	103	90	-1.23	167.77	0.50
b1	484	1809	88	346	347	512	694	27.93	180.77	0.38
b2	312	586	113	166	117	265	262	11.19	172.40	0.50
b3	254	335	88	63	94	191	162	-4.39	175.97	0.50
b4	149	211	34	59	17	110	93	-1.22	165.40	0.39

MODEL (image C): black matt desk										
face/ position	Simulated Illuminance Values Cubic Illuminance meter						Calculated lower order properties of the light field			
	0	1	2	3	4	5	intensity	altitude	azimuth	diffuseness
	(lux)	"	"	"	"	"	E_{sr}	(α)	(ϕ)	($D_{normalized}$)
a1	501	1498	67	241	282	527	566	21.01	181.96	0.35
a2	260	440	36	97	80	234	187	5.95	176.27	0.38
a3	133	226	18	40	33	106	90	5.57	174.12	0.33
a4	81	133	23	28	26	59	58	6.28	172.33	0.45
b1	481	1806	68	305	346	503	678	27.29	181.65	0.35
b2	284	569	38	110	87	248	224	11.01	175.77	0.35
b3	153	281	16	35	45	114	106	8.38	176.00	0.30
b4	92	167	22	31	17	68	65	6.07	170.85	0.36

Table M.2 The cubic illuminance values and the calculated lower order properties of the light field from the simulations in paragraph 9.2.2 of the various adjusted models (model D-F).

MODEL (image D): horizontal overhang										
face/ position	Simulated Illuminance Values Cubic Illuminance meter						Calculated lower order properties of the light field			
	0	1	2	3	4	5	intensity	altitude	azimuth	diffuseness
	(lux)	"	"	"	"	"	E_{sr}	(α)	(ϕ)	($D_{normalized}$)
a1	310	581	28	107	124	330	242	7.48	182.39	0.36
a2	176	293	21	68	52	151	125	6.74	174.51	0.38
a3	109	161	15	31	23	78	67	2.23	170.93	0.35
a4	81	112	21	25	21	55	51	0.24	169.13	0.44
b1	319	740	27	130	142	336	290	14.22	181.56	0.34
b2	197	354	22	80	57	165	145	9.37	173.86	0.36
b3	133	206	15	25	37	89	81	4.42	174.23	0.32
b4	107	139	20	26	17	67	60	-2.53	167.10	0.35

MODEL (image E): light transmittance 47%										
face/ position	Simulated Illuminance Values Cubic Illuminance meter						Calculated lower order properties of the light field			
	0	1	2	3	4	5	intensity	altitude	azimuth	diffuseness
	(lux)	"	"	"	"	"	E_{sr}	(α)	(ϕ)	($D_{normalized}$)
a1	276	825	36	128	146	290	307	20.32	181.66	0.34
a2	143	246	21	54	40	130	103	5.70	175.86	0.37
a3	81	130	12	23	18	61	52	3.72	172.78	0.33
a4	61	83	15	17	15	44	38	-1.74	171.09	0.42
b1	264	993	37	162	178	270	367	26.87	181.03	0.34
b2	155	315	23	59	45	138	122	10.35	176.06	0.34
b3	95	162	11	19	27	68	62	6.27	175.41	0.31
b4	75	110	14	19	17	48	46	2.38	169.71	0.37

MODEL (image F): horizontal louvers										
face/ position	Simulated Illuminance Values Cubic Illuminance meter						Calculated lower order properties of the light field			
	0	1	2	3	4	5	intensity	altitude	azimuth	diffuseness
	(lux)	"	"	"	"	"	E_{sr}	(α)	(ϕ)	($D_{normalized}$)
a1	248	574	22	104	106	239	224	15.53	179.51	0.34
a2	144	267	16	59	42	124	109	9.80	174.38	0.36
a3	98	136	13	30	21	69	59	1.13	169.82	0.36
a4	68	93	17	22	19	45	43	1.30	168.49	0.45
b1	223	586	20	110	103	211	225	19.59	178.62	0.35
b2	170	327	17	63	42	123	126	11.79	171.77	0.32
b3	116	177	12	22	34	70	70	5.62	172.87	0.32
b4	83	120	16	23	17	48	50	3.23	166.47	0.37

Table M.3 The cubic illuminance values and the calculated lower order properties of the light field from the simulations in paragraph 9.2.2 of the various adjusted models (model G-H)

MODEL (image G): horizontal louvers + white desk										
face/ position	Simulated Illuminance Values Cubic Illuminance meter						Calculated lower order properties of the light field			
	0	1	2	3	4	5	intensity	altitude	azimuth	diffuseness
	(lux)	"	"	"	"	"	E_{sr}	(α)	(ϕ)	($D_{normalized}$)
a1	246	563	33	121	114	244	229	16.25	179.38	0.39
a2	173	278	52	87	55	128	129	8.31	167.62	0.50
a3	134	162	43	47	31	100	82	-7.59	167.77	0.49
a4	89	111	21	31	24	58	54	-0.58	166.48	0.47
b1	228	608	29	126	111	219	238	20.58	178.23	0.37
b2	168	354	53	94	58	127	149	16.24	169.84	0.46
b3	147	195	47	32	50	106	91	-4.35	175.00	0.47
b4	91	128	20	33	17	58	56	1.88	165.12	0.41

MODEL (image H): white shiny desk										
face/ position	Simulated Illuminance Values Cubic Illuminance meter						Calculated lower order properties of the light field			
	0	1	2	3	4	5	intensity	altitude	azimuth	diffuseness
	(lux)	"	"	"	"	"	E_{sr}	(α)	(ϕ)	($D_{normalized}$)
a1	520	1491	81	262	284	529	573	20.85	180.95	0.37
a2	289	455	94	132	94	240	213	4.29	171.65	0.50
a3	223	251	66	69	47	157	128	-9.96	166.59	0.47
a4	153	181	33	44	36	101	87	-4.60	167.51	0.43
b1	482	1802	78	350	353	505	694	28.39	180.70	0.38
b2	308	567	96	153	104	249	248	10.75	171.45	0.47
b3	258	325	72	51	77	181	151	-5.93	173.85	0.44
b4	177	216	31	48	17	109	95	-4.93	163.73	0.34

M2. SIMULATION NOVEMBER 3, 11:00H CLEAR SKY

The raw data of the simulated cubic illuminance values from the various simulations based upon the reference model on a clear simulated sky are shown in table M.4-6.

Table M.4 The cubic illuminance values and the calculated lower order properties of the light field from the simulations on November 3, 11:00h Clear Sky of the various adjusted models (model A-C).

REFERENCE MODEL (image A) - November 3, 11:00h Clear sky										
face/ position	Simulated Illuminance Values Cubic Illuminance meter						Calculated lower order properties of the light field			
	0	1	2	3	4	5	intensity	altitude	azimuth	diffuseness
	(lux)	"	"	"	"	"	E_{sr}	(α)	(ϕ)	($D_{normalized}$)
a1	1764	2411	322	893	638	1296	1220	7.50	167.64	0.51
a2	1055	1316	91	430	285	657	635	4.94	164.73	0.42
a3	544	777	63	153	120	343	325	3.64	168.77	0.34
a4	330	481	78	107	99	214	214	4.32	169.36	0.44
b1	1838	2551	345	1026	636	1212	1299	10.57	163.14	0.52
b2	1081	1489	91	497	288	661	696	8.82	163.83	0.42
b3	602	888	60	126	194	337	363	7.07	171.47	0.35
b4	388	574	74	107	17	227	224	0.25	163.83	0.29

MODEL (image B): white matt desk										
face/ position	Simulated Illuminance Values Cubic Illuminance meter						Calculated lower order properties of the light field			
	0	1	2	3	4	5	intensity	altitude	azimuth	diffuseness
	(lux)	"	"	"	"	"	E_{sr}	(α)	(ϕ)	($D_{normalized}$)
a1	1806	2428	368	931	658	1301	1249	7.31	166.57	0.52
a2	1107	1369	247	535	335	711	716	3.98	162.07	0.52
a3	728	855	197	220	162	496	421	-6.92	166.87	0.46
a4	408	505	96	144	124	284	251	-1.09	168.62	0.48
b1	1829	2592	378	1050	667	1214	1325	11.58	163.31	0.53
b2	1155	1507	247	624	344	673	780	8.62	158.69	0.52
b3	797	947	216	172	244	521	456	-6.01	171.55	0.46
b4	424	579	91	152	17	283	249	-2.75	162.43	0.35

MODEL (image C): black matt desk										
face/ position	Simulated Illuminance Values Cubic Illuminance meter						Calculated lower order properties of the light field			
	0	1	2	3	4	5	intensity	altitude	azimuth	diffuseness
	(lux)	"	"	"	"	"	E_{sr}	(α)	(ϕ)	($D_{normalized}$)
a1	1794	2426	327	886	620	1293	1221	6.80	167.06	0.50
a2	1082	1328	83	433	283	670	641	4.43	164.58	0.42
a3	519	796	54	146	114	333	321	5.55	169.73	0.33
a4	269	432	69	97	92	192	190	6.99	171.93	0.45
b1	1779	2556	334	1022	642	1211	1292	11.70	164.13	0.52
b2	1083	1497	83	492	286	647	695	9.20	163.61	0.41
b3	541	897	50	120	176	330	352	9.32	173.28	0.33
b4	294	505	65	102	17	189	193	4.55	165.23	0.32

Table M.5 The cubic illuminance values and the calculated lower order properties of the light field from the simulations in paragraph 9.2.2 of the various adjusted models (model D-F).

MODEL (image D): horizontal overhang										
face/ position	Simulated Illuminance Values Cubic Illuminance meter						Calculated lower order properties of the light field			
	0	1	2	3	4	5	intensity	altitude	azimuth	diffuseness
	(lux)	"	"	"	"	"	E_{sr}	(α)	(ϕ)	($D_{normalized}$)
a1	1550	1614	303	699	485	1130	932	-3.72	165.08	0.53
a2	916	1092	74	404	245	565	548	4.80	162.88	0.44
a3	482	644	56	136	105	305	279	1.71	168.20	0.36
a4	282	388	70	98	90	182	181	3.42	168.49	0.48
b1	1607	1787	313	794	492	1087	1001	0.94	161.92	0.53
b2	973	1233	74	425	249	565	593	6.90	162.38	0.42
b3	537	757	53	111	166	299	315	5.61	170.89	0.35
b4	327	473	66	103	17	192	192	0.28	162.52	0.32

MODEL (image E): light transmittance 47%										
face/ position	Simulated Illuminance Values Cubic Illuminance meter						Calculated lower order properties of the light field			
	0	1	2	3	4	5	intensity	altitude	azimuth	diffuseness
	(lux)	"	"	"	"	"	E_{sr}	(α)	(ϕ)	($D_{normalized}$)
a1	1007	1359	180	493	324	712	678	6.44	166.16	0.49
a2	594	743	58	230	145	371	352	3.54	164.80	0.41
a3	305	446	40	80	60	206	183	2.09	170.04	0.33
a4	163	244	38	53	47	115	107	3.71	171.05	0.43
b1	1018	1420	187	551	337	671	712	9.90	163.44	0.50
b2	620	809	59	283	148	366	386	7.02	161.90	0.42
b3	331	492	40	65	99	195	199	5.44	172.16	0.34
b4	180	291	36	57	17	114	113	3.48	165.97	0.32

MODEL (image F): horizontal louvers										
face/ position	Simulated Illuminance Values Cubic Illuminance meter						Calculated lower order properties of the light field			
	0	1	2	3	4	5	intensity	altitude	azimuth	diffuseness
	(lux)	"	"	"	"	"	E_{sr}	(α)	(ϕ)	($D_{normalized}$)
a1	1066	978	257	556	314	687	638	-5.28	155.19	0.59
a2	657	711	47	273	169	363	370	3.19	160.16	0.44
a3	326	466	34	103	71	174	196	6.67	165.00	0.35
a4	176	231	41	69	58	103	112	5.34	164.93	0.50
b1	1111	1006	272	612	314	657	670	-3.48	150.59	0.60
b2	678	719	46	336	164	331	392	6.20	154.18	0.46
b3	334	485	32	75	127	175	205	9.23	171.38	0.38
b4	185	257	38	72	17	97	112	2.73	158.57	0.38

Table M.6 The cubic illuminance values and the calculated lower order properties of the light field from the simulations of the various adjusted models (model G-H) on November 3, 11:00h clear sky.

MODEL (image G): horizontal louvers + white desk										
face/ position	Simulated Illuminance Values Cubic Illuminance meter						Calculated lower order properties of the light field			
	0	1	2	3	4	5	intensity	altitude	azimuth	diffuseness
	(lux)	"	"	"	"	"	E_{sr}	(α)	(ϕ)	($D_{normalized}$)
a1	1083	972	278	571	337	700	652	-6.04	154.75	0.61
a2	689	688	125	333	194	378	405	0.80	154.89	0.54
a3	406	463	101	139	88	254	233	-5.00	163.06	0.47
a4	226	243	47	80	66	143	129	-3.76	164.89	0.50
b1	1148	962	301	648	314	664	687	-6.09	146.90	0.61
b2	681	776	124	371	187	353	426	6.89	153.54	0.52
b3	434	480	111	92	155	245	241	-4.56	169.51	0.49
b4	230	295	45	85	17	143	132	-2.33	160.75	0.37

MODEL (image H): white shiny desk										
face/ position	Simulated Illuminance Values Cubic Illuminance meter						Calculated lower order properties of the light field			
	0	1	2	3	4	5	intensity	altitude	azimuth	diffuseness
	(lux)	"	"	"	"	"	E_{sr}	(α)	(ϕ)	($D_{normalized}$)
a1	1761	2414	346	941	664	1301	1242	8.33	167.16	0.52
a2	1117	1334	223	526	323	679	701	3.73	160.71	0.51
a3	737	819	178	206	146	464	404	-7.82	164.84	0.44
a4	447	506	94	137	112	290	252	-4.69	166.48	0.45
b1	1805	2562	366	1077	655	1196	1320	12.21	162.51	0.53
b2	1168	1509	221	584	326	665	763	7.66	159.36	0.49
b3	796	925	193	156	246	486	442	-5.26	170.76	0.45
b4	490	593	89	147	17	296	261	-5.76	161.00	0.32

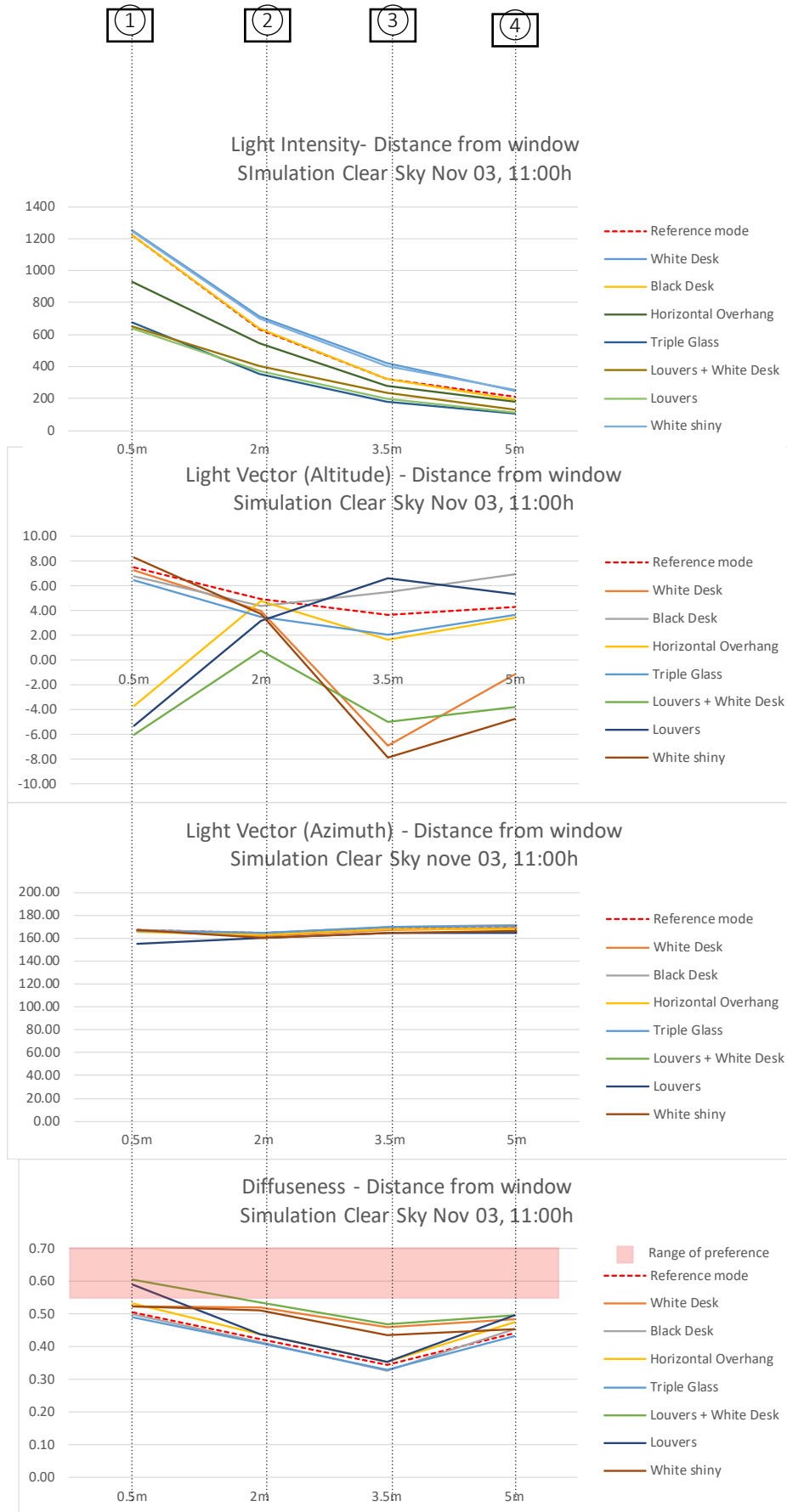


Figure M.7 Light intensity, light direction (altitude, azimuth) and light diffuseness in simulations with Clear sky on November 3, 11:00h.

N ADDITIONAL VISUALIZATION

In the recommendations it is mentioned that the table should be turned in order to prevent observers from facing the window during a meeting. However, it is assumed that in some cases the strong directionality of the light and the low diffuseness could cause a disturbing shadow on parts of the face. This is tested in the set-up below (figure N.1). Due to limited availability of the meeting space Ct2.72, this measurement was executed in Ct6.75.

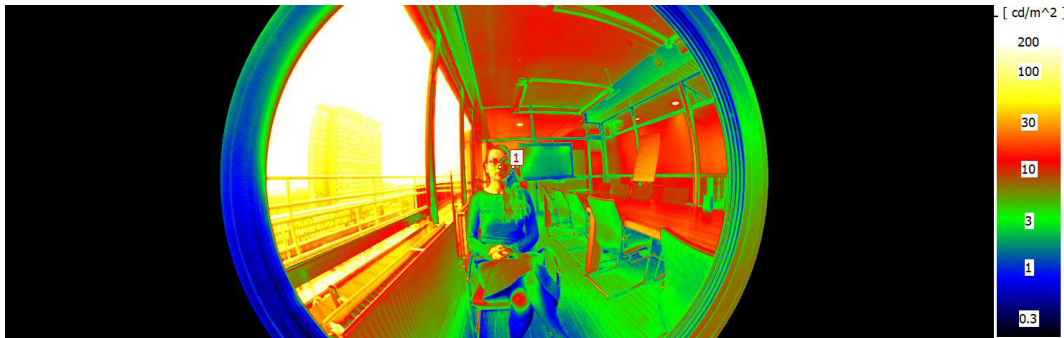


Figure N.1 A false-color image of a fish eye image in which a person sits parallel to the window. Results presented in table N.1

Table N.1 The luminance values and ratios measured in figure N.1.

	min	max	mean	ratio (max/mean)	ratio (max/mean)
	cd/m ²	cd/m ²	cd/m ²		
square 1	0,95	96,1	27,6	1:101	1:3,5

